Unicast versus broadcast in cellular networks

Juan Carlos Vargas Rubio

COLLEGE SCIENCES
DOCTORAL POUR L'INGENIEUR
BRETAGNE ET LE NUMERIQUE

IMT Atlantique
Bretagne-Pays de la Loire
École Mines-Télécom

THESE DE DOCTORAT DE

L'ÉCOLE NATIONALE SUPERIEURE MINES-TELECOM ATLANTIQUE
BRETAGNE PAYS DE LA LOIRE - IMT ATLANTIQUE

ECOLE DOCTORALE N° 648
SPIN : Sciences pour l'ingénieur et le numérique

Spécialité : Informatique

Par

Juan Carlos VARGAS RUBIO

Unicast versus Broadcast in Cellular Networks

Thèse présentée et soutenue sur le campus de Rennes d'IMT Atlantique, le 23 mars 2023
Unité de recherche : IRISA
Thèse N° : 2023IMTA0341

Rapporteurs avant soutenance :

Véronique VEQUE	Professeure, Université Paris-Saclay
David GOMEZ-BARQUERO	Professeur, Universitat Politecnica de Valencia

Composition du Jury :

Président :	Loutfi NUAYMI	Professeur, IMT Atlantique
Examinateurs :	Véronique VEQUE	Professeure, Université Paris-Saclay
	David GOMEZ-BARQUERO	Professeur, Universitat Politecnica de Valencia
	Toufik AHMED	Professeur, ENSEIRB-MATMECA
	Aymen JAZIRI	Ingénieur de recherche, SIRADEL
Dir. de thèse :	Xavier LAGRANGE	Professeur, IMT Atlantique
Co-dir. de thèse :	Cédric THIENOT	CTO, Firecell (ENENSYS Technologies pendant la thèse)

Invité(s)

Richard LHERMITTE	CTO, ENENSYS Technologies

Dedicated to the loving memory of my father, Juan Carlos Vargas Hernandez, who always put his loved ones before himself. He supported me in every possible way even from a distance. He encouraged me to pursue my dreams and was alongside me at every step of the way, I know he'll always be.

To my grandfather, Campo Elias Rubio Romero, who wanted me to learn and love math. I'll always remember when I was a kid and he offered me a prize for learning the multiplication tables. It worked.

Acknowledgement

I have many people to thank for this amazing journey that has been my academic life. I'll do my best.

When I told people that Xavier Lagrange was my thesis director they would say things like "he's intelligent and very exigent" or "you already have 50% of your PhD", and they were right. But, what impressed me more about Xavier was his commitment with our work. He was always there to answer all my questions or to review our papers 24 hours before the deadline. His guidance and ideas were key for the success of this thesis. Thank you!

Cédric, even though we didn't work side by side physically, I think we made a good team during these years. Your feedback helped me understand why our research was important not only for science but also for the industry. Even though you were swamp with work, you always had time to discuss about the thesis, thank you!

I want to thank the jury members for being a part of this thesis. In particular Veronique Vêque and David Gomez Barquero for evaluating the manuscript and their valuable feedback.

To all my friends, colleagues, staff, professors and directives from IMT Atlantique, it has been a pleasure working by your side. In particular, I want to thank Maria Le Goff and Jhon Puentes who helped me to come to France and do my masters at IMT. I thank as well my friends from the master, Julian, Nicolas, Christopher, Gino, Barbara, Checho, Jhonny, Liz, Morten, Alejo. Leaving my life in Colombia was hard but your company made everything easier, we had fun. Cesar, my boss and friend during my internship, life in Grenoble was great thanks to you. To ADER, Tania, Renzo, Routa, Farah, Tommy, Laudin, Georgios, Aris, you made me feel welcome from the first day and we had the best of times. I'll always cherish our coffee breaks, BBQs, trips, wedding parties, and more.

To all the team at Enensys, these three years have been a very enriching experience. I've had the opportunity to meet very skilled and experienced engineers and good people. Benoît, Christophe, Williams, Ricardo, thanks for your feedback and help, your industry experience in MBMS was very valuable for me. Richard, Séverine, Régis, thank you for trusting me and offering me the opportunity to work at Enensys.

I would not have a PhD If hadn't become an engineer first. I'm very thankful with the Distrital University of Bogota for giving me the opportunity to become a professional. In particular, I'd like to thank professor Gustavo Puerto for stablishing relations with IMT Atlantique. Thanks to you, me and many other students from the university have realized their dream of studying abroad. I want to thank my friends and teammates Liz, Jonier, Cristian Rodriguez and Cristian Aguazaco. I'm not sure I'd have done it without you.

To my family, I'll never have enough words to express my gratitude. As I get older I realize the immense value of everything you did and still do for me. To my aunts Martha and Judith, thank you for always being there for me and my sister. To my grandfather, Campo Elias, the one responsible for me loving math, I'll always remember you. To my sister, Diana, I love you very much, thank you for taking care of my parents while I was doing this thesis, I could not have done it without you. To my mom, Maria Rubio, this PhD is as mine as it is yours, you have always believed in us, ever since we were little kids you always believed we could get this far. I'll always love you. To my dad, Juan Carlos Vargas Hernandez, thank you for working so hard for us, you'll always be in my heart, I'll love you forever.

Finally, to my dear wife, Jenny Tatiana Moreno Perea, the love of my life, thank you for being by my side all these years. I'm excited to think about everything life has in store or us. I love you.

To all, even the ones that I did not mention explicitly, I'm grateful for having you in my life.

Vive la France et vive la Colombie.

Abstract

Data traffic on mobile networks is increasing every year, especially video content. However, spectrum is scarce and expensive and operators need to optimize its use. In scenarios where the same content is transmitted at the same time to many devices in the same geographical area, the preferred solution to reduce bandwidth consumption is broadcast transmission.

Unicast transmission benefits from link adaptation techniques. However, the same content is transmitted as many times as the number of users demanding the same service. Conversely, a single broadcast transmission can cover a large number of users. Nevertheless, the bitrate in broadcast is fixed considering the users with the worst channel quality. Multicast-Broadcast Single-Frequency-Network (MBSFN) is a broadcast technique in which a group of synchronized cells transmit the same waveform. On the other hand, with Single-Cell Point-To-Multipoint (SC-PTM) each cell performs broadcast transmission independently. The problem is to determine when is it better to use unicast, MBSFN or SC-PTM.

In our work, we compare the performance of unicast, MBSFN and SC-PTM through system level simulations and analytical models. We consider base stations located according to Poisson distributions, the use of beamforming in unicast and different broadcast configurations. The core contribution of this thesis is an analytical method to calculate the number of users demanding the same content from which MBSFN or SC-PTM become more efficient than unicast. We prove that a switching mechanism based on this user threshold reduces bandwidth utilization and energy consumption. This method is based on stochastic geometry results for wireless networks.

Keywords

Unicast, Broadcast, MBMS, MBSFN, SC-PTM, MooD, beamforming, stochastic geometry, coverage, energy consumption, MCC, group communications.

RÉSUMÉ DE LA THÈSE EN FRANÇAIS

La vidéo est un facteur important de la charge des réseaux cellulaires en raison de la popularité croissante des services de streaming et de télévision linéaire. En 2022, on estime que le trafic vidéo représente 69% du trafic de données mobiles et devrait passer à 79% en 2027 avec l'adoption des technologies de réalité virtuelle/augmentée. Ces chiffres sont d'autant plus impressionnants que le trafic de données sur les réseaux mobiles a augmenté de 40 % entre le premier trimestre de 2021 et le premier trimestre de 2022, et que cette tendance devrait se poursuivre dans les années à venir. En outre, le nombre d'appareils mobiles capables d'afficher des services gourmands en bande passante tels que la vidéo ultra-haute définition (UHD) et la vidéo à 360 degrés devrait augmenter. Ces services disruptifs seront soutenus par la 4G et la 5G. En fait, la part de la 5G dans le trafic de données mobiles devrait atteindre 60 % en 2027, contre 10 % en 2021.

La demande sans cesse croissante de contenu multimédia de haute qualité dans les réseaux cellulaires exige la mise en œuvre de techniques de gestion efficace des ressources radio, car le spectre est limité et coûteux. Afin de fournir une bonne qualité de service, les opérateurs cherchent des alternatives pour réduire l'utilisation des ressources radio lorsque plusieurs utilisateurs demandent le même contenu vidéo dans une zone géographique donnée. La transmission par diffusion est la solution privilégiée pour les scénarios dans lesquels le même contenu est transmis à de nombreux utilisateurs en même temps. Lorsqu'une vidéo est très populaire, le contenu peut être poussé par la transmission de diffusion et ensuite stocké dans le cache du récepteur, même avant la demande de l'utilisateur. Cela permet de décharger le réseau et de maintenir une bonne qualité de service. Parmi les cas d'utilisation, citons la télévision mobile, le streaming vidéo d'événements populaires et les communications de groupe dans des scénarios de mission critique.

Dans les situations d'urgence, les premiers intervenants doivent communiquer de manière rapide et fiable, c'est ce qu'on appelle les communications essentielles à la mission (MCC). Les MCC dépendent de réseaux de radio mobile professionnelle (PMR) sécurisés et fiables. Les réseaux PMR utilisaient autrefois des formes d'onde et des méthodes de multiplexage spécifiques, différentes des technologies cellulaires commerciales. Cependant, les réseaux PMR fonctionnent aujourd'hui sur les bandes LTE (Long Term Evolution) et devraient

fonctionner avec la 5G. En particulier, la solution pour la transmission de diffusion dans LTE, Multimedia Broadcast Multicast Service (MBMS), est la technologie privilégiée pour la transmission des services de communication de groupe. Les communications de groupe sont destinées à distribuer le même contenu à plusieurs utilisateurs en même temps et de manière contrôlée, garantissant l'efficacité des opérations.

Cette thèse s'est déroulée dans le cadre d'une Convention Industrielle de Formation par la Recherche (CIFRE). Une convention CIFRE est financée en partie par le ministère français de l'enseignement supérieur et de la recherche et implique un établissement d'enseignement supérieur, une entreprise et le doctorant. Pour cette thèse, IMT Atlantique et Enensys Technologies ont formé la convention CIFRE. La société Enensys est basée à Rennes, France. Elle fournit des solutions pour optimiser, sécuriser et monétiser l'ensemble de la chaîne des médias, sur tous les types de réseaux de diffusion : satellite, terrestre, haut débit et mobile. Depuis sa création en 2004, le groupe réalise de 80 à 90 % de son chiffre d'affaires à l'export. C'est une entreprise portée par l'innovation, Enensys possède un portefeuille de 60 brevets internationaux. Enensys dispose d'une solution de bout en bout pour la diffusion sur les réseaux 4G et 5G. Il s'agit de la solution MBMS la plus avancée du marché, avec les plus grands déploiements commerciaux.

Contribution des Travaux

Les contributions de notre travail de thèse sont les suivantes :

— Nous comparons les performances en termes du rapport signal sur interférence plus bruit (SINR) des techniques de transmission Unicast et Multicast Broadcast Single Frequency Network (MBSFN) par le biais de simulations au niveau du système. Nous considérons la formation de faisceau (beamforming) pour l'unicast et différentes configurations de zone MBSFN. Notamment une grande zone MBSFN (à l'échelle nationale) et des zones MBSFN avec un nombre limité de stations de base. Le modèle de propagation et le modèle d'antenne sont tirés de la littérature.

— Nous proposons un modèle pour calculer le nombre d'utilisateurs par cellule dans la zone MBSFN, appelé seuil d'utilisateur, pour passer de l'unicast au MBSFN afin de réduire l'utilisation des ressources radio. Le modèle tient compte de la distribution de probabilité du SINR lors de l'utilisation de la diffusion individuelle et du MBSFN. La distribution du SINR dépend du nombre d'antennes utilisées pour la formation de faisceau, du nombre de stations de base (BS) dans la zone MBSFN, de la densité

des stations de base (nombre moyen de stations de base par kilomètre carré), entre autres paramètres du système.

— Nous proposons une méthode pour calculer analytiquement le seuil d'utilisateur afin de réduire l'utilisation des ressources radio. Nous calculons le seuil d'utilisateur pour passer de l'unicast au MBSFN et le seuil d'utilisateur pour passer de l'unicast au Single-cell Point-to-Multipoint (SC-PTM). La méthode est basée sur une équation permettant de calculer la distribution du SINR pour un utilisateur situé en tout point d'une zone MBSFN.

— Nous adaptons les modèles de consommation d'énergie pour l'unicast de la littérature afin de comparer la consommation d'énergie en MBSFN, SC-PTM et unicast. Nous analysons séparément le côté UE et le côté BS. En outre, nous proposons un modèle analytique pour calculer le seuil d'utilisateur pour passer de l'unicast à MBSFN ou SC-PTM afin de réduire la consommation d'énergie de l'UE et de la station de base.

— Nous avons effectué des simulations au niveau du système afin d'identifier les scénarios de mission critique dans lesquels la transmission par diffusion (MBSFN et SC-PTM) est plus efficace que la transmission unicast du point de vue de l'utilisation des ressources.

Révision technique de la transmission en diffusion dans les réseaux cellulaires

Notre analyse est basée sur le modèle de référence proposé par le 3GPP dans [3]. Le modèle de propagation est basé sur Okumura-Hata-Cost231 avec effet de masque et évanouissement. De plus, ce travail prend en compte les antennes omnidirectionnelles, les antennes tri-sectorielles et les antennes directrices utilisant le beamforming.

Le 3GPP a développé une spécification d'interface point-à-multipoint (PTM) pour les réseaux cellulaires appelée MBMS. Dans l'interface radio, MBMS peut utiliser deux techniques de transmission différentes : MBSFN ou SC-PTM. Dans MBSFN, plusieurs cellules transmettent le même signal, la même forme d'onde, de manière synchrone aux utilisateurs intéressés, tandis que SC-PTM fait référence à la transmission en diffusion dans une seule cellule. Les transmissions MBSFN et SC-PTM visent à couvrir les utilisateurs présentant les pires conditions de canal dans la zone de diffusion, c'est-à-dire les utilisateurs ayant le rapport signal sur interférences plus bruit (SINR) le plus faible.

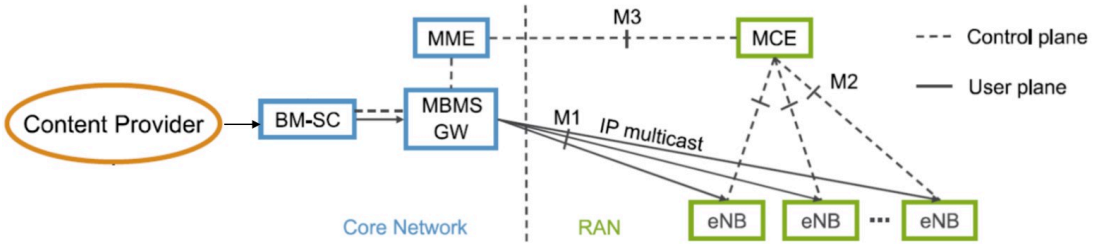

FIGURE 1 – Architecture MBMS [19]

L'architecture MBMS présentée dans la Figure 1 a été définie par le 3GPP dans la release 9.

Le BM-SC (Broadcast Multicast Service Center), situé dans le coeur de réseau, est le point d'entrée du contenu et il est responsable de l'authentification/autorisation à la fois du fournisseur de contenu et de l'utilisateur, de la facturation de l'utilisateur, de la configuration du flux de données global à travers le coeur de réseau et du codage au niveau de l'application. Le MBMS gateway est un nœud logique qui distribue les données MBMS du BM-SC aux stations de base en utilisant le multicast IP. De plus, l'entité de coordination multi-cellules/multidiffusion (MCE) est un nœud logique dans le réseau d'accès radio (RAN) chargé de l'allocation des ressources radio pour la transmission multidiffusion multi-cellules en utilisant la technique MBSFN.

MBSFN est une technique de transmission simultanée consistant en plusieurs cellules qui transmettent des formes d'onde identiques en même temps. L'UE combine les signaux arrivant qui sont perçus comme une seule transmission souffrant de la propagation par trajets multiples, tout comme dans les transmissions Unicast.

La zone de proximité réseau où toutes les cellules peuvent être synchronisées et effectuer des transmissions MBSFN est appelée la zone de synchronisation MBSFN. Elles sont capables de prendre en charge une ou plusieurs zones MBSFN. Une zone MBSFN est un groupe de cellules coordonnées pour transmettre la même forme d'onde simultanément. C'est généralement une zone compacte sans aucun trou comme présenté dans la Figure 2.

Le SC-PTM a été introduit dans la release 13 du 3GPP pour prendre en charge les services MBMS dans une seule cellule. Il utilise la même architecture présentée précédemment, mais le réseau peut décider dynamiquement quelles cellules transmettent en mode SC-PTM, tandis que dans le MBSFN, la zone MBSFN est statique. Puisque le Unicast et le SC-PTM sont basés sur le même canal physique et ont la même structure de trame radio, les ressources radio peuvent être partagées de manière flexible entre le unicast et le SC-PTM dans la même sous-trame.

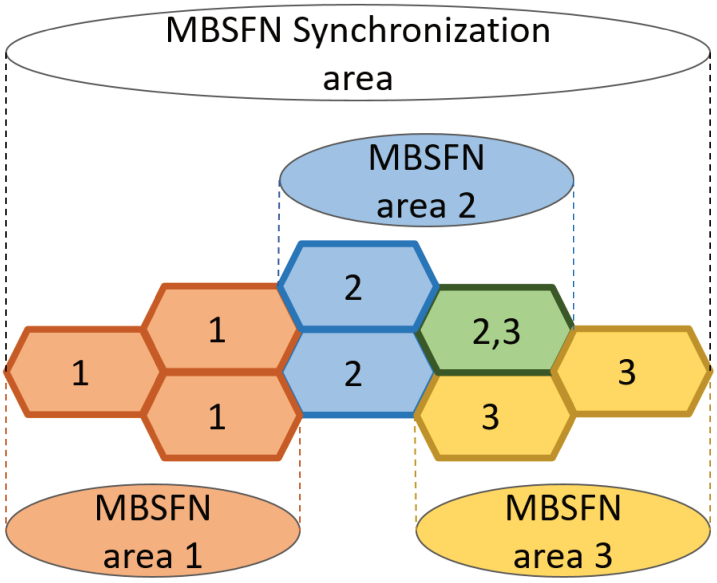

FIGURE 2 – Zone de synchronisation MBSFN et zone MBSFN

L'opération MBMS à la demande (MooD) permet l'activation et la désactivation automatiques et transparentes des services MBMS. Lorsqu'il devient plus efficace d'exécuter un service unicast en tant que service MBMS, le système peut activer une session MBMS pour le service.

MBSFN versus Unicast dans les systèmes cellulaires

Nous présentons une comparaison de performance entre la transmission Unicast (UC) et la transmission MBSFN dans les réseaux cellulaires d'un point de vue de l'utilisation des ressources. Nous introduisons un modèle pour calculer la distribution du SINR pour un utilisateur final recevant en mode UC et MBSFN. Nous utilisons ce modèle pour comparer les deux modes de transmission en termes de puissance du signal utile et des interférences. Ensuite, nous calculons le nombre minimum d'utilisateurs par cellule, téléchargeant les mêmes données, pour lequel une transmission MBSFN est plus efficace que plusieurs transmissions Unicast.

Pour tenir compte de l'irrégularité des réseaux opérationnels, nous considérons des stations de base situées selon un Processus de Poisson Ponctuel (PPP) avec une intensité λ_{BS} comme indiqué dans la Figure 3. L'intensité λ_{BS} représente le nombre moyen de stations de base (BS) par kilomètre carré. Par conséquent, dans le reste de ce document,

nous l'appelons densité des BS. Le modèle PPP s'est avéré produire des résultats plus proches des performances des déploiements réels de réseaux cellulaires par rapport au modèle hexagonal typique.

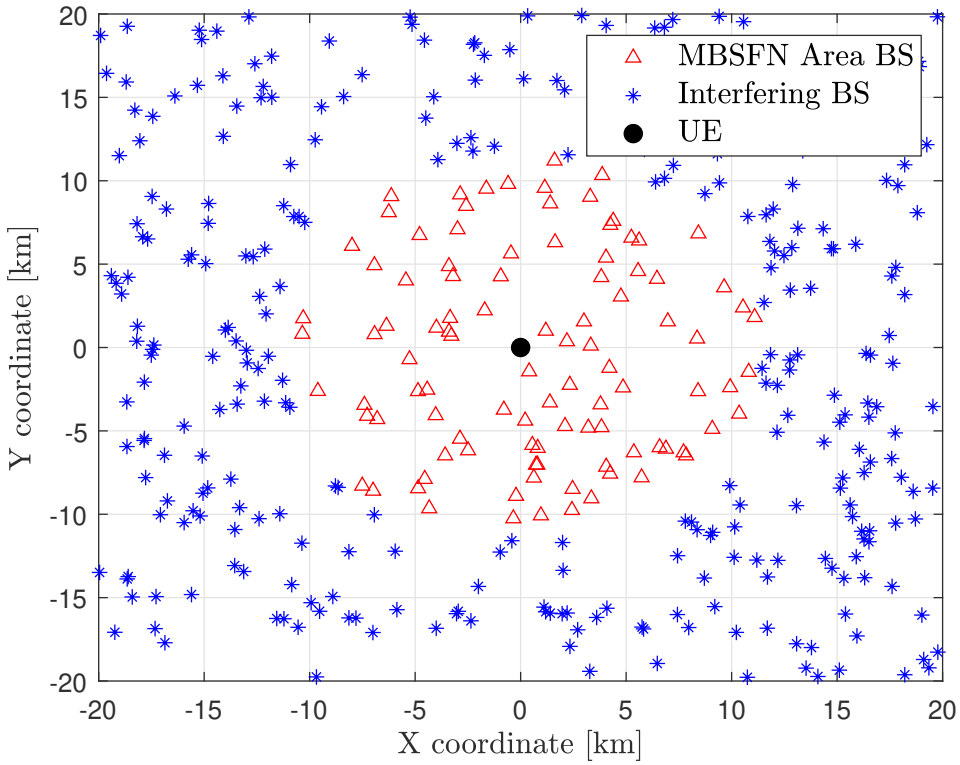

FIGURE 3 – Zone MBSFN avec 100 BS dans une superficie où les BS sont placées en suivant un PPP de densité $\lambda_{\text{BS}} = 0.25$ BS/km^2.

Nous calculons la fonction de répartition cumulative (CDF) du SINR perçu par un utilisateur lors de la réception en mode UC et en mode MBSFN à l'aide de la méthode de Monte Carlo. Nous considérons une surface très large pour localiser les BS et analysons chaque mode de transmission séparément. En mode MBSFN, nous considérons des BS distribuées selon le PPP comme dans la Figure 3, mais avec tous les BS appartenant à la zone MBSFN. Nous considérons un UE situé au centre de la surface simulée, à l'origine du plan. Nous considérons également des stations de base tri-sectorielles pour les modes UC et MBSFN, et le beamforming uniquement pour le mode UC. À chaque itération, un nouveau PPP pour l'emplacement des BS est généré et le SINR pour un UE en modes UC et MBSFN est calculé.

La Figure 4 montre la CDF du SINR pour un récepteur en mode UC, incluant le

beamforming avec un nombre différent d'antennes par secteur (M), et en mode MBSFN en considérant une grande zone MBSFN de 1600 km2. Comme prévu, la technique du beamforming augmente le SINR en mode UC, plus le nombre d'antennes par secteur (M) est élevé, plus le SINR est élevé, grâce à l'augmentation de la puissance du signal. Cependant, le mode MBSFN offre un SINR plus élevé que tous les cas UC en raison de la réduction des interférences. Remarquez dans la Figure 4 que la densité des BS n'a pas un effet significatif lors de la transmission en mode UC. La puissance d'interférence augmente lorsque la densité des BS augmente, atténuant l'effet de l'augmentation de la puissance du signal. En revanche, lors de la transmission en mode MBSFN, plus la densité des BS est élevée, plus le SINR est élevé. Un plus grand nombre de BS dans la zone MBSFN augmente la puissance du signal tout en maintenant une faible interférence.

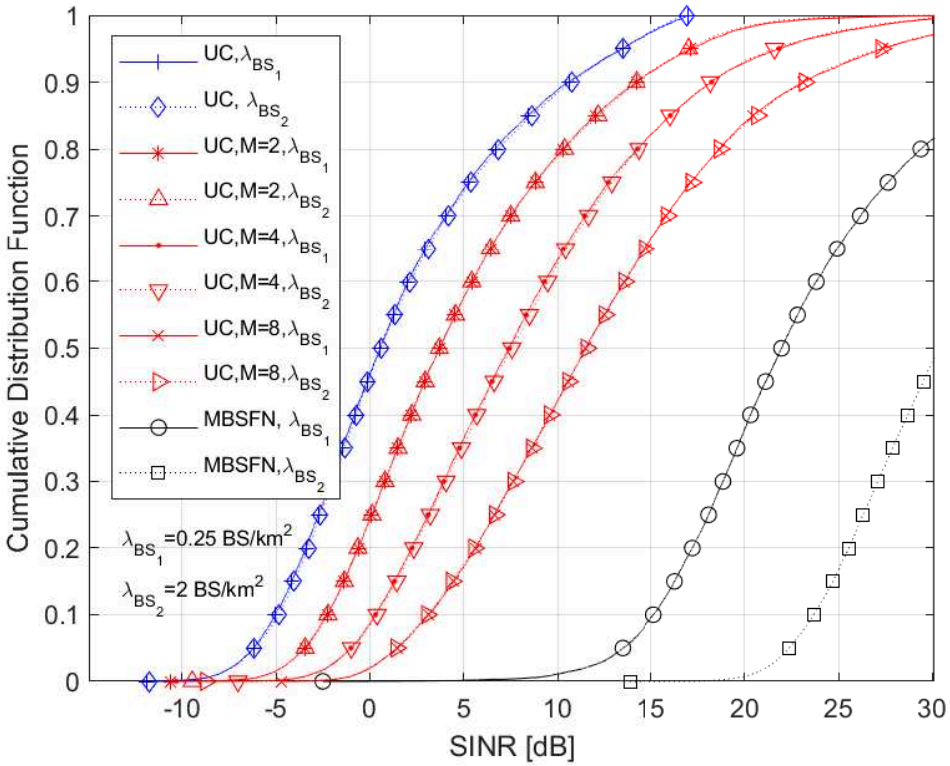

FIGURE 4 – CDF du SINR perçu par un utilisateur en mode Unicast (UC), incluant le beamforming avec différents nombres d'antennes (M), et en mode MBSFN, en considérant tous les BS comme faisant partie de la zone MBSFN, pour différentes valeurs de densité des BS.

Seuil Utilisateur

Nous définissons le seuil utilisateur (U_T) comme le nombre d'utilisateurs par cellule dans la zone MBSFN à partir duquel le mode unicast consomme plus de ressources que le mode MBSFN.

La Figure 5 présente le seuil utilisateur (U_T) en fonction du nombre de cellules dans la zone MBSFN (N_{SFN}) pour différentes configurations Unicast. Remarquez que même lorsque une zone MBSFN est formée par seulement 2 stations de base (6 cellules) et que les transmissions UC sont effectuées à l'aide du beamforming avec 8 antennes par secteur, MBSFN est plus efficace que l'unicast lorsqu'il y a au moins 8 utilisateurs par cellule demandant le même contenu.

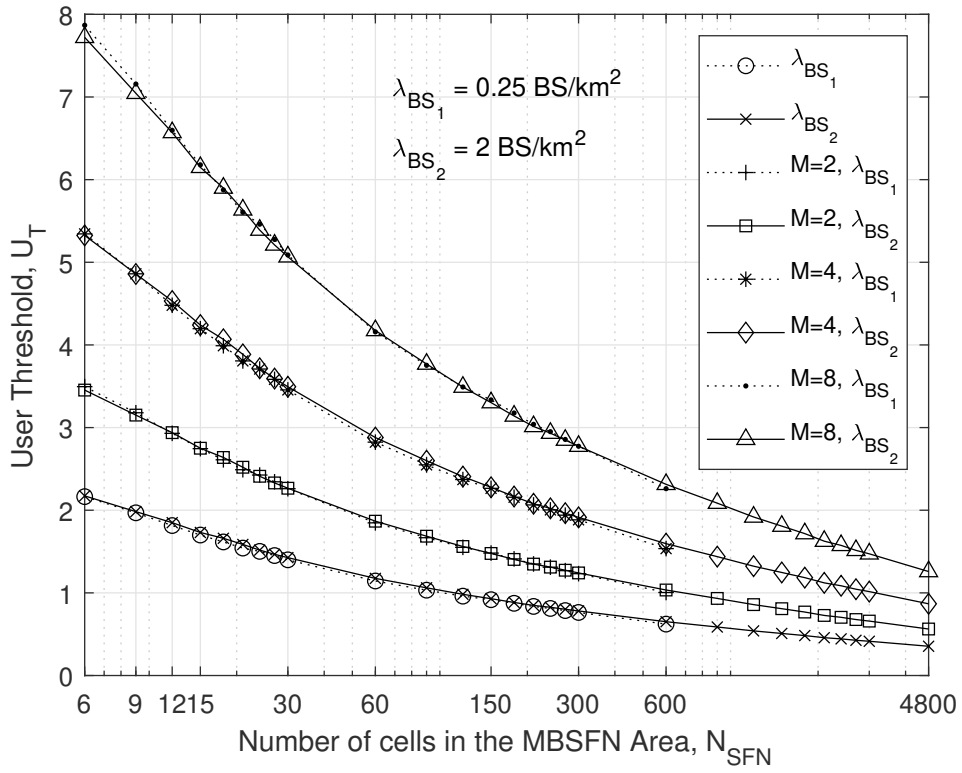

FIGURE 5 – Seuil de l'utilisateur (U_{T}) par rapport au nombre de cellules dans la zone MBSFN (N_{SFN}) pour différentes configurations UC et différentes valeurs de densité de BS, λ_{BS}.

Analyse de l'utilisation des ressources et de la consomation d'énergie pour MBMS

Dans cette thèse on présente des expressions analytiques permettant de calculer la distribution du SINR pour les utilisateurs recevant en mode Unicast, MBSFN et SC-PTM. Les expressions analytiques sont développées en utilisant des outils de géométrie stochastique. Nous intégrons ces expressions avec le modèle de seuil utilisateur et proposons une méthode de calcul analytique. Nous présentons également un modèle de consommation d'énergie pour le MBMS. Nous développons des expressions analytiques pour calculer la consommation d'énergie des stations de base (BS) et des équipements utilisateur (UE) lors de la réception en unicast, MBSFN et SC-PTM. À l'aide de ces expressions, nous calculons le seuil utilisateur pour passer de l'unicast à la diffusion (BC) afin de réduire la consommation d'énergie.

En mode de transmission MBSFN, le schéma de modulation et de codage (MCS), et donc le débit de données, sont fixes. Les valeurs sont basées sur les utilisateurs du groupe de diffusion ayant le SINR le plus faible et l'objectif de couverture. Par conséquent, il est important de trouver une expression permettant de calculer la probabilité de couverture en mode MBSFN pour un UE situé n'importe où dans la zone MBSFN. Cela permet d'étendre l'analyse des performances, notamment pour prendre en compte le cas d'un utilisateur à la frontière de la zone MBSFN.

Nous considérons que la zone MBSFN est formée par les stations de base situées à une distance $r \leq R_{\mathrm{s}}$ de l'origine. L'UE peut être situé à une distance ξR_{s} de l'origine, telle que $0 \leq \xi \leq 1$, comme illustré dans la Figure 6. L'expression analytique permettant de calculer la distribution du SINR en mode MBSFN est obtenu à partir de ce modèle.

Le seuil utilisateur pour passer du mode unicast au mode MBSFN en fonction de ξ est présenté dans la Figure 7. Ces résultats ont été obtenus avec les expressions analytiques développées dans la thèse. Nous considérons deux valeurs de densité de stations de base, $\lambda_{\mathrm{BS}} = 4$ BS/km^2 et $\lambda_{\mathrm{BS}} = 12$ BS/km^2. La première observation est que, pour une même valeur de R_{s}, le seuil utilisateur est plus bas pour une densité de stations de base plus élevée. Cela est dû au fait que le SINR fourni par une transmission MBSFN augmente avec une densité de stations de base plus élevée. En revanche, la probabilité de couverture en unicast ne dépend pas de la densité des stations de base. Par conséquent, pour l'ensemble des paramètres considérés dans cette étude, la valeur du seuil utilisateur dépend de la configuration du réseau MBSFN. Nous observons que la valeur du seuil utilisateur reste

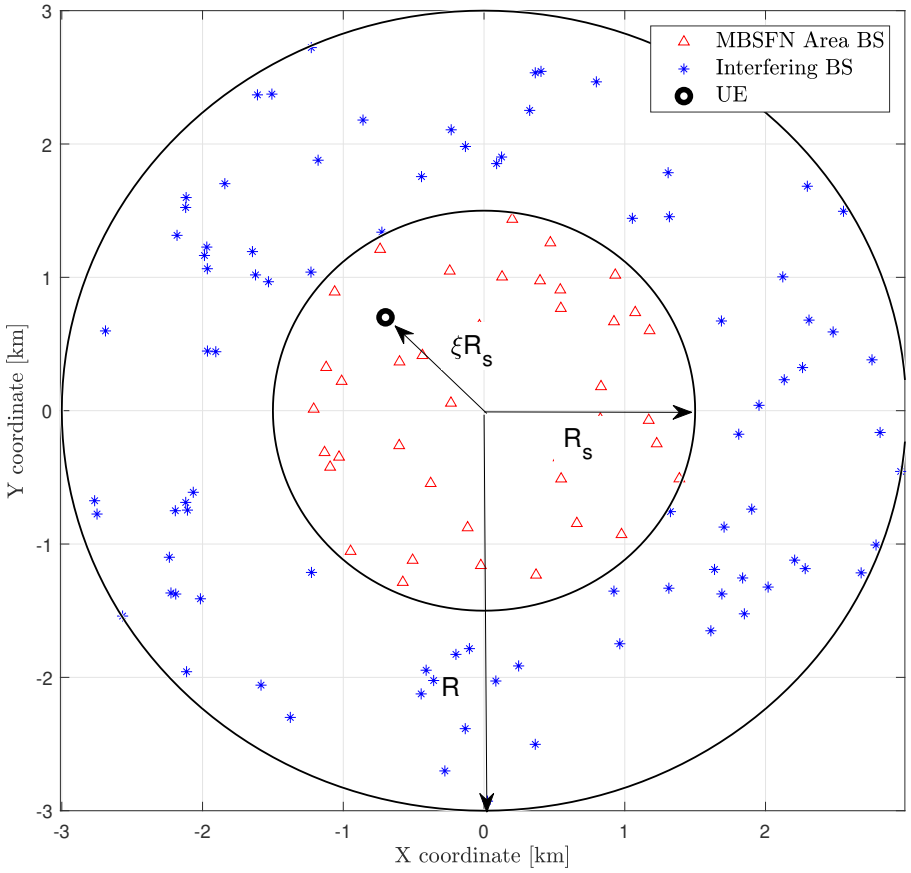

FIGURE 6 – Modèle étendu pour la distribution du SINR en mode MBSFN.

presque constante pour $R_s = 2.5$ km dans l'intervalle $0 < \xi < 0.5$, en particulier pour la densité de stations de base plus élevée. Une zone MBSFN plus grande n'améliorerait pas radicalement les performances du MBSFN. En revanche, si l'on considère une petite zone MBSFN ou $\xi > 0.5$, le seuil utilisateur change radicalement.

La Figure 8 présente le rapport entre la consommation d'énergie des stations de base en mode unicast ($E_{\mathrm{BS_{UC}}}$) et en mode MBSFN ($E_{\mathrm{BS_{SFN}}}$). Nous considérons une zone MBSFN de 19,6 km^2 ($R_s = 2.5$ km) et une zone de service de 9,8 km^2 ($\xi = 0.7071$). Avec la transmission MBSFN, les stations de base consomment moins d'énergie qu'en mode unicast lorsque la densité d'utilisateurs est supérieure à 3.8 UE/km^2 pour $\lambda_{\mathrm{BS}} = 12$ BS/km^2. Pour des densités de stations de base plus faibles, jusqu'à 1,2 BS/km^2, la valeur de λ_{UE} qui rend $\frac{E_{\mathrm{BS_{UC}}}}{E_{\mathrm{BS_{SFN}}}} = 1$ diminue. Cependant, si $\lambda_{\mathrm{BS}} < 1.2$ BS/km^2, il est nécessaire d'avoir plus

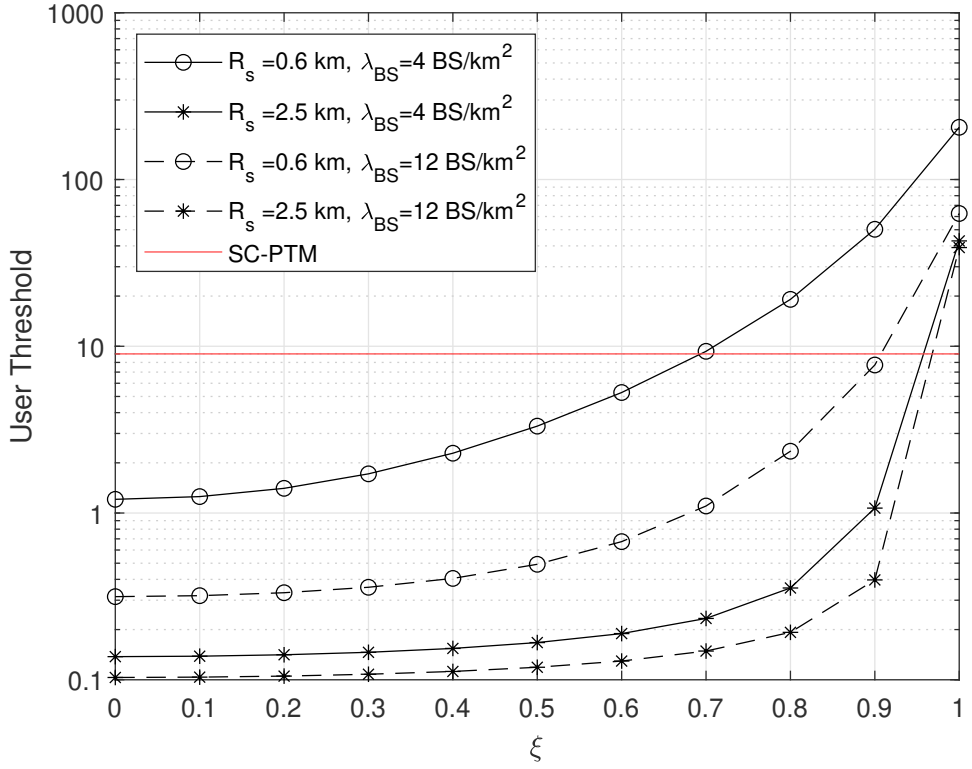

FIGURE 7 – Seuil utilisateur pour passer du mode unicast au mode MBSFN en fonction de ξ, en tenant compte de différentes valeurs de R_{s} et λ_{BS}.

d'utilisateurs pour que le MBSFN soit plus efficace. Dans ce scénario, $\lambda_{\mathrm{BS}} = 1.2$ BS/km^2 minimise la consommation d'énergie des stations de base en mode MBSFN pour toutes les densités d'utilisateurs. De plus, on observe que le rapport d'énergie des stations de base augmente avec la densité d'utilisateurs, par exemple, avec $\lambda_{\mathrm{BS}} = 4$ BS/km^2 et $\lambda_{\mathrm{UE}} = 10$ UE/km^2, les stations de base consomment 5 fois plus d'énergie en mode unicast qu'en mode MBSFN.

Comparaison de MBSFN, SC-PTM et Unicast pour les communications critiques de mission

Les services de communications critiques de mission (MCC) sont actuellement fournis via des réseaux dédiés de radiocommunication professionnelle mobile (PMR) sécurisés et fiables. Ces services comprennent la voix, la transmission de données et la diffusion de

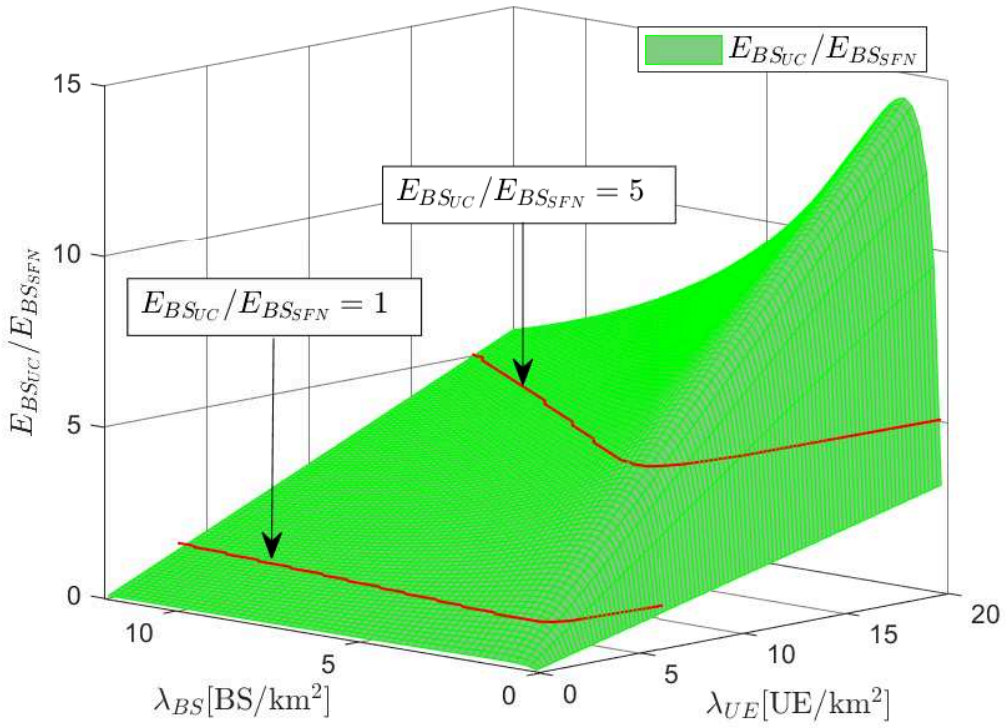

FIGURE 8 – Rapport entre la consommation d'énergie des stations de base en mode unicast et en mode MBSFN pour différentes valeurs de λ_{BS} et λ_{UE}, en considérant $R_{\mathrm{s}} = 2.5$ km et $\xi = 0.7071$ km.

vidéos. En cas d'urgence, un accès rapide au streaming vidéo peut améliorer la perception de la situation et faciliter les opérations de sauvetage. Ainsi, afin d'améliorer les capacités des réseaux PMR et de bénéficier des avantages de la mutualisation, des technologies cellulaires standard basées sur les réseaux cellulaires de quatrième génération (4G) et de cinquième génération (5G) ont été adoptées pour les MCC. En particulier, le service de diffusion multimédia multicast (MBMS) est adapté à la transmission de services de communication de groupe. Dans ce chapitre, nous comparons le mode MBSFN, le mode Single-Cell Point-to-Multipoint SC-PTM et le mode Unicast dans des scénarios critiques de mission du point de vue de l'utilisation des ressources radio.

Conclusions

Dans cette thèse, nous fournissons tout d'abord une comparaison entre unicast et MBSFN. Nous considérons des stations de base équipées d'antennes tri-sectorielles réparties selon une distribution de Poisson. Nous avons montré que lorsqu'une zone MBSFN couvre une très grande surface, la diffusion MBSFN surpasse la transmission unicast en termes de SINR, même si l'unicast utilise la formation de faisceau avec jusqu'à huit antennes par secteur. À l'inverse, si la zone MBSFN comporte un nombre limité de cellules, le SINR est plus faible. Le scénario le plus difficile pour le MBSFN est une zone MBSFN de seulement deux stations de base par rapport à une diffusion unique utilisant la formation de faisceaux avec huit antennes par secteur. Dans ce cas, le seuil d'utilisateurs à partir duquel le MBSFN devient plus efficace que l'unicast est de huit équipements utilisateurs (UE) par cellule.

Nous cherchons ensuite à fournir un moyen plus rapide de calculer le seuil de rentabilité de MBSFN, compte tenu de la dynamique de la localisation des utilisateurs. Nous avons développé une équation permettant de calculer la distribution du SINR pour un UE situé à n'importe quel endroit de la zone MBSFN. En utilisant cette équation et la formule pour la probabilité de couverture en monodiffusion, nous proposons une méthode analytique pour calculer le seuil de rentabilité en nombre d'utilisateurs pour passer de l'unicast à MBSFN ou SC-PTM. Le paramètre clé de cette méthode est l'emplacement de l'utilisateur le plus proche de la limite de la zone MBSFN. Si ce paramètre est mis à jour en temps réel, la valeur du seuil de l'utilisateur peut être ajustée dynamiquement.

Ensuite, nous avons développé un modèle analytique pour calculer la consommation d'énergie de l'UE et de la station de base (BS) lors de l'utilisation de MBSFN et SC-PTM en nous basant sur les modèles de monodiffusion de la littérature. De plus, nous avons développé des équations pour calculer le seuil d'utilisateur à partir duquel MBSFN et SC-PTM réduisent la consommation d'énergie de l'UE ou de la BS par rapport à l'unicast. Nous avons prouvé que le seuil en nombre d'utilisateurs pour réduire la consommation d'énergie de la station de base est le même que le seuil pour réduire l'utilisation des ressources radio, à la fois en mode SC-PTM et MBSFN. Nous avons également prouvé que le seuil de l'utilisateur pour réduire la consommation d'énergie de l'UE est inférieur au seuil de l'utilisateur pour réduire la consommation d'énergie de la station de base, en particulier pour le MBSFN.

L'un des cas d'utilisation les plus importants des MBMS est la communication de groupe

dans des scénarios de mission critique (MC). Nous considérons un modèle dans lequel les cellules dans la zone MBSFN peuvent décider de ne pas participer à la transmission MBSFN si elles ne comptent aucun UE intéressé par le flux diffusé. De plus, nous considérons le cas où les utilisateurs MC sont en veille sur des cellules en dehors de la zone MBSFN et doivent décider de rester en unicast ou de passer en veuille sur une cellule MBSFN. Les UE sont localisés suivant une distribution de Poisson, ainsi que la BS. Nos résultats montrent que pour augmenter le SINR dans la zone MBSFN lorsque la densité d'UE est élevée, il faut augmenter la densité de BS. Inversement, si la densité d'UE est faible, un SINR plus élevé est obtenu en réduisant la densité de BS. D'autre part, le rapport SINR dans le système SC-PTM diminue avec la densité d'UE et augmente avec la densité de BS. En outre, les résultats en termes de efficacité spectrale et de seuil d'utilisateur ont montré que le paramètre dominant est la densité d'UE. Si la densité d'UE est élevée, MBSFN est plus efficace que SC-PTM. Au contraire, le SC-PTM est plus efficace que le MBSFN pour les faibles densités d'UE.

PUBLICATIONS

Publications in peer-reviewed international conferences:

[1] P. Angot, V. Lepec, A. Nochimowski, P. Gonon, C. Thienot, and **Vargas-Rubio, J.C.** « Taking Steps Towards Greener Streaming ». In: *IBC 2022 International Broadcasting Convention 2022*. Amsterdam, Netherlands, Sept. 12, 2022.

[2] **Vargas, Juan**, Cedric Thienot, and Xavier Lagrange. « Analytical Calculation of the User Threshold for the Switching between Unicast and Broadcast in Cellular Networks ». In: *NOMS 2022 IEEE/IFIP Network Operations and Management Symposium*. Budapest, Hungary, Apr. 25, 2022, pp. 1–6.

[3] **Vargas, Juan**, Cedric Thienot, and Xavier Lagrange. « MBSFN and SC-PTM as Solutions to Reduce Energy Consumption in Cellular Networks ». In: *ISCC 2022 IEEE Symposium on Computers and Communications*. Rhodes Island, Greece, June 30, 2022.

[4] **Vargas, Juan**, Cédric Thienot, Christophe Burdinat, and Xavier Lagrange. « Broadcast-Multicast Single Frequency Network versus Unicast in Cellular Systems ». In: *WiMob 2020 16th International Conference on Wireless and Mobile Computing, Networking and Communications*. Oct. 2020.

[5] **Vargas, Juan**, Cédric Thienot, and Xavier Lagrange. « Comparison of MBSFN, SC-PTM and Unicast for Mission Critical Communication ». In: *WPMC 2021 24th International Symposium on Wireless Personal Multimedia Communications*. Dec. 2021.

Table of Contents

List of Figures

List of Tables

Acronyms

3G	Third-Generation cellular networks
3GPP	Third Generation Partnership Project
4G	Fourth-Generation cellular networks
5G	Fifth-Generation cellular networks
5GMS	5G Media Streaming
5G MBS	5G Multicast Broadcast Services
ADPD	Associated Delivery Procedure Description
AF	Application Function
AMF	Access and Mobility Management Function
APCO	Association of Public-Safety Communications Officials
API	Application Programming Interface
APP	Application
ARQ	Automatic Repeat Request
AS	Application Server
BB	Baseband
BC	Broadcast
BM-SC	Broadcast-Multicast Service-Center
BPM	Broadcast Provisioning Manager
BS	Base Station
CCDF	Complementary Cumulative Distribution Function
CDD	Cyclic Delay Diversity
CDN	Content Delivery Network
CDF	Cumulative Distribution Function
CIFRE	Convention Industrielle de Formation par la Recherche
CP	Cyclic Prefix
CSA	Common Subframe Allocation
CSI	Channel State Information

D2D	Device-to-Device
DASH	Dynamic Adaptive Streaming over HTTP
dB	decibel
DHCP	Dynamic Host Configuration Protocol
DL	Downlink
DLSCH	Downlink Shared Channel
DU	Distributed Unit
eMBB	enhanced Mobile Broadband
eMBMS	evolved MBMS
EHF	Extremely High Frequency
EPC	Evolved Packet Core
FeMBMS	Further evolved MBMS
HARQ	Hybrid Automatic Repeat Request
HTTP	Hypertext Transfer Protocol
HLS	HTTP Live Streaming
ISD	Inter-Side Distance
LTE	Long Term Evolution
MAC	Medium Access Control
MBMS	Multimedia Broadcast Multicast Service
MBS	Multicast Broadcast Service
MB-SMF	Multicast-Broadcast Session-Management-Function
MBSF	Multicast Broadcast Service Function
MBSFN	Multicast-Broadcast Single-Frequency-Network
MBSTF	Multicast Broadcast Service Transport Function
MB-UPF	Multicast-Broadcast User-Plane-Function
MC	Mission Critical
MCC	Mission Critical Communications
MCCH	Multicast Control Channel
MCE	Multi-cell/Multicast Coordination Entity
MCH	Multicast Channel
MCPTT	Mission Critical Push-to-Talk

MCS	Modulation and Coding Scheme
MIMO	Multiple-Input Multiple-Output
MooD	MBMS operation on Demand
MPD	Media Presentation Description
MSA	MCH Subframe Allocation
MSH	Media Session Handler
MSI	MCH Scheduling Information
MSP	MCH Scheduling Period
MTCH	Multicast Traffic Channel
MW	Middleware
NEF	Network Exposure Function
NF	Network Functions
NFV	Network Functions Virtualization
NG-RAN	Next-Generation RAN
NR	New Radio
OFDM	Orthogonal Frequency-Division Multiplexing
OTT	Over-The-Top
P25	Project 25
PCF	Policy Control Function
PDF	Probability Density Function
PDCCH	Physical Downlink Control Channel
PDU	Protocol Data Unit
PDSCH	Physical Downlink Shared Channel
PGW	Packet Data Network Gateway
PMCH	Physical Multicast Channel
PMR	Professional Mobile Radio
PPP	Poisson Point Process
PSS	Packet-switched Streaming Service
PTM	Point-to-Multipoint
PTP	Point-to-Point
QoS	Quality of Service

RAN	Radio Access Network
RF	Radio Frequency
RRC	Radio Resource Configuration
RV	Random Variable
SAI	Service Area Identifier
SC	Single-Cell
SC-PTM	Single-Cell Point-to-Multipoint
SE	Spectral Efficiency
SFN	Single Frequency Network
SIB	System Information Block
SINR	Signal to Interference-plus-Noise Ratio
SIR	Signal to Interference Ratio
SMF	Session Management Function
SNR	Signal to Noise Ratio
SSE	System Spectral Efficiency
TB	Transport Block
TCCA	Tetra and Critical Communication Association
TETRA	Terrestrial Trunked Radio
TETRAPOL	Terrestrial Trunked Radio Police
TM	Transmission Mode
TRX	transceiver
TTI	Transmission Time Interval
UC	Unicast
UE	User Equipment
UHF	Ultra High Frequency
UHD	Ultra High Definition
UPF	User Plane Function
URI	Uniform Resource Identifier
URLLC	Ultra-Reliable Low-Latency Communication
USD	User Service Description

Chapter 1

Introduction

1.1 Context of the Thesis Work

Video is an important factor of the load in cellular networks due to the growing popularity of streaming and linear services. In 2022, video traffic is estimated to account for 69 percent of mobile data traffic and expected to increase to 79 percent in 2027 with the adoption of virtual/augmented reality technologies [23]. This is more impressive considering that mobile network data traffic grew 40 percent between the first quarter (Q1) of 2021 and Q1 2022 and the tendency is expected to continue in the years to come [23]. Additionally, the number of mobile devices capable of displaying bandwidth-hungry services such as Ultra High Definition (UHD) video and 360-degree video is expected to increase [42]. This disruptive services will be supported by Fourth-Generation cellular networks (4G) and Fifth-Generation cellular networks (5G). In fact, 5G's share of mobile data traffic is forecast to be 60 percent in 2027 versus 10 percent in 2021 [23].

This ever increasing demand for high quality multimedia content in cellular networks requires the implementation of techniques for efficient radio resource management since spectrum is limited and expensive. In order to provide a good quality of service, operators are searching for alternatives to reduce the radio resource utilization when several users are demanding the same video content on a given geographical area. Broadcast transmission is the preferred solution for scenarios in which the same content is transmitted to many users at the same time. When a video is very popular, contents could be pushed via broadcast transmission and then stored in the cache of the receiver, even prior to user demand [24]. Thus, offloading the network and maintaining good service quality. Some use cases are mobile TV and video streaming of popular events.

In emergency situations, first responders communicate in a timely and reliable manner, this is called Mission Critical Communications (MCC). MCC depend on secure and reliable Professional Mobile Radio (PMR) networks. PMR networks used to work using specific waveforms and multiplexing methods different from commercial cellular technologies.

However, nowadays PMR networks work on LTE bands and are expected to work with 5G. In particular, the solution for broadcast transmission in LTE, MBMS, is the preferred technology for the transmission of group communication services. Group communications are intended to distribute the same content to multiple users at the same time in a controlled manner. During an emergency, rescue and security teams use group communications for coordination of actions. Thus, group communications are key to ensure efficient operations.

This thesis takes place in the framework of an Industrial Agreement for Training Through Research (Convention Industrielle de Formation par la Recherche (CIFRE)). A CIFRE agreement is partially financed by the french ministry of higher education and research and involves a higher education institution, a company and the PhD candidate. For this thesis, IMT Atlantique [14] and Enensys Technologies [49] formed the CIFRE agreement. Enensys is based in Rennes, France. The company has solutions to optimize, secure and monetize the entire media chain, on all types of broadcast networks: satellite, terrestrial, broadband and mobile. Since its creation in 2004, the group realizes from 80 to 90 percent of its revenues in export. It is a company driven by innovation, Enensys has a portfolio of 60 international patents. Enensys has an end-to-end solution for broadcast over 4G and 5G networks. It includes a server (MediaCast Mobile) in charge of LTE Broadcast provisioning and a middleware (CubeAgent Mobile) to manage broadcast content reception in the end device. It is an advanced MBMS solution on the market, with very large MBMS commercial deployments.

1.2 Contribution of the Thesis Work

The most common transmission technique in cellular networks is unicast transmission. The base station makes an independent transmission for each user. This enables the use of link adaptation techniques that adjust the bitrate according to the channel quality of each UE. The better the channel quality, the higher the bitrate. However, the same data is transmitted as many times as the number of users demanding the same service.

On the other hand, with the broadcast transmission technique, the base station or group of base stations make a single transmission to a potentially infinite number of users located in the same geographical area. The bitrate is the same for all the UE and it is determined based on the users with the worst channel quality among the UE interested in the same content.

There exist two different broadcast techniques. In the first one, a group of cells are

synchronized and transmit the same waveform at the same time. It is called MBSFN. The second one consist on broadcast transmission in one cell, SC-PTM. There exist many commonalities between unicast and SC-PTM, the same data and control channels are used, neighboring cells generate interference and the length of the guard interval used to reduce inter-symbol interference (Cyclic Prefix (CP)) is the same. Conversely, MBSFN uses its own data and control channels, occupies the entire bandwidth in the subframes allocated for broadcast transmission, uses a longer CP to enable larger Inter-Side Distance (ISD) between the cells in the MBSFN area and reduces interference specially at cell borders because neighboring cells provide useful signal power.

There exist a standardized method to enable the switching between unicast and broadcast called MBMS operation on Demand (MooD). This method is based on the consumption report procedure in which the UE signal their interest in the content. However, there is not an standardized method to determine the number of users from which broadcast transmission outperforms unicast. This user threshold is usually fixed manually by the network operator. The problem is that the exact value of the user threshold depends on may system parameters. Some of them are fixed during deployment as the ISD, the size of the MBSFN area or the antenna configuration. Other parameters change constantly, particularly, the users location. Therefore, the value of user threshold is different depending on the scenario and it may change in real time according to the users location.

In this thesis we compare the performance of unicast, SC-PTM and MBSFN in different scenarios in terms of SINR, spectral efficiency and energy consumption. We consider deployments with base stations located according to a PPP. This enables the use of stochastic geometry theorems and results for wireless networks available in the literature. The contributions of our thesis work can be accounted as:

— We compare the performance in terms of SINR of Unicast and Multicast Broadcast Single Frequency Network (MBSFN) transmission techniques through system level simulations. We consider beamforming for unicast and different MBSFN area configurations. Notably a large MBSFN area (nation wide) and MBSFN areas with a limited number of base stations. The propagation model and antenna model are taken from literature.

— We propose a model to calculate the number of users per cell in the MBSFN area, called User Threshold, to switch from unicast to MBSFN in order to reduce radio resource utilization. The model considers the probability distribution of the SINR

when using unicast and MBSFN. The SINR distribution depends on the number of antennas used for beamforming, the number of BS in the MBSFN area, the base station density (average number of base stations per square kilometer), among other system parameters.

— We propose a method to calculate analytically the user threshold to reduce radio resource utilization. We calculate the user threshold to switch from unicast to MBSFN and the user threshold to switch from unicast to SC-PTM. The method is based on an equation to calculate the SINR distribution for a user located at any point inside an MBSFN area.

— We adapt power consumption models for unicast from the literature to compare the energy consumption in MBSFN, SC-PTM and unicast. We analyze separately the UE side and the BS side. Furthermore, we propose an analytical model to calculate the user threshold to switch from unicast to MBSFN or SC-PTM in order to reduce UE and Base Station energy consumption.

— We performed system level simulations to identify the Mission Critical Scenarios in which broadcast transmission (MBSFN and SC-PTM) are more efficient than unicast from a resource utilization perspective.

1.3 Organization of the Thesis Report

The thesis report is organized into six chapters, which include:

— In Chapter 2 we present a synopsis of the characteristic of broadcast transmission in cellular networks. We summarize the standardization efforts done by the Third Generation Partnership Project (3GPP) for MBMS up to Release 17. We describe each broadcast transmission technique (MBSFN and SC-PTM) highlighting their differences and commonalities. We also describe the the standardized mechanism for the switching between unicast and broadcast, MBMS operation on Demand (MooD).

— In Chapter 3 we compare unicast and MBSFN in terms of radio resource utilization. We use Monte Carlo simulations to calculate the SINR distribution for users receiving in unicast and MBSFN under different system configurations. Particularly, we consider the use of the beamforming technique in unicast mode and MBSFN areas

with different sizes. Then, we propose a model to calculate the user threshold for the switching between unicast and MBSFN.

— In Chapter 4 we developed an extension for the equation to calculate the SINR distribution of a user located in the center of an MBSFN area. This extension enables the calculation of the SINR distribution of a user located at any place inside the MBSFN area, particularly the borders. We also propose energy consumption models for SC-PTM and MBSFN based on unicast models from the literature. The energy consumption is analyzed separately for the UE and the Base Stations. Then, we use the equation to propose an analytical method, aided by numerical calculations, to obtain the user threshold to switch from unicast to MBSFN or from unicast to SC-PTM in order to reduce radio resource utilization and energy consumption.

— In Chapter 5 we compare unicast, MBSFN and SC-PTM in terms of SINR and Spectral Efficiency, when used for group communication in Mission Critical Scenarios. In Mission Critical scenarios we have more exigent coverage requirements and we aim to cover a surface with a fixed size called the mission critical area. We use Monte Carlo simulations with Base Stations and UE following PPP distributions. We define the user threshold as the number of users per square kilometer from which broadcast modes become more efficient than unicast.

— In Chapter 6 we present the conclusion of this thesis work. We summarize the contributions of each part of this work, propose our conclusive remarks and identify the prospective work directions.

Chapter 2

Technical Review of Broadcast Transmission in Cellular Networks

This chapter presents an overview of the technical aspects of broadcast transmission in cellular networks. The objective is to describe what has been done in terms of technological advancements and standardisation efforts to enable broadcast transmission in 4G LTE and 5G. The 3GPP has worked on the specifications for MBMS since Release 9 in 2009. Since then, several enhancements have been provided for MBMS implementation in LTE in Releases 10-14 and 5G in Releases 16-17. We make a review of these specifications and highlight which are the open issues that are addressed in our work.

In Section 2.1 and Section 2.2 we describe the propagation models and antenna models considered in our work for the simulation of unicast and broadcast networks. Then, in Section 2.3 we present an overview of the standardisation efforts done by the 3GPP for broadcast transmission in cellular networks called MBMS. MBMS can use two broadcast transmission techniques, MBSFN and SC-PTM. Afterwards, we explain how MBSFN and SC-PTM work in LTE systems in Section 2.4 and Section 2.5 respectively. Additionally, in Section 2.6 we describe how the mechanism to switch from unicast to MBMS, MooD, works. An important part of the chapter, Section 2.7, is dedicated to the specifications for media distribution in 5G. Particularly, we describe the architectures proposed for 5G Media Streaming (5GMS), LTE-based 5G Broadcast and 5G Multicast Broadcast Services (5G MBS). Finally, in Section 2.8 we summarize this review and highlight the commonalities between broadcast transmission in 4G and 5G.

2.1 Propagation Model

Our analysis is based on the reference model proposed by the 3GPP in [3]. The propagation model is based on Okumura-Hata-Cost231 with shadowing and fading.

2.1.1 Path Loss

Path loss refers to the attenuation of an electromagnetic wave as it propagates through space. Considering the Macro cell propagation model in Urban area, the path loss in dB can be calculated as [3]

$$P_{\mathrm{L}} = 40(1 - 4 \times 10^{-3} h_{\mathrm{BS}}) \log_{10} r - 18 \log_{10} h_{\mathrm{BS}} + 21 \log_{10} f_{\mathrm{c}} + 80, \tag{2.1}$$

where

— f_{c} is the carrier frequency in MHz

— r is the distance between UE and BS in kilometers.

— h_{BS} is the base station antenna height in metres, measured from the average rooftop level.

Considering h_{BS} of 15 metres, the path loss is given by

$$P_{\mathrm{L_{dB}}} = 58.83 + 37.6 \log_{10}(r) + 21 \log_{10}(f_{\mathrm{c}}). \tag{2.2}$$

Furthermore, when considering f_{c} in GHz

$$P_{\mathrm{L_{dB}}} = 121.78 + 37.6 \log_{10}(r) + 21 \log_{10}(f_{\mathrm{c}}). \tag{2.3}$$

For simplicity, we express the path loss in linear scale. We rewrite (2.3) as a function of the path loss exponent, α, and the path loss factor, k, considering the distance r in meters, such that

$$P_{\mathrm{L}} = 10^{\frac{P_{\mathrm{L_{dB}}}}{10}} = \frac{r^{\alpha}}{k}, \tag{2.4}$$

where

$$\alpha = 3.76 \tag{2.5}$$

$$k = 0.1265 \times {f_c}^{-2.1} \tag{2.6}$$

Considering this model, the received signal power P_{rx} for a user located at a distance r from the BS is calculated as

$$P_{\text{rx}} = P_{\text{tx}} k r^{-\alpha}, \tag{2.7}$$

where P_{tx} is the base station transmission power.

2.1.2 Fading

Fading refers to the attenuation of a signal due to multipath propagation. We model fading as an exponential random variable, h, with average $\mu = 1$ as in [11]. Therefore, the received signal power considering path loss and fading is calculated as

$$P_{\text{rx}} = P_{\text{tx}} k r^{-\alpha} h, \tag{2.8}$$

where $h \sim exp(1)$.

2.1.3 Shadowing

Shadowing is the effect of received signal power fluctuations due to obstructions (buildings, mountains, etc.) between the transmitter and receiver. Shadowing is usually modeled as a Log-Normal random variable $y = \exp(\chi)$, where χ follows a Normal distribution $\chi \sim N(0, {\sigma_\chi}^2)$. This variable is expressed in linear scale but shadowing is usually characterized in terms of the standard deviation of y_{dB}

$$y_{\text{dB}} = 10 \log_{10}(\exp(\chi)) = \frac{10}{\ln 10}\chi, \tag{2.9}$$

therefore, $\sigma_{\text{y}_{\text{dB}}} = \frac{10}{\ln 10}\sigma_\chi$.

To take into account that obstacles close to the receiver are common obstacles for all BS, we consider a correlation between the shadowing for the same receiver and different BS [34]. Then, the Log-Normal variable is composed of two independent coefficients

$$\exp(\chi) = \exp(\chi_{\text{c}}) \exp(\chi_i), \tag{2.10}$$

where $\exp(\chi_c)$ represents the part of shadowing common to all BSs for a certain receiver and $\exp(\chi_i)$ is different for each BS, see Figure 2.1. Both follow independent Log-Normal laws.

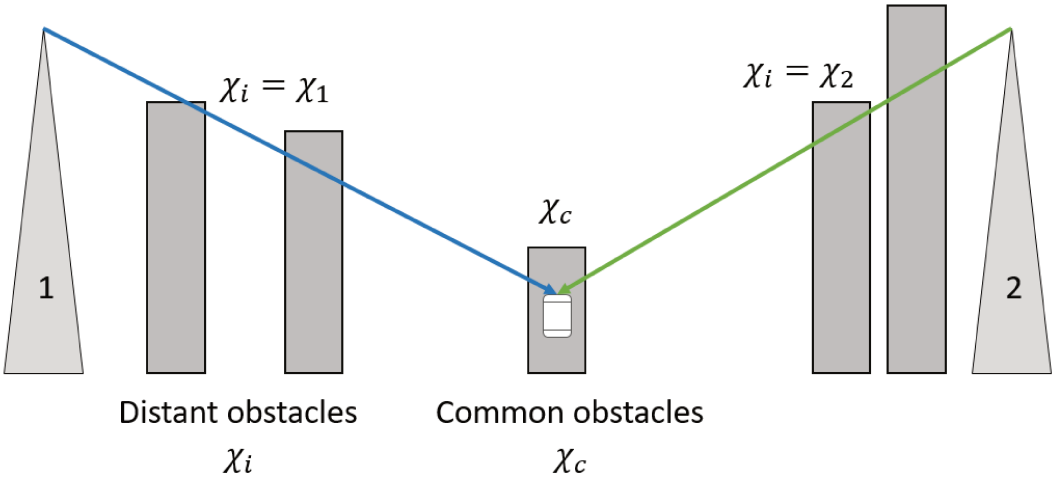

Figure 2.1 – Shadowing due to objects distant and close from the UE.

This means that $\chi = \chi_c + \chi_i$ and ${\sigma_\chi}^2 = {\sigma_{\chi_c}}^2 + {\sigma_{\chi_i}}^2$. The correlation coefficient ρ is given by

$$\rho = \frac{{\sigma_{\chi_c}}^2}{{\sigma_\chi}^2}. \tag{2.11}$$

Finally, the received signal power considering path loss, fading and shadowing is calculated as

$$P_{rx} = P_{tx} k r^{-\alpha} h \exp(\chi_c) \exp(\chi_i). \tag{2.12}$$

2.1.4 Noise

The noise power (P_N) is the aggregation of the thermal noise spectral density for the given occupied bandwidth (W) and the receiver noise figure (γ) and its value in dB is calculated as

$$P_{NdB} = \gamma + 10 \log_{10}(k_B T_k W), \tag{2.13}$$

where k_B is the Boltzmann's constant and $T_k = 300$ K is the receiver system temperature.

The signal received by a UE is weak and noisy and is amplified. The power amplifier in the receive chain amplifies the signal and inevitably the noise. Additionally, the amplifier itself adds noise. The noise figure, γ, is given by

$$\gamma = 10 \log_{10}(F), \tag{2.14}$$

where F is the noise factor. It is the ratio of the Signal to Noise Ratio (SNR) at the input of the amplifier and the SNR at the output, such that

$$F = \frac{SNR_i}{SNR_o}. \tag{2.15}$$

The lower the noise figure, the lower the noise added by the amplifier.

2.2 Base Station Antenna Model

This section provides the models we use for the antennas at the base stations. This work considers omnidirectional antennas, tri-sector antennas and directive antennas using beamforming.

2.2.1 Omnidirectional Antennas

Omnidirectional antennas radiate equal power in all directions in a plane. The three dimensional radiation patter of an omnidirectional antenna is doughnut-shaped. We denote the gain of the antenna as g.

2.2.2 Tri-sector Antennas

Telecommunication operators use Tri-sector Antennas to deploy three cells using only one base station site. Furthermore, since the antenna in each sector radiates in a certain direction, interference is reduced with respect to omnidirectional antennas.

In this work, we consider that each sector has a 120°-width. The antenna pattern in decibel (dB) for each sector in the direction θ measured from the antenna boresight, can be calculated as stated in [3]

$$G_{\mathrm{dB}}(\theta) = G_{\mathrm{A}} - \min\left\{12\left(\frac{\theta}{\theta_{3\mathrm{dB}}}\right)^2, G_{\mathrm{FB}}\right\}, \tag{2.16}$$

where G_{A} is the antenna gain in the boresight direction in dB, $\theta_{3\mathrm{dB}}$ is the 3 dB beam width, G_{FB} is the antenna front to back ratio and $-180° \leq \theta \leq 180°$. In this study it is assumed that the antenna boresight angles for the three sectors are 30°, 150° and 270° counterclockwise for all BSs. We represent the magnitude of the electromagnetic field, $\sqrt{G(\theta)}$, of a tri-sector antenna in Figure 2.2

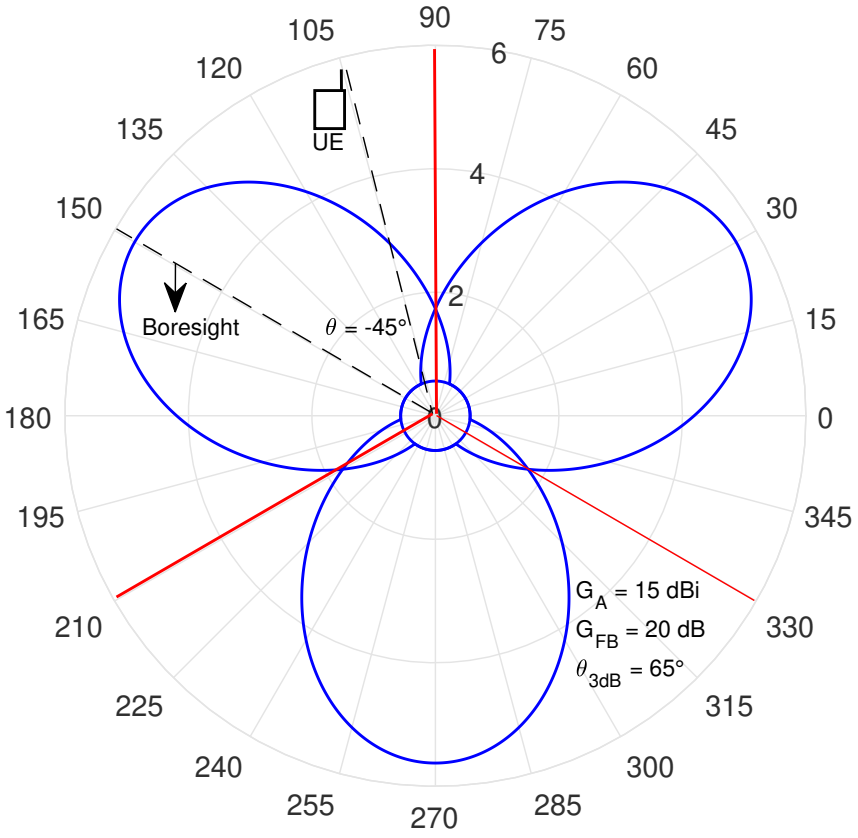

Figure 2.2 – Radiation pattern of tri-sector antenna

2.2.3 Beamforming

Beamforming is a technology in which several antennas work together to create a beam pointed in a specific direction. Beamforming increases the power radiated in a specific direction and reduces the power radiated in other directions. We consider tri-sectored BSs in which each sector has a linear array of M antennas capable of performing beamforming. The transmission power is divided among the M antennas. For each antenna the transmission power is $\frac{P_{Tx}}{M}$. In each sector, the array is placed on the axis perpendicular to the boresight. The direction towards which the beam is pointed is characterized by

the steering angle, ϕ, which is measured from the antenna boresight, see Figure 2.3. The expression to calculate the array pattern for one sector in the direction θ can be derived from [33, 38, 51] as

$$A(\theta,\phi) = \begin{cases} \frac{\sin^2(M\frac{\pi}{2}(\sin(\phi)-\sin(\theta)))}{M\sin^2(\frac{\pi}{2}(\sin(\phi)-\sin(\theta)))}G(\theta) & \theta \neq \phi \\ MG(\theta) & \theta = \phi \end{cases}, \tag{2.17}$$

where $G(\theta)$ is the radiation pattern of each elementary antenna (2.16) and $-60° \leq \phi \leq 60°$.

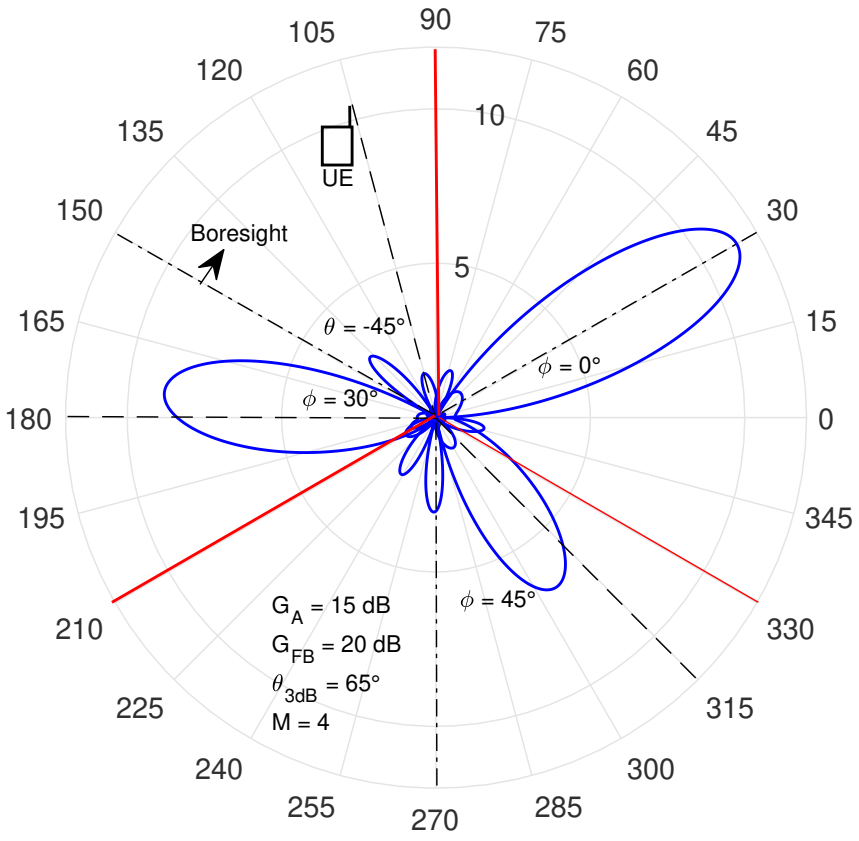

Figure 2.3 – Radiation pattern of tri-sectored BS capable of performing beamforming

We represent the array gain for three sectors in Figure 2.3. In each sector the beam is steered in a different direction. Notice that the maximum gain is obtained when $\phi = 0$, i.e. when the beam is steered in the boresight direction. Observe as well that when $\phi \neq 0$ the highest gain is obtained in a direction different from the steering direction, e.g., when $\phi = 30°$ the highest gain is obtained in $\theta \approx 25°$. This is because each antenna is not omnidirectional.

2.3 Overview of Broadcast transmission in Cellular Networks

The Third Generation Partnership Project (3GPP) developed a Point-to-Multipoint (PTM) interface specification for cellular networks called MBMS. In the radio interface MBMS can use two different transmission techniques: MBSFN or SC-PTM. In MBSFN multiple cells transmit the same signal, same waveform, synchronously to the interested users while SC-PTM refers to broadcast transmission in one cell. MBSFN and SC-PTM transmission are aimed to cover the users with the worst channel conditions in the broadcast area, i.e. users with lowest SINR. More detail about MBSFN and SC-PTM is given in Section 2.4 and Section 2.5 respectively.

2.3.1 MBMS Standardization

The 3GPP has standardized BC solutions since Release 6 with the MBMS interface specification for 3G. It was conceived as a pre-planned and static mobile TV service based on SFN transmission [28]. MBMS was not significantly enhanced in Release 7, and Release 8 focuses on the requirements for the new 4G LTE technology. In Release 9, eMBMS appears as the LTE version of MBMS. Radio resources are time multiplexed between UC and eMBMS allowing maximum 6 subframes per frame for eMBMS. Additionally, new physical, transport, and logic channels are defined together with three new logical entities in the core network architecture, see Subsection 2.3.2 for further detail.

Release 10 states that MBMS download delivery method, normally used for file transmission, should support the delivery of Dynamic Adaptive Streaming over HTTP (DASH) content. DASH is an adaptive bitrate streaming technique that enables high quality streaming of multimedia content delivered from Hypertext Transfer Protocol (HTTP) web servers. Furthermore, this release mentions a UE counting procedure in the Radio Access Network (RAN). Based on the number of interested UEs, the network can decide to enable or disable MBSFN transmission [53, Chapter 11]. Release 11 specifies mechanisms for MBSFN to provide service continuity in multi-frequency deployments [1]. In 2015, Release 12 introduced MooD which allows automatic MBMS activation and deactivation based on consumption reports. Consumption Reports are sent by the UEs directly to the Broadcast-Multicast Service-Center (BM-SC), i.e. they are transparent to the RAN. Consumption reporting replaced the RAN level UE counting procedure. Release 12 also

specifies eMBMS support for Group Communication in Mission Critical scenarios.

The option to perform BC transmission in only one cell was presented in Release 13 as SC-PTM [19, Chapter 19]. SC-PTM benefits from a flexible and dynamic radio resource allocation for BC transmissions, allowing BC and UC transmission in the same subframe and a reduced end-to-end latency. Later, Release 14 introduced Further evolved MBMS (FeMBMS). It includes a receive-only mode to allow devices without operator subscription to receive BC content. Other enhancements are a 100% carrier allocation for MBMS transmission and a 200 µs CP to support large inter-site distances [28]. The fifth generation of cellular networks (5G) arrives in Release 15 which mainly focuses in UC transmissions. Then, in Release 16, a further study item evaluates the ability of FeMBMS to support an SFN of cells with a coverage radius of up to 100 km (implying even longer CP) and mobile reception with speeds up to 250 km/h [27]. Finally, Release 17 is expected to include standalone BC enhancements, for instance, introducing the support of 6/7/8 MHz carrier bandwidths. Multicast operations for 5G with simultaneous/dynamic switching between BC and UC transmissions are also included [46].

We see that BC transmission in cellular networks has been a subject of interest in 3GPP for many years. However, there are still open issues specially concerning the radio resource utilization efficiency of BC transmissions. For instance, there is not an standardized method to calculate the number of users to switch from UC to MBMS.

2.3.2 MBMS Architecture in LTE

The 3GPP defined a PTM interface specification for cellular networks called MBMS. In the radio interface MBMS uses the MBSFN transmission technique. The MBMS architecture presented in Figure 2.4 was defined by the 3GPP in Release 9.

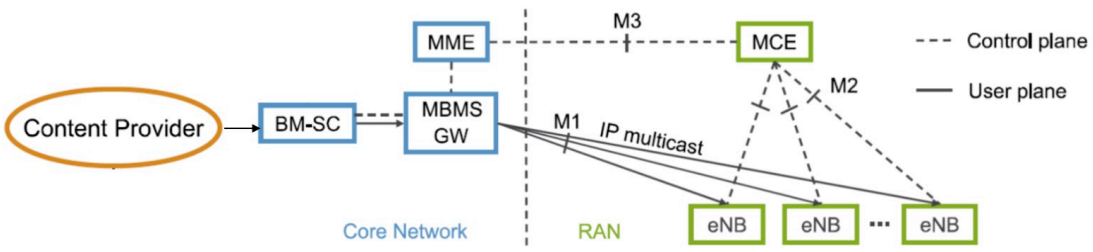

Figure 2.4 – LTE eMBMS Architecture [19]

Broadcast Multicast Service Center

The BM-SC, located in the core network, is the entry point for content and it is responsible for authentication/authorization of both the content provider and the user, charging the user, configuration of the overall data flow through the core network and application level coding. The data flow is ciphered by the BM-SC. Hence the flow is ciphered on the whole transmission chain, from the BM-SC till the UE.

Service announcement is one of the primary duties of BM-SC. The BM-SC generates a session start message when it is ready to send data. The message comprises the Quality of Service (QoS) parameters [13].

MBMS Gateway

The MBMS gateway is a logical node that distributes the MBMS data from the BM-SC to base stations using IP multicast. It has three major responsibilities: broadcasting the packets to all BS (more generally to the RAN), managing session start/stop and charging information collection for each terminal having an active session [13].

Multi-cell/Multicast Coordination Entity

The Multi-cell/Multicast Coordination Entity (MCE) is a logical node in the RAN responsible for the allocation of radio resources to multi-cell MBMS transmission using the MBSFN technique [28]. It takes decisions about establishing the radio bearer of a new MBMS Service as per the availability of radio resources. It also decides some radio details like the Modulation and Coding Scheme (MCS). There is no direct UE to MCE signaling but MCE is involved in the control signaling of an MBMS session. Each BS is served by a single MCE but an MCE can control one or more cells.

2.4 Multicast-Broadcast Single-Frequency-Network

MBSFN is a simulcast transmission technique consisting of multiple cells transmitting identical waveforms at the same time. The UE combine the arriving signals which are seen as a single transmissions suffering from multipath propagation, as in UC transmissions, see Figure 2.5.

MBSFN provides several benefits:

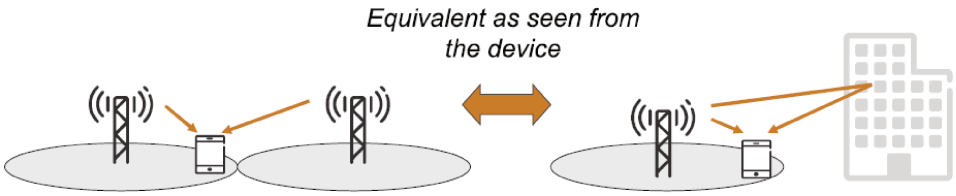

Figure 2.5 – Equivalence between simulcast transmission and multi-path propagation [19].

— Higher received signal power, especially at the border between cells involved in the MBSFN transmission

— Reduced interference power, especially at cell border, since neighboring cells provide useful signal power and not interference power as in unicast

— Diversity gain. Diversity schemes enable the combining of multiple signals to reduce the effect of excessively deep fades. Diversity schemes minimize the effect of fading since deep fades rarely occur simultaneously during the same time interval on two or more paths, see Figure 2.6. In the case of MBSFN, the Macro-diversity gain is used for combining two or more signals, which are obtained via independently fading paths received from two or more different antennas at different base-station sites.

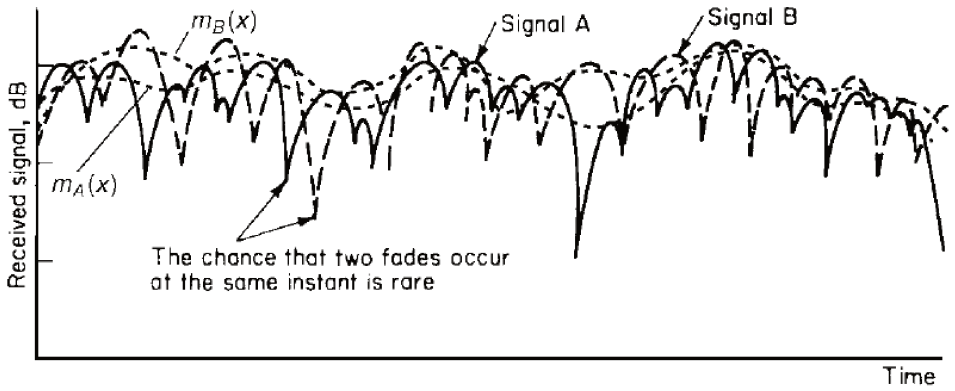

Figure 2.6 – Uncorrelated fading signals [35]

Altogether, this represents significant improvements in the BC reception quality and therefore higher BC data rates can be achieved.

2.4.1 MBSFN Synchronization Area and MBSFN Area

The network proximity where all cells that are synchronizable and can perform MBSFN transmission is called the MBSFN Synchronization Area. They are capable of supporting

one or more MBSFN Areas. A cell can belong to only one synchronization area but it can belong to several, up to eight, MBSFN areas, see Figure 2.7. An MBSFN area is a group of cells that are coordinated to transmit the same waveform at the same time. It is generally a compact area without any hole. However, it is possible to exclude some cells from an MBSFN transmission though these cells are geographically located in the MBSFN area. An MBSFN Area Reserved Cell is defined as a cell within a MBSFN Area which is not contributing in the MBSFN Transmission. The cell can transmit for other services. MBSFN area are static and do not vary over time.

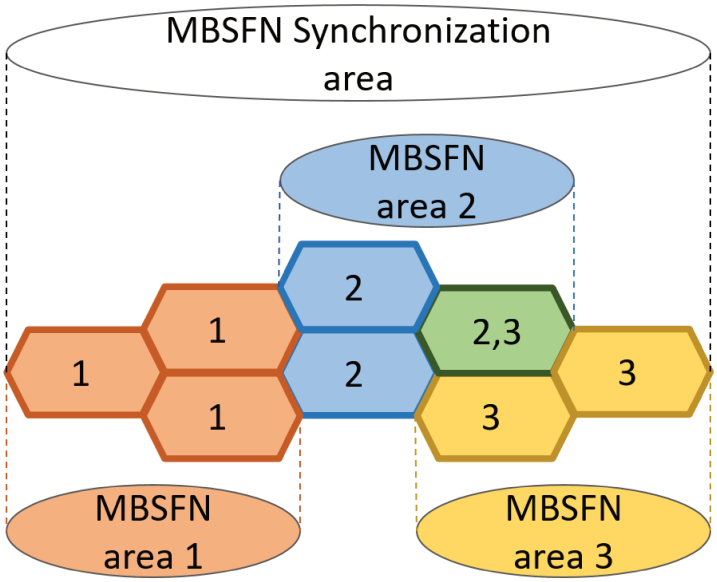

Figure 2.7 – MBSFN Synchronization Area and MBSFN Area.

2.4.2 MBSFN Channel Structure

The transport channel that supports MBSFN transmission is the Multicast Channel (MCH). Two types of logical channels are multiplexed in the MCH:

— Multicast Traffic Channel (MTCH).

— Multicast Control Channel (MCCH).

The MTCH carries MBMS data corresponding to a certain MBMS service. If the number of services to be provided in a MBSFN area is large, multiple MTCHs can be configured. On the other hand, the MCCH carries control information necessary for

reception of a certain MBMS service, including subframe allocation and MCS for each MCH. Thre is one MCCH per MBSFN area.

One or several MTCH and one MCCH are multiplexed at the Medium Access Control (MAC) layer to form an MCH transport channel. The MAC header contains the multiplexing information so the device can de-multiplex the information upon reception. The MCH is transmitted using MBSFN in one MBSFN area.

MCH processing is, for the most part, the same that for Downlink Shared Channel (DLSCH), with some exceptions:

— In MBSFN, cells transmit using the same radio resources. Thus, the MCH transport format and resource allocation can not be dynamically adjusted by each BS. Instead, the transport format is determined by the MCE and signaled to the devices on the MCCH. This poses a chicken-and-egg problem solved by the reception of the System Information Block (SIB) 13, as explained later.

— The MCH transmission simultaneously targets multiple devices and therefore no feedback (Automatic Repeat Request (ARQ)) is used.

— Multi-antenna transmission (transmit diversity and spatial multiplexing) does not apply to MCH transmission.

The MCH is mapped to the Physical Multicast Channel (PMCH) and transmitted in MBSFN subframes, see Figure 2.8. An MBSFN subframe has two parts: a control region used for regular unicast signaling and an MBSFN region used for transmission of the MCH. MCH transmissions use the extended CP to cover the timing difference between the signals received from different cells in the MBSFN area. The 'hole' in Figure 2.8 is used to keep the start timing of the MBSFN region fixed irrespective of the CP used for the control region.

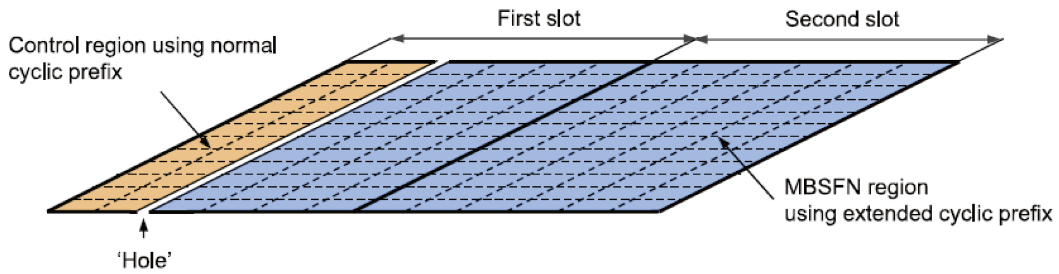

Figure 2.8 – Resource-Block structure for MBSFN subframes [19].

From the UE point of view, the radio channel over which the MCH propagates is the aggregation of the channel of each cell in the MBSFN area. To enable coherent demodulation of the MCH, special reference symbols are transmitted in the MBSFN subframe as shown in Figure 2.9. These reference symbols are transmitted by each cell in the MBSFN area using the same time-frequency positions. MBSFN transmission in combination with specific MBSFN reference signals can be seen as a transmission using a specific antenna port, referred to as antenna port 4 in 3GPP standards.

The frequency-domain density of MBSFN reference signals is higher than the density of cell-specific reference symbols (used in unicast transmission). This is needed as the aggregated channel of all MBSFN area cells is equivalent to a highly time-dispersive or, equivalently, highly frequency-selective channel. Consequently, a higher density in the frequency domain reference symbols is needed.

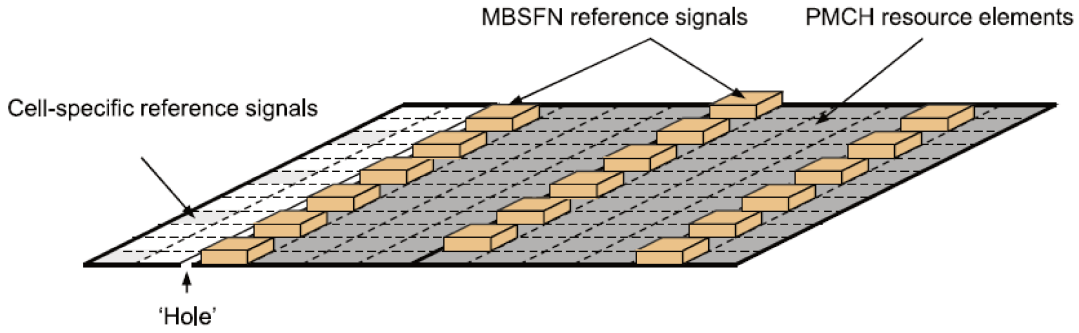

Figure 2.9 – Reference Signal structure for PMCH [19].

2.4.3 Scheduling of MBSFN Services

The MCH transmission takes place in the form of Transport Blocks (TBs). In each Transmission Time Interval (TTI) only one TB is transmitted and it is mapped to a MBSFN subframe in which all the MBSFN resources should be utilized, normally the entire bandwidth.

The MCHs transmitted by cells in the same MBSFN area occupy subframes within a pattern of MBSFN subframes. This pattern is common for each cell in the area and it is called Common Subframe Allocation (CSA) Pattern. According to [7], the CSA pattern repeats in every CSA period. The actual MCH Subframe Allocation (MSA) for each MCH carrying MTCHs is defined by the CSA pattern, the CSA period, and the corresponding MSA end, that are all signaled on MCCH. The MSA end indicates the last subframe of

the MCH within the CSA period. The MCHs are time multiplexed within the CSA period. During one MCH Scheduling Period (MSP), which is configurable per MCH and can be larger than the CSA period (from 80 ms to 10.24 s), the BS applies MAC multiplexing of different MTCHs and optionally MCCH to be transmitted on this MCH. An example of MBMS scheduling is presented in Figure 2.10. In this example the scheduling period for the first MCH is 16 frames which is equal to the CSA period, and the scheduling period for the second MCH is 32 frames, corresponding to two CSA periods, therefore the scheduling information is transmitted once every 32 frames.

The MSA is periodic and at the beginning of each MSP a MAC control element is used to transmit the MCH Scheduling Information (MSI). The MSI indicates which subframes are used by each MTCH during the MSP. Notice from Figure 2.10 that not all the available MBSFN subframes in the CSA pattern need to be utilized for MBMS transmission.

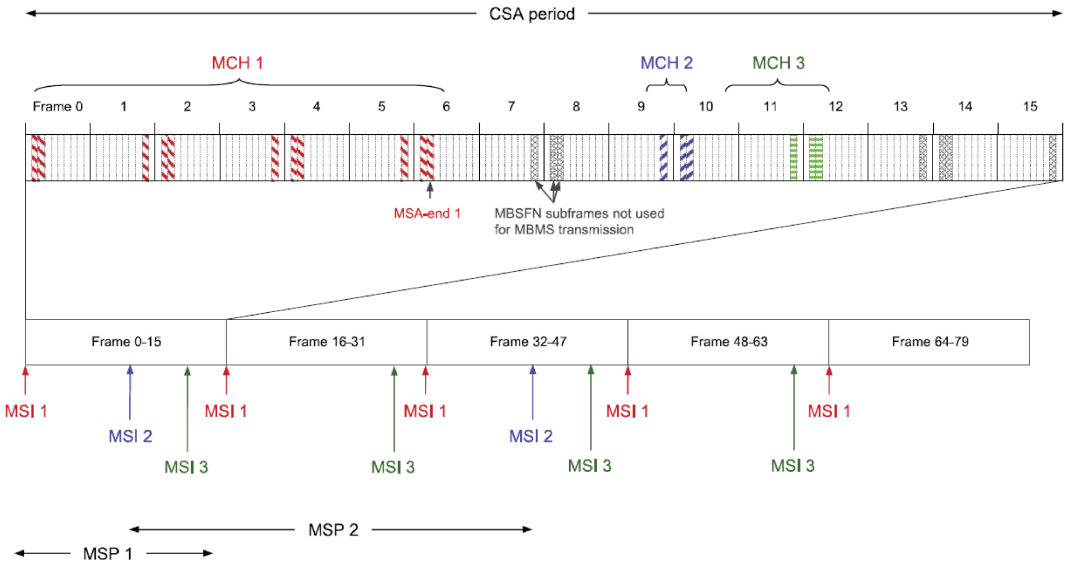

Figure 2.10 – Example of scheduling of MBMS services [19].

MCH is characterized by a semi-static transport format and semi-static scheduling as these characteristics remain the same at least during a MCCH modification period. MCCH modification may be necessary when starting a new service. The entire MCCH information will be transmitted periodically based on a repetition period. Changes/Updates to the MCCH can only occur at specific time instants, at the beginning of the modification period. A modification period is defined as an integer multiple of the repetition period. This is illustrated in Figure 2.11.

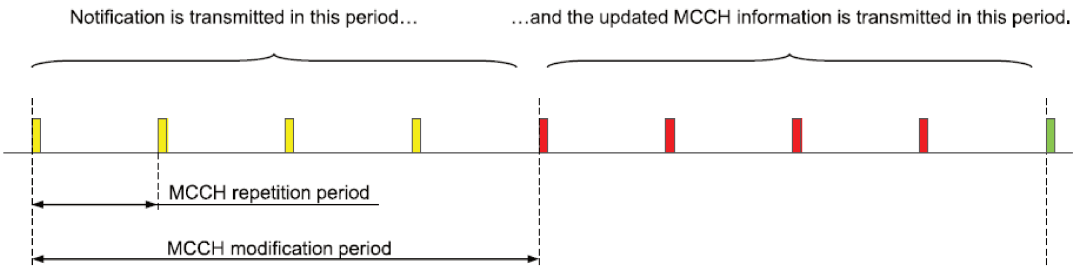

Figure 2.11 – MCCH transmission schedule [19].

Since the information necessary to decode the MCH is provided in the MCCH which is itself mapped in the MCH, a mechanism to solve this chicken-and-egg problem is necessary. There is an MCCH-specific transport format which is provided in the SIB 13. The SIB 13 also provides information about the scheduling and modification periods of the MCCH (but not about CSA period, CSA pattern, ans MSP, which are in the MCCH itself). To summarize, reception of a MBMS service is achieved by the following steps:

— Receive SIB 13 to obtain knowledge on how to receive the MCCH for this particular MBSFN area

— Receive the MCCH to obtain information about the CSA and MSP for the broadcast service

— Receive the MSI at the beginning of each MSP. With this information the device knows in which subframes it can find the service of interest

2.5 Single-Cell Point-to-Multipoint

SC-PTM was introduced in 3GPP Release 13 to support MBMS services in one cell. It uses the same architecture presented in Subsection 2.3.2 but the network can dynamically decide which cells transmit in SC-PTM mode while in MBSFN the MBSFN area is static.

The Single-Cell (SC) MTCH which carries the information to be transmitted using SC-PTM, is mapped to the DLSCH. Therefore, dynamic scheduling of the DLSCH is used, as in unicast. SC-PTM transmits to multiple devices at the same time, thus ARQ feedback and Channel State Information (CSI) reports are not used. However, SC-PTM supports three Transmission Modes (TMs): TM 1 - Single transmit antenna, TM 2 - Transmit diversity and TM 3 - Open loop spatial multiplexing with Cyclic Delay Diversity (CDD). On the other hand, MBSFN only supports TM 1 [19]. TM 2 and TM 3 make use of two

or more antennas in a cell to transmit the same information which provides diversity and helps to mitigate fading. Furthermore, SC-PTM uses the normal CP while MBSFN uses the extended CP, thus SC-PTM can transmit more symbols per subframe.

For SC-PTM, radio resources could be dynamically assigned by Physical Downlink Control Channel (PDCCH) based on the real time traffic load TTI by TTI. Since Unicast and SC-PTM are based on Physical Downlink Shared Channel (PDSCH) and have the same radio frame structure, radio resources could be flexibly shared between unicast and SC-PTM in the same subframe as shown in Figure 2.12.

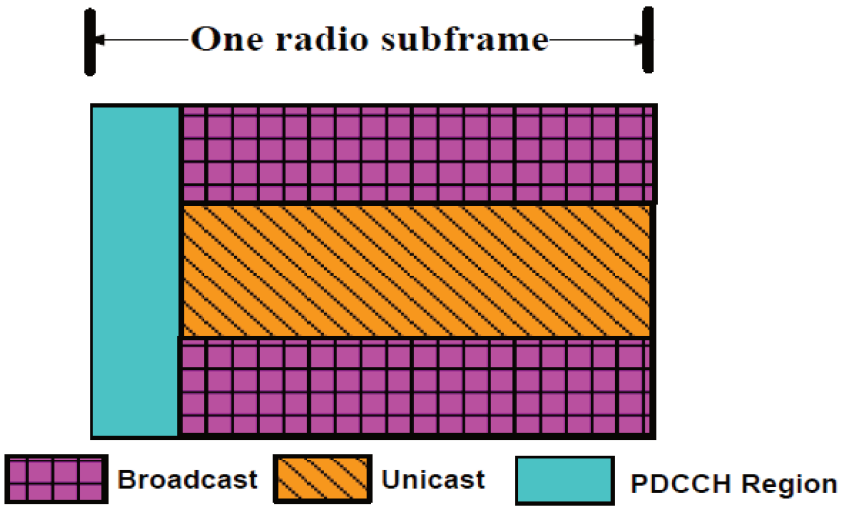

Figure 2.12 – Unicast and SC-PTM multiplexed in the same Subframe [29].

The dynamic scheduling of SC-PTM allows a shorter set-up latency with respect to MBSFN. For MBSFN, the time to setup and notify the receiving group members of the MBMS bearer setup for a new group communication is dominated by the MCCH modification period which can take the value 5.12 s or 10.2 s. To reduce latency in MBSFN, MBMS bearers have to be pre-established but even so the session establishment time can be of up to 525 ms due to the MCCH repetition period and MSP [29]. Furthermore, synchronization between cells is not necessary in SC-PTM which could further reduce latency.

The disadvantage of SC-PTM with respect to MBSFN is the lower useful signal power and increased interference power since neighboring cells transmit different signals. This is particularly important at cell borders since the SC-PTM transmission should cover all users in the cell. UE at cell border may decrease the transmission bit rate due to their low SINR.

2.6 MBMS operation on Demand (MooD)

MooD was introduced in 3GPP Release 12. MooD enables automatic and seamless MBMS service activation and deactivation based on the UE service consumption reporting [28]. When it becomes more efficient to run a unicast service as an MBMS service, the system may activate an MBMS session for the service [32].

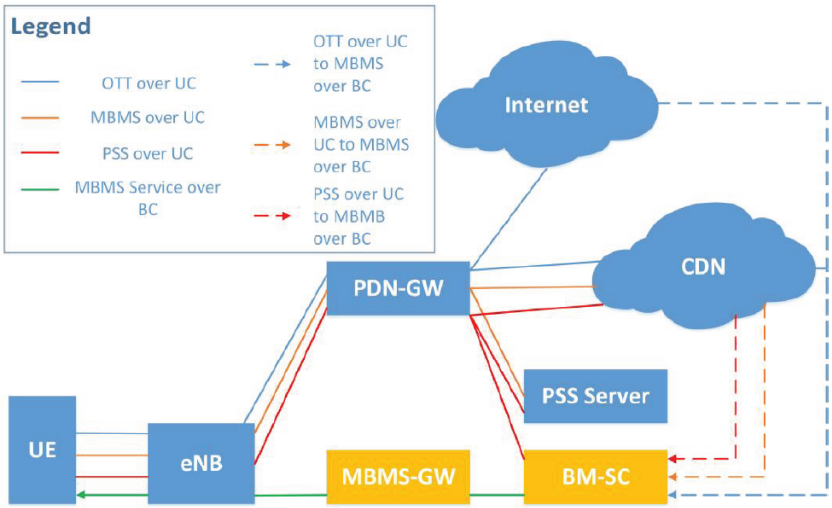

Figure 2.13 – High-Level 3GPP LTE MooD solution architecture [17].

When the BM-SC determines a high attachment rate of a unicast service, it decides to activate an MBMS user service to carry the same content over the MBMS bearer. Figure 2.13 shows the paths for delivery of Over-The-Top (OTT), Packet-switched Streaming Service (PSS) and MBMS over Unicast and the path for MBMS over Broadcast. Additionally, it illustrates the paths that are activated when the BM-SC decides to offload the delivery of OTT, PSS or MBMS to MBMS over Broadcast. We see that the Content Delivery Network (CDN) sends the content directly to the BM-SC for BC delivery.

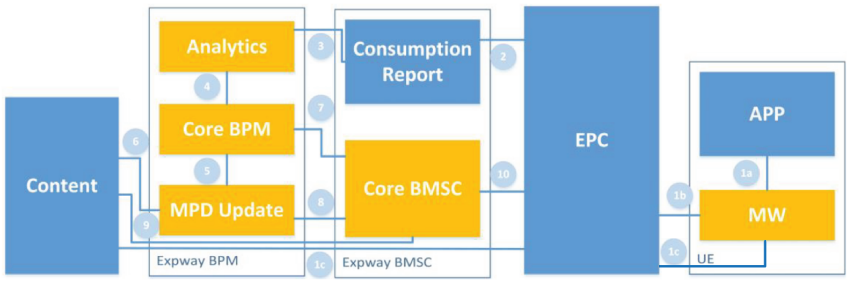

Figure 2.14 – Detailed 3GPP LTE MooD solution architecture [17].

A more detailed description of the MooD working mode, particularly for the delivery of DASH content, is presented in Figure 2.14. This solution is proposed in the framework of the 5G-Xcast project [10] in which Enensys-Expway participated [50].

1. a) In the UE, the Application (APP) requests the content to the Middleware (MW) (knwon as MBMS client in 3GPP standards [4]). b) The MW acts as a proxy server. c) Initially the content is delivered over Unicast directly from the content source.
2. The MW sends Consumption Reports to the Consumption Report server in the BM-SC. They are sent as data in the user plane using the Evolved Packet Core (EPC) unicast path (Packet Data Network Gateway (PGW), SGW), and not as control information.
3. The Analytics server in the Broadcast Provisioning Manager (BPM) pulls the Consumption Report or the Consumption Report Server pushes the content to the Analytics server.
4. The Analytics server decides to deliver popular content over Multicast if the number of users demanding the same content in the serving area is higher than a threshold fixed by the BPM administrator.
5. The BPM updates the manifest (Media Presentation Description (MPD) for DASH content), in order to add multicast and unicast profiles (Unified MPD).
6. The manifest update is sent to the content provider.
7. The BPM instructs the BM-SC to send the content over MBMS.
8. The BM-SC retrieves the unified MPD.
9. The BM-SC retrieves the video segments.
10. The BM-SC performs Service Announcement and delivers content to UE.

2.6.1 MBMS Consumption Reporting

The decision to switch from unicast to MBMS is taken based on the consumption reports sent by the UE to the BM-SC. The BM-SC sends Service Announcements to advertise MBMS services. A service announcement contains several metadata fragments including the User Service Description (USD). The USD contains a reference to an Associated Delivery Procedure Description (ADPD) which contains the Consumption Report configuration. The consumption report configuration contains:

— ***samplePercentage:*** only a subset of UE are required to send consumption reporting, the attribute *samplePercentage* allows defining the proportion of UE that shall send reports.

— ***randomTimePeriod:*** refers to the time window length over which a MBMS client shall calculate a random time for the initiation of the consumption report procedure. This is used to avoid many UE sending consumption reports at the same time.

— ***offsetTime:*** the time that a MBMS client shall wait after sending a consumption report before computing a random time within the time window given by randomTimePeriod.

— ***reportInterval:*** the server may ask the UE to send ongoing consumption reports at a given time interval. *randomTimePeriod* « *reportInterval*.

— ***reportClientId:*** specifies if the UE have to send its unique identifier.

— ***serviceURI:*** the Uniform Resource Identifier (URI) of the server where the UE must send the Consumption Report Request.

— ***location:*** indicates to report Cell-ID or Service Area Identifier (SAI).

On the other hand, the MBMS client in the UE send the Consumpton Report Request message to the BM-SC using HTTP POST request. The message contains the following mandatory parameters:

— ***serviceId:*** Same that in the USD

— ***consumptionType:*** declares the consumption report as belonging to one of the following types:

1. Start of consumption of the on the MBMS bearer.
2. Transition of UE consumption of the service from unicast to MBMS bearer.
3. Stop of consumption of the Service on the MBMS bearer.
4. Transition of UE consumption of the Service from MBMS bearer to unicast.
5. Ongoing consumption of the Service over MBMS upon the expiration of the 'report interval' timer.
6. Location change while consuming the MBMS User Service on the MBMS bearer.
7. Start of consumption of the Service on unicast.
8. Stop of consumption of the Service on unicast.

9. Ongoing consumption of the Service on unicast, upon the expiration of the 'report interval' timer.
10. Location change while consuming the Service on unicast.

The Consumption Report Request can contain the following optional parameters:

— ***clientId:*** identifies the reporting UE. Sent if the attribute *reportClientId* was present in the consumption report configuration.

— ***reportTime:*** identifies the time when the report is generated by the UE.

— ***location:*** represents the UE's location or the list of MBMS SAI.

2.7 5G Media Distribution

Video delivery accounts for more than half of the world's mobile data traffic [41]. Thus, the distribution of media content is one of the priorities of the 5G standardization organizations.

2.7.1 5G Architecture

The 5G brings an ensemble of new technologies, architectures and protocols that support new use cases that were not possible with the former 4G LTE technology. A key technology for 5G is Network Functions Virtualization (NFV). NFV separates the Network Functions (NF) from hardware. NF run in a virtualized environment and offer services to other Network Functions (NF) and consumers.

The 5G reference architecture is presented in Figure 2.15. Control plane NF communicate with each other using NF services. An NF service consist of operations based on either a request-response or a subscribe-notify model [28]. Hereafter we mention the functionalities supported by some of the 5G NFs.

— ***Access and Mobility Management Function (AMF):*** the AMF supports registration management, connection management, mobility management, access authentication and authorization, and security context management [21].

— ***User Plane Function (UPF):*** supports packet routing and forwarding, packet inspection, QoS handling, among others [21].

— ***Session Management Function (SMF):*** supports session management (session establishment, modification, release), UE IP address allocation and management,

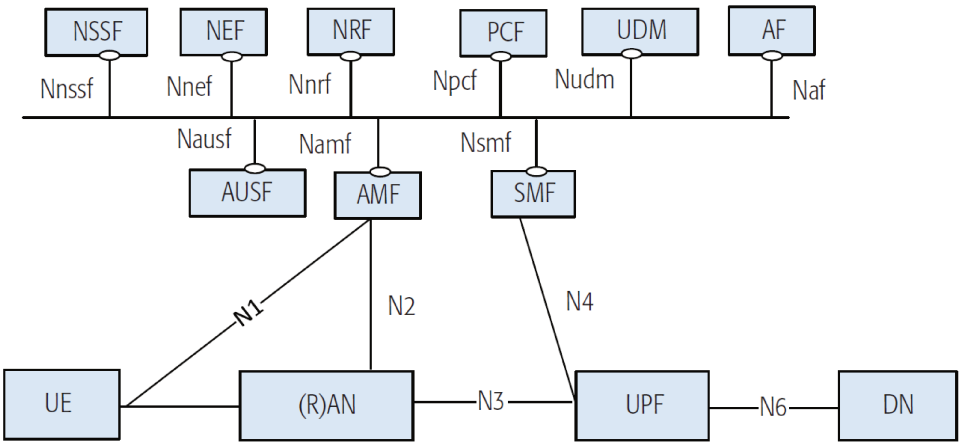

Figure 2.15 – Service Based 5G Architecture © 2018, IEEE [28].

Dynamic Host Configuration Protocol (DHCP) functions, downlink data notification, etc. [21].

— ***Network Exposure Function (NEF):*** provides means to securely expose the services and capabilities provided by 3GPP network functions to third parties, or non-3GPP environments [21].

— ***Policy Control Function (PCF):*** the PCF determines the resources and services that can be used to support connected devices. It determines customers data allocations, whether they are fixed or mobile subscribers, and even what entertainment services they may have subscribed to through their operator, etc. [40].

One of the main 5G use cases is enhanced Mobile Broadband (eMBB). It refers to services requiring a high data rate, e.g. 4K and 8K video streaming and virtual and augmented reality. Furthermore, eMBB should be able to deliver high quality content to a massive audience in a geographically restricted area. In order to satisfy the requirements for eMBB, the 3GPP standardized in Release 16 the 5GMS architecture. On top of that, Release 17 brings the specifications for LTE-based 5G Broadcast and 5G MBS.

2.7.2 5G Media Streaming

A 5GMS system is an assembly of Application Functions, Application Servers and interfaces from the 5G Media Streaming architecture that support either downlink media streaming services or uplink media streaming services, or both [8].

In this work we are interested in the downlink scenario. Therefore, the Unicast Downlink

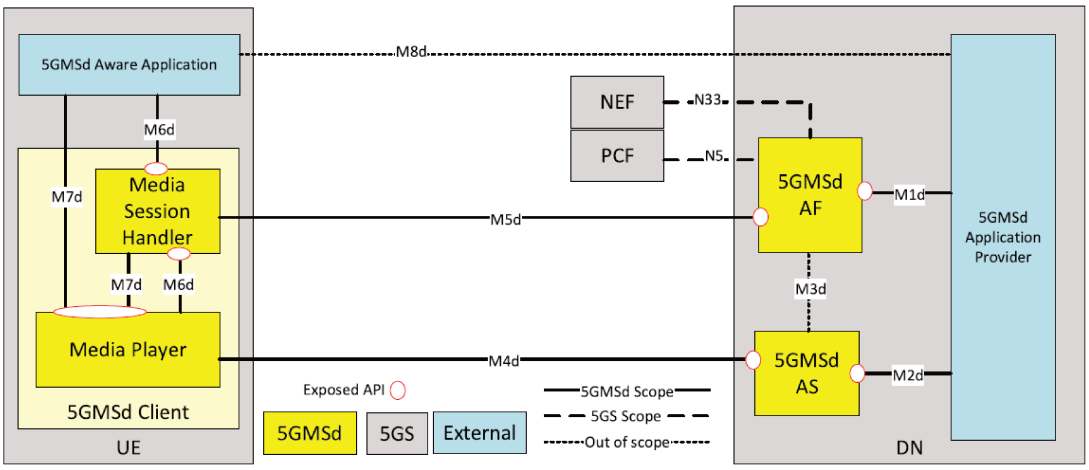

Figure 2.16 – 5G Media Streaming User Service Architecture [8]

5GMS Services Architecture is presented in Figure 2.16. Two blocks from this architecture are not in the scope of 5GMS nor 5G system specifications, the 5GMS Application Provider and the 5GMS-Aware Application. The 5GMS Application Provider uses 5GMS for streaming services. It provides a 5GMS Aware-Application on the UE to make use of 5GMS Client and network functions using interfaces and Application Programming Interfaces (APIs) defined in 5GMS.

The following functions are defined:

— ***5GMS Client for downlink:*** Receiver of 5GMS downlink media streaming service. It contains two subfunctions:

  — ***Media Session Handler (MSH):*** It communicates with the 5GMS Application Function (AF) in order to establish, control and support the delivery of a media session.

  — ***Media Player:*** It communicates with the 5GMS Application Server (AS) in order to stream the media content and may communicate with the 5GMS-Aware Application for media playback and to the MSH for media session control.

— ***5GMS AF for downlink:*** Embodies the control plane aspects such as provisioning, configuration and reporting [43]. It may relay or initiate a request for different PCF treatment or interact with other network functions via the NEF.

— ***5GMS AS for downlink:*** An Application Server which hosts 5G media functions. It provides 5GMS services to 5GMS Clients (data plane) supporting pull-based

content retrieval protocols (DASH, HTTP Live Streaming (HLS)). Note that there may be different realizations of the 5GMS AS, for example a CDN.

2.7.3 LTE-Based 5G Broadcast

3GPP Release 17 defined an architecture for 5G Media Streaming on top of LTE-based 5G Broadcast using MBMS user services. This harmonized architecture is presented in Figure 2.17. This architecture allows 5GMS-based downlink media streaming to be deployed as an MBMS-aware Application on top of MBMS. The 5GMS Media Player is served by a Media Server that is part of the MBMS Client and which acts as a proxy for the 5GMS AS when media objects are transmitted via MBMS. The Media Session Handler acts as an MBMS-Aware Application and initiates service acquisition. This architecture offers the content to the Media Player from two different "data networks", one from the 5GMS Application Server in the network and one from the local proxy in the MBMS Client.

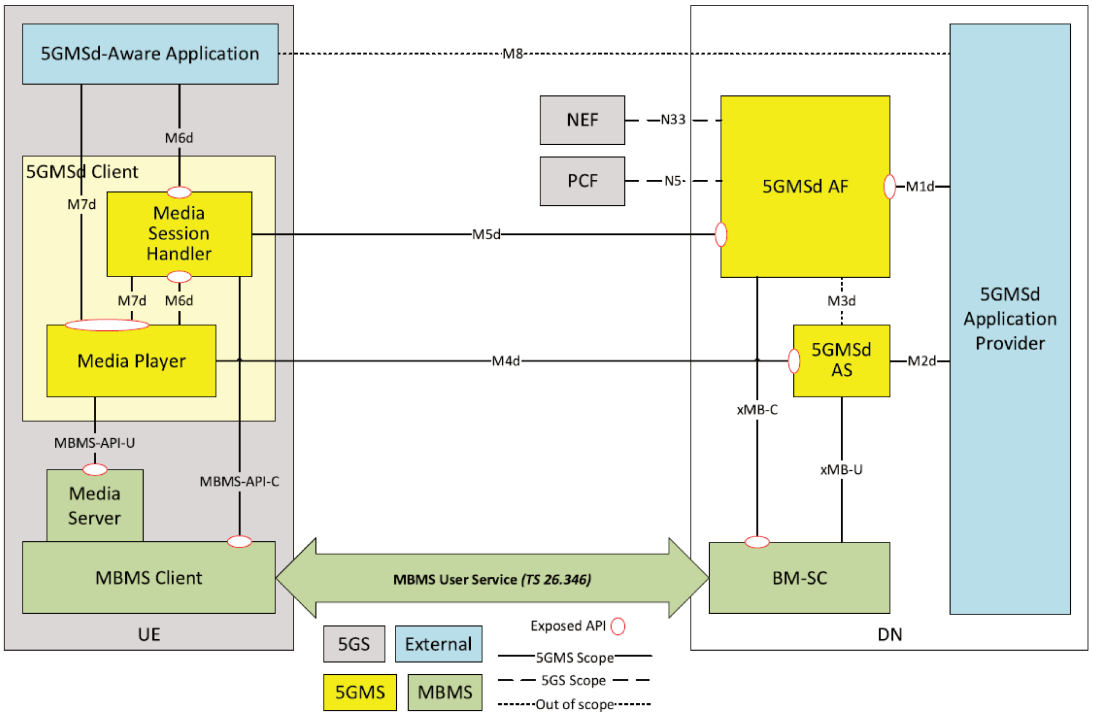

Figure 2.17 – 5G Media Streaming over MBMS User Service Architecture [8].

2.7.4 5G Multicast Broadcast Services

With 5G Multicast Broadcast Services (5G MBS) in Release 17, the 3GPP adds broadcast and multicast capabilities to the 5G New Radio (NR) system, and 5G Media Streaming (5GMS). There are some important differences between 5G MBS and LTE MBMS:

— Only SC-PTM supported in NR RAN which means no support for MBSFN. MBSFN is only used in LTE-based 5G broadcast.

— Support of Multicast Services with autonomous RAN based switching between Point-to-Point (PTP) and PTM transmission modes. In LTE MooD, the switching is managed by the BM-SC.

Furthermore, 5G MBS aims to reuse physical channels and signals, without new numerologies to facilitate its deployment. The 5G system architecture leverages the unicast 5G system architecture wherever possible.

The 5G MBS architecture is presented in Figure 2.18. Four new functions are added to support broadcast and multicast services and some 5G functions are enhanced with new functionalities. In the user plane we have:

— ***Multicast Broadcast Service Transport Function (MBSTF):*** Provides generic packet transport functionalities available to any IP multicast enabled application, such as framing, multiple flows, packet encoding and multicast/broadcast delivery of input files as objects or object flows [43].

— ***Multicast-Broadcast User-Plane-Function (MB-UPF):*** Provides user plane transport functionality for 5G MBS data via shared tunnel or unicast delivery.

In the control plane we have:

— ***Multicast Broadcast Service Function (MBSF):*** Provides control plane functionality to configure 5G MBS sessions, including determination of transport parameters, selection of MB-SMF, etc.

— ***Multicast-Broadcast Session-Management-Function (MB-SMF):*** Provides session management and control of 5G MBS transport, including QoS, UE join/leave procedures, RAN and MB-UPF configuration of MBS data tunneling [43].

Additionally, some 5G Core functions are enhanced:

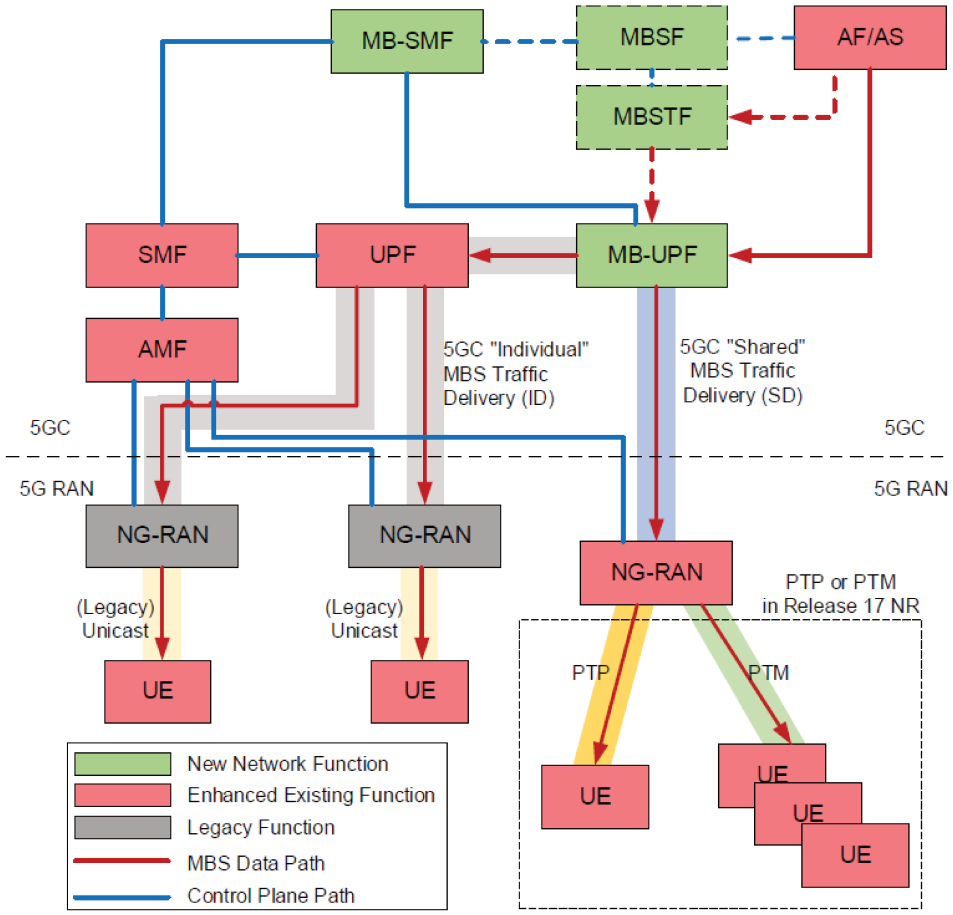

Figure 2.18 – 5G Multicast Broadcast Services Architecture © 2022, IEEE [48]

— ***AMF:*** Transfers Multicast Broadcast Service (MBS) signaling between MB-SMF and Next-Generation RAN (NG-RAN), and manages paging procedures for UE in multicast mode during service activation. It selects appropriate NG-RAN nodes for broadcast and group notification of multicast session activation towards UE.

— ***NG-RAN:*** Provides support of 5G MBS shared tunnel, and PTM/PTP delivery of MBS data.

— ***SMF:*** It is enhanced to handle UE's multicast session join or leave and to determine the MBS traffic delivery method to use.

— ***UPF:*** It is enhanced to deliver multicast data to UE via Protocol Data Unit (PDU) session

— ***PCF:*** it is is upgraded to support QoS handling for MBS session [48].

In addition to this architecture, some features are added to NG-RAN. For NR multicast

mode, flexible switching between PTM and PTP by the NG-RAN node is allowed, even supporting a Hybrid Automatic Repeat Request (HARQ) retransmission by PTP of an initial packet delivered via PTM. Furthermore, flexible scheduling between unicast and Multicast is possible. There is no need for static subframe allocation as in MBSFN.

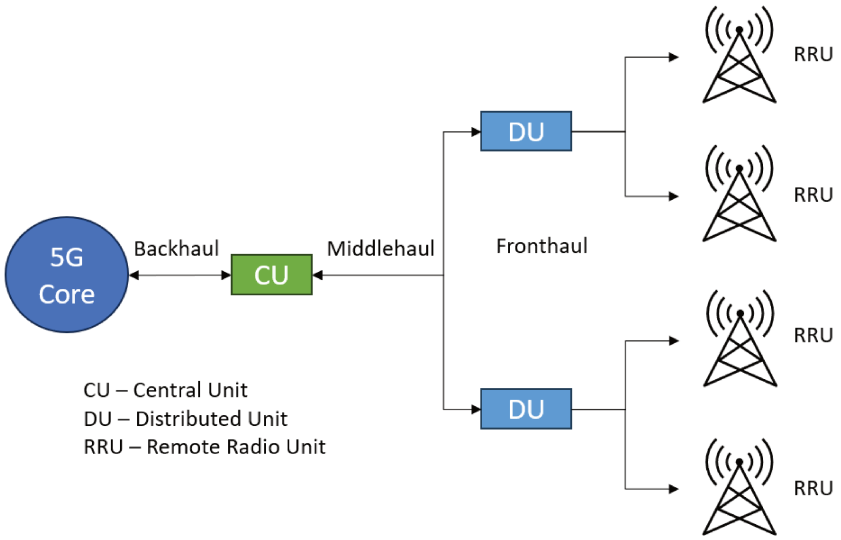

Figure 2.19 – 5G Functional Split.

5G MBS does not support wide area MBSFN transmission. However, small area SFN transmission is possible. It is limited to a group of cells connected to same Distributed Unit (DU) and is transparent to UE, see Figure 2.19.

The 5G MBS user service architecture is presented in Figure 2.20. This architecture supports operator and third-party applications using 5G MBS for media distribution. An MBS Application Provider may communicate with the MBSF to establish a 5G MBS User Service. The MBSF establish QoS and 5G MBS delivery. It also provisions the MBSTF to accept data from the application provider and deliver it to the MBSTF Client. The MBSF Client discovers the announced User Services and sets up the relevant delivery functions in order to receive the data.

2.8 Summary

In this chapter present an overview of the technical aspects related to broadcast transmission in cellular networks. We started presenting the propagation model and antenna model considered in our work to study data transmission in cellular networks. The

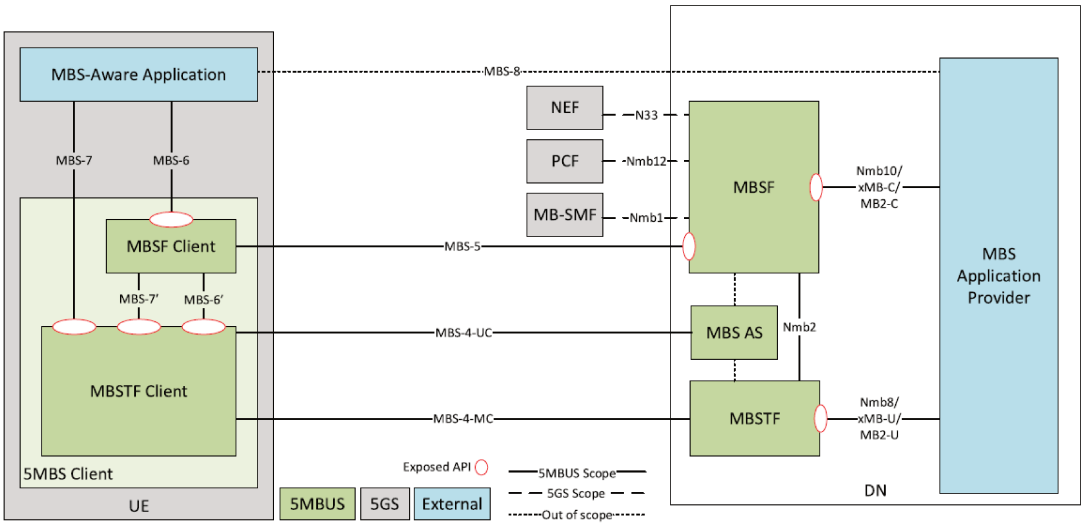

Figure 2.20 – 5G Multicast Broadcast Services User Service Architecture [9].

propagation model is based on the reference model proposed by the 3GPP with shadowing and fading. For the antennas we consider three cases: omnidirectional antennas, tri-sector antennas and beamforming. These models are taken from the literature and are used in the following chapters.

Afterwards, we focus on broadcast transmission. We present an overview of the standardisation efforts done by 3GPP to specify MBMS and the LTE MBMS architecture. MBMS can use two transmission techniques, MBSFN and SC-PTM. We explain in detail how these two broadcast transmission techniques work in LTE. Afterwards, we present the mechanism that enables seamless switching between unicast and MBMS in LTE, MBMS operation on Demand (MooD). We present the content of the messages exchanged between the UE and the BM-SC to manage the switching, notably the Consumption Reporting mechanism. We see that the consumption report considers the option to transmit the UE location to the BM-SC. However, the criteria for the switching between unicast and MBMS is not standardised and it is up to the BM-SC administrator. In the following chapters we propose methods to adjust the switching criteria using the information that may be provided by the consumption reports: the number of users demanding the broadcast service and their location.

Towards the end of this chapter we present some of the effort the 3GPP has done to standardise media distribution in 5G cellular networks. We present a short overview of the 5G core network and its more important functions. Then, we focus on 5G Media

Streaming (5GMS) systems for which 3GPP has standardized an architecture following the principles of the 5G core network, notably the separation between user plane and control plane. In Release 16 5GMS considered only unicast transmission but in Release 17 an architecture for LTE-based 5G broadcast is provided. This architecture enables the transmission of 5GMS services in downlink over MBMS. However, the interaction between the BM-SC and the UE remains as in LTE. Afterwards, we present the 3GPP architecture that adds broadcast and multicast capabilities in 5G systems without using MBMS, it is the 5G Multicast Broadcast Services (5G MBS) architecture. 5G MBS considers the SC-PTM transmission technique and MBSFN is restricted to the cells connected to the same Distributed Unit (DU). From these standardisation efforts we see that in 5G the MBSFN technique continues working over LTE RAN. Furthermore, in the radio interface, 5G SC-PTM or 5G MBS is similar to LTE SC-PTM since it was already compatible with unicast. One important difference, is that the decision to switch from unicast to SC-PTM is taken by the RAN and not by the BM-SC as in LTE MBMS.

In the following chapter we present a detailed comparison between unicast and MBSFN in terms of interference, SINR and coverage. Furthermore, we provide a model to calculate the number of users per cell from which MBSFN becomes more efficient that unicast in terms of radio resource utilization.

Chapter 3

MBSFN versus Unicast in Cellular Systems

This chapter presents a performance comparison between UC and MBSFN transmission in cellular networks from a resource utilization perspective. We introduce a model to calculate the SINR distribution for a UE receiving in UC and MBSFN mode. We use this model to compare both transmission modes in terms of useful signal power and interference. Then, we calculate the minimum number of users per cell downloading the same data from which a MBSFN transmission is more efficient than multiple UC transmissions.

In Section 2.3 we introduce the BC transmission mode in cellular networks and present a review of its standardization from the 3GPP Release 6 to the future Release 17. Additionally, a state-of-the-art on the comparison between UC and BC is presented. Then, in Section 3.2, we present the models to calculate the SINR distribution for a user receiving in MBSFN mode and UC mode considering beamforming in UC and BC areas of different sizes. Afterwards, in Section 3.3 we propose a model to compare the radio utilization efficiency of UC and MBSFN mode. More precisely we calculate the user threshold, the number of users per cell in the MBSFN area from which the MBSFN mode becomes more efficient than the UC mode. Finally, in Section 3.4 we summarize our study underlining the most important contributions.

3.1 State-of-the-art on the comparison between Unicast and MBSFN

MBSFN transmission consists in a group of cells, called MBSFN area, that transmit the same signal to a group of users in the BC area. Since it is a single transmission, the bitrate is the same for all users, see Section 2.4 for more detail. The MCS of the transmission is set aiming to cover the user with the lowest SINR, therefore, MBSFN transmissions do

not benefit from link adaptation. On the other hand, UC transmissions benefit from link adaptation and the possibility of using the beamforming technique but the same data is transmitted as many times as the number of users demanding the same service.

The problem is to identify at which point it becomes more efficient to transmit in MBSFN mode rather than in UC mode from a resource utilization perspective. A user with a very low SINR can degrade the performance of MBSFN transmissions. On the other hand, transmitting the same content several times in the same region is inefficient. The difficulty lies in the various irregularities in cellular systems, such as different BS densities, number of users demanding the same service, user's location, size of the MBSFN area, antennas capabilities, propagation effects, etc. Nevertheless, some authors have addressed this problem.

In [16], authors propose a method to identify when it is convenient to change from UC to multicast transmission in a single cell scenario. They define an SINR threshold which is set by the user with the best instantaneous channel with respect to the average channel. If the minimum SINR among multicast users is higher than the SINR threshold, then multicast transmission is executed. In [22], authors prove the benefits of multicast over UC when the average channel quality is high and there is a large number of users in the cell. They also proved that multicast performs better when the channel has low dynamicity, a low standard deviation of the SINR. However, both of these works consider BC transmission only in one cell. Models to calculate the SINR distribution for a receiver in MBSFN mode are presented in [44] and [47]. In [44] authors consider a regular hexagonal lattice and the effect of path-loss, fading and shadowing. On the other hand, authors in [47] consider Poisson distributed BS and use stochastic geometry to derive an approximation of the coverage probability in an large MBSFN network, but they consider omnidirectional antennas and do not consider shadowing.

3.2 SINR in Unicast and MBSFN

In this section, we derive the expressions for the SINR perceived by a UE in MBSFN mode and UC mode. Then, we compare both transmission modes in terms of signal power, interference power and SINR.

3.2.1 Base Station Location Model

To take into account the irregularity of operational networks, we consider base stations located according to a PPP with intensity λ_{BS} as shown in Figure 3.1. The intensity λ_{BS} is the average number of BSs per square kilometer, therefore, in the remainder of this document we call it BS density. The PPP model has proven to yield results closer to the performance of real cellular network deployments compared to the typical hexagonal model [11].

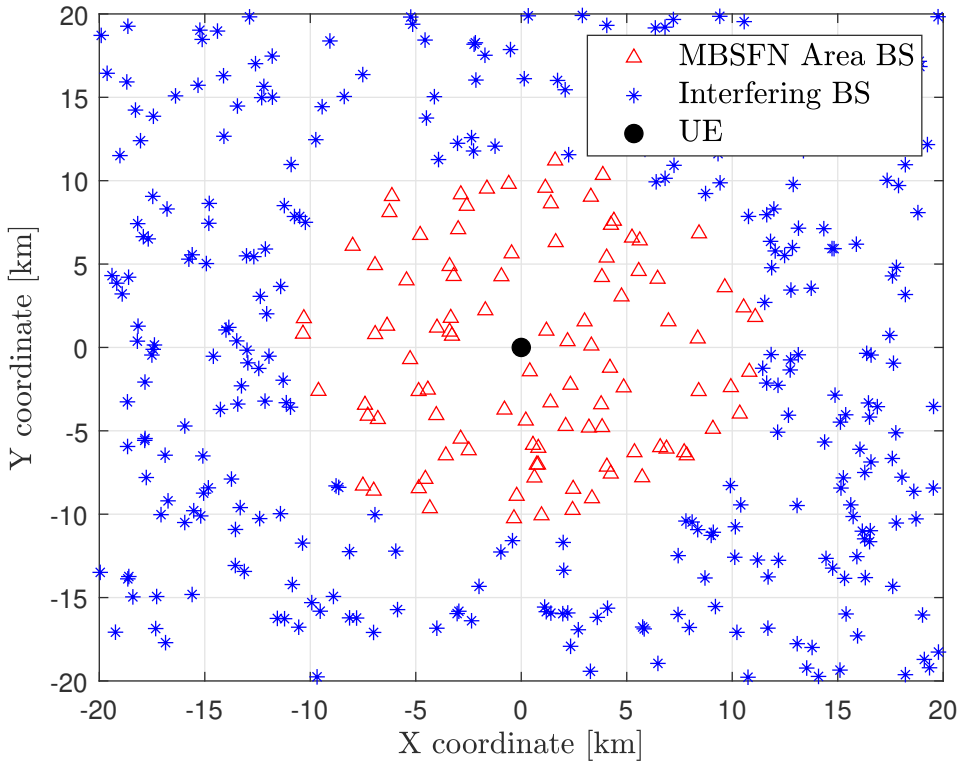

Figure 3.1 – MBSFN area of 100 BS on a surface where BS are located following a PPP with density $\lambda_{\text{BS}} = 0.25$ BS/km^2.

3.2.2 SINR in Unicast mode

Hereafter we present how to calculate the SINR perceived by a UE in UC mode. We consider PPP-distributed BSs and in Figure 3.1 but with all BSs transmitting in unicast mode. In UC mode, only the serving cell provides useful signal power (P_{UC}) and

neighboring cells generate interference (I_{UC}). The SINR for a receiver in UC mode can be calculated as

$$S_{UC} = \frac{P_{\mathrm{UC}}}{P_{\mathrm{N}} + I_{\mathrm{UC}}}, \tag{3.1}$$

where P_{N} is the noise power, see Section 2.1, and P_{UC} and I_{UC} are the useful signal power and interference power respectively. P_{UC} is calculated as

$$P_{\mathrm{UC}} = P_{\mathrm{tx}} k r_{\mathrm{s}}^{-\alpha} h_{\mathrm{s}} e^{\chi_{\mathrm{c}}} e^{\chi_{\mathrm{s}}} \Omega(\theta_{\mathrm{s}}, \phi_{\mathrm{s}}), \tag{3.2}$$

where the sub-index s stands for serving cell and $\Omega(\theta_i, \phi_i)$ is the antenna gain of the BS in the direction θ_i when the beam is steering in the direction ϕ_i, if beamforming is used. We consider three cases according to the antenna deployment in the base station:

1. BS with omnidirectional antennas. In this case $\Omega(\theta_i, \phi_i) = g$, refer to Subsection 2.2.1.
2. BS with tri-sector antennas. We use $\Omega(\theta_i, \phi_i) = G(\theta_i)$, refer to Subsection 2.2.2. Take into account that only one cell generates useful signal power. It is, from the serving base station one sector provides useful signal power (serving cell) and the other two sectors generate interference as well as all sectors from other base stations.
3. Tri-sector BS with cells capable of performing the beamforming technique. Here we use $\Omega(\theta_i, \phi_i) = A(\theta_i, \phi_i)$, refer to Subsection 2.2.3. We assume that the beam of the serving cell is steered towards the UE, it is $\theta_{\mathrm{s}} = \phi_{\mathrm{s}}$. Then, according to (2.17), $\Omega(\theta_{\mathrm{s}}, \phi_{\mathrm{s}}) = A(\theta_{\mathrm{s}}, \phi_{\mathrm{s}}) = MG(\theta_{\mathrm{s}})$.

The interference power, I_{UC}, is calculated as follows

$$I_{\mathrm{UC}} = P_{\mathrm{tx}} k e^{\chi_{\mathrm{c}}} \sum_{i \in \psi / i \neq s} r_i^{-\alpha} h_i e^{\chi_i} \Omega(\theta_i, \phi_i), \tag{3.3}$$

where ψ represents the set of cells and the sub-index i denotes cell i. If base stations are tri-sectored, $\Omega(\theta_i, \phi_i) = G(\theta_i)$ and, if beamforming is used, $\Omega(\theta_i, \phi_i) = A(\theta_i, \phi_i)$. Notice that P_{UC} and I_{UC} have the factor $P_{\mathrm{tx}} k e^{\chi_{\mathrm{c}}}$ in common, therefore we can rewrite (3.1) as follows

$$S_{UC} = \frac{\hat{P}_{\mathrm{UC}}}{\frac{P_{\mathrm{N}}}{P_{\mathrm{tx}} k e^{\chi_{\mathrm{c}}}} + \hat{I}_{\mathrm{UC}}}, \tag{3.4}$$

where

$$\hat{P}_{\mathrm{UC}} = \frac{P_{\mathrm{UC}}}{P_{\mathrm{tx}} k e^{\chi_c}}, \tag{3.5}$$

and

$$\hat{I}_{\mathrm{UC}} = \frac{I_{\mathrm{UC}}}{P_{\mathrm{tx}} k e^{\chi_c}}. \tag{3.6}$$

Beamforming Interference Model

The interference models we use for omnidirectional antennas and tri-sector antennas consider the same antenna configuration for all BSs. Figure 3.2 illustrates the interference model in unicast mode when tri-sector antennas are used. It considers three cells from different BS sites and two UEs. The beam in each sector is pointed in the boresight direction. Thus, the power received from interfering cells depends only on the angle between the boresight and the UE, θ.

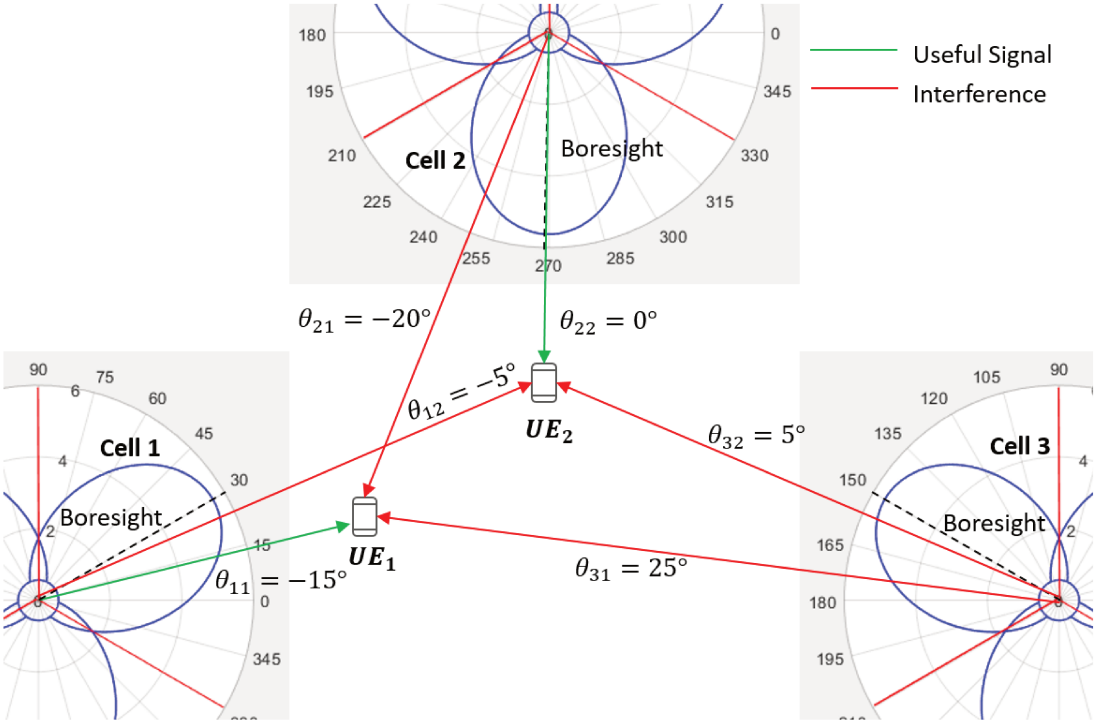

Figure 3.2 – Interference model considering Tri-sector antennas.

However, when using beamforming, the power received from interfering cells depends on θ and the steering angle of the beam, ϕ. Figure 3.3 illustrates the interference model when using beamforming. The serving cell for UE_1 is Cell 1, therefore the beam is pointed

towards the user and $\theta_{11} = \phi_1 = 0°$. Similarly, the serving cell for UE_2 is Cell 3 thus, $\theta_{32} = \phi_3 = 30°$. Notice that Cell 2 generates interference power for UE_1 and UE_2, and it depends on the steering angle ϕ_2 which is arbitrarily set to 45°. Therefore, we need a model to set the steering angle of interfering beams.

We need to calculate the probability distribution of ϕ under the assumption that beams from interfering sectors serve other users. To do so, we run several Monte Carlo simulations in which we place a user in the center of the plane and point the beams of the closest sectors towards it, $\theta_{\mathrm{s}} = \phi_{\mathrm{s}}$. Then, we calculate the received signal power from each beam and select the one that provides the highest as the serving cell. In Figure 3.4 we present the empirical PDF of the angle between the boresight of the serving sector and the UE, θ_{s}. Then, we estimate a probability model that follows this distribution. It is a normal distribution with zero mean and a standard deviation of 0.665 truncated in $[-\pi/3, \pi/3]$. The PDF of θ_s, $f(\theta_s)$, for $-\pi/3 < \theta_s < \pi/3$, is given by

$$f(\theta_s) = \frac{1}{0.665} \times \frac{\phi(\frac{\theta_s}{0.665})}{\Phi(\frac{\pi/3}{0.665}) - \Phi(\frac{-\pi/3}{0.665})}, \tag{3.7}$$

where

$$\phi(x) = \frac{1}{\sqrt{(2\pi)}} \exp(-\frac{1}{2}x^2), \tag{3.8}$$

is the PDF of the standard normal distribution and

$$\Phi(x) = \frac{1}{\sqrt{(2\pi)}} \int_{-\infty}^{x} e^{-\frac{t^2}{2}} dt, \tag{3.9}$$

is the CDF.

We verified that the data follows this distribution with a Kolmogorov-Smirnov test. This test is used to determine if a sample (an empirical set of data) comes from a population with a specific distribution. If the test yields a probability value (p-value) higher than 0.05 then the sample follows the distribution with a reliability of 95%. In our case, we obtained a p-value of 0.428. Thus, we use this distribution to set the steering angle of all the interfering cells in our simulations.

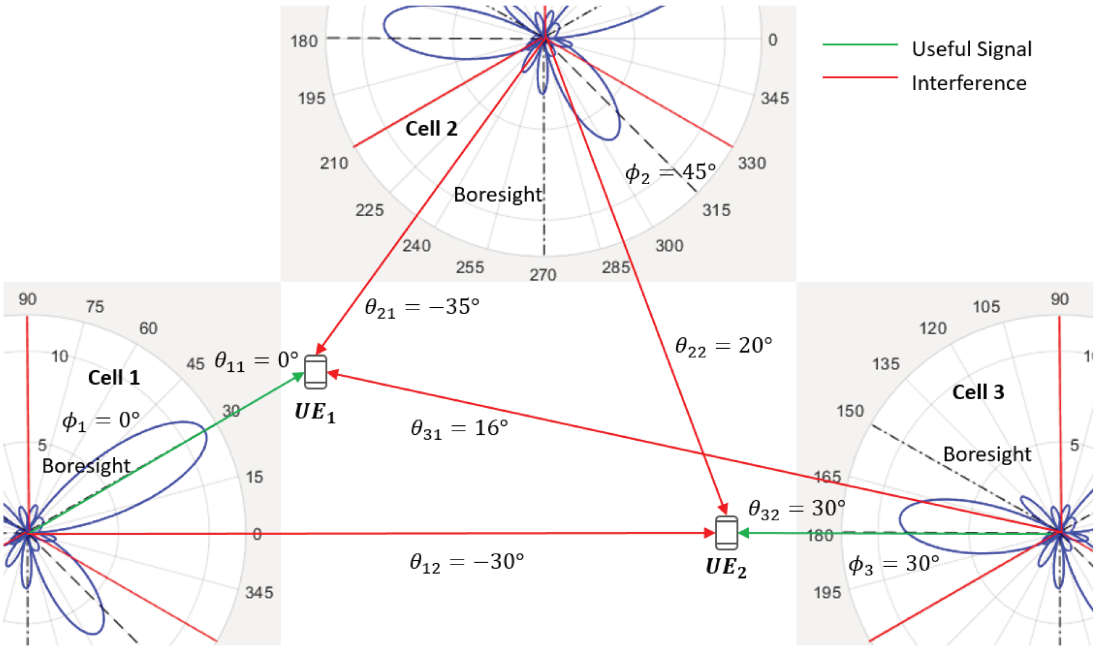

Figure 3.3 – Interference model considering Beamforming

3.2.3 SINR in MBSFN mode

In MBSFN mode, all cells belonging to the MBSFN area transmit the same waveform at the same time to the group of BC users. However, if MBSFN base stations are located far from the user, they may not contribute to the useful signal power but rather to the interference power.

Interference in MBSFN mode

Consider a BS i, different from the serving BS, in a MBSFN area located at a distance r_i from a UE. Depending on the delay time with respect to the serving BS (τ_i) and the length of the Cyclic Prefix (T_{CP}), the received signal power can be useful, partially useful or interference. Note that we approximate the real distance r_i to the modified distance $r_{i_{\mathrm{m}}}$. It is assumed that the receiver is synchronized with the serving BS which is located at a distance r_{s}. Thus, $\tau_i = \frac{r_i - r_{\mathrm{s}}}{c}$, where c is the speed of light. Based on the model presented in [36], the usefulness of the signals received during a MBSFN transmission can be derived as

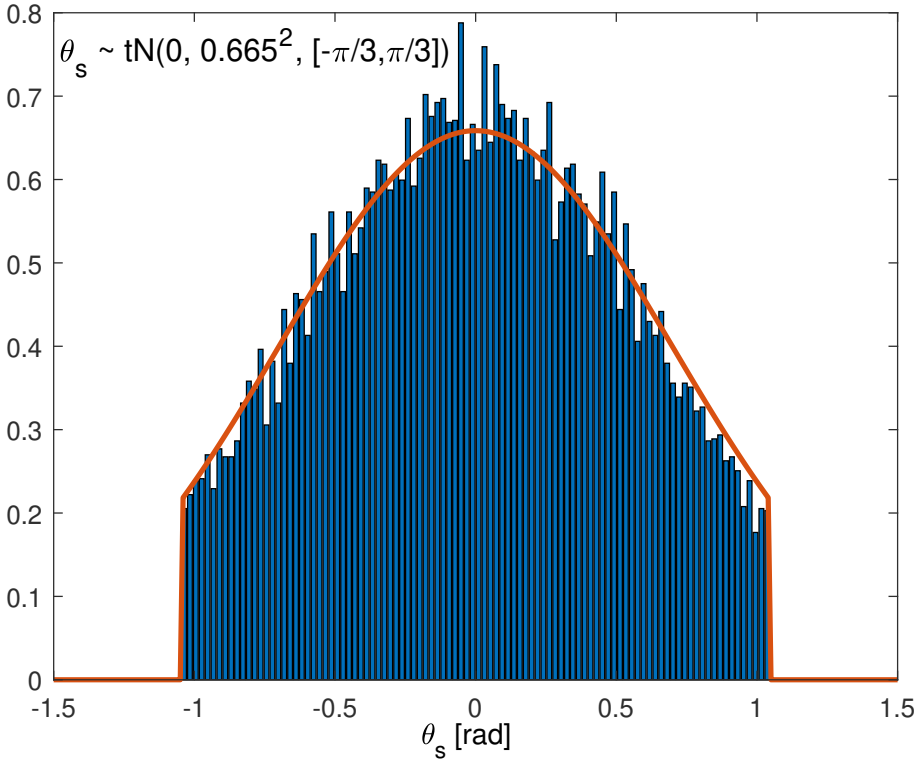

Figure 3.4 – PDF of the steering angle of the serving BS (θ_s)

$$\delta_i = \begin{cases} 1 & 0 \leq r_i - r_\mathrm{s} \leq c\,T_\mathrm{CP} \\ (1 + \frac{T_\mathrm{CP}}{T_\mathrm{u}} + \frac{r_\mathrm{s} - r_i}{c\,T_\mathrm{u}})^2 & c\,T_\mathrm{CP} < r_i - r_\mathrm{s} \leq c\,T_\mathrm{f} \\ 0 & r_i - r_\mathrm{s} > c\,T_\mathrm{f} \end{cases}, \tag{3.10}$$

where T_u is the useful symbol time and $T_\mathrm{f} = T_\mathrm{CP} + T_\mathrm{u}$ is the total OFDM symbol time. Using (3.10) we account for the fact that BS located far from the UE do not contribute to the useful signal power even if they belong to the MBSFN area.

SINR calculation in MBSFN mode

The SINR for a receiver in MBSFN mode can be calculated as

$$S_\mathrm{SFN} = \frac{P_\mathrm{SFN}}{P_\mathrm{N} + I_\mathrm{SFN}}, \tag{3.11}$$

where P_SFN and I_SFN are the useful signal power and interference power respectively.

P_{SFN} is calculated as

$$P_{\text{SFN}} = P_{\text{tx}} k e^{\chi_{\text{c}}} \sum_{i \in \psi_{\text{SFN}}} \delta_i r_i^{-\alpha} h_i e^{\chi_i} \Omega(\theta_i, \phi_i), \tag{3.12}$$

where ψ_{SFN} represents the set of cells belonging to the MBSFN area.

$$I_{\text{SFN}} = P_{\text{tx}} k e^{\chi_{\text{c}}} \left(\sum_{i \in \psi_{\text{SFN}}} (1 - \delta_i) r_i^{-\alpha} h_i e^{\chi_i} \Omega(\theta_i, \phi_i) + \sum_{i \notin \psi_{\text{SFN}}} r_i^{-\alpha} h_i e^{\chi_i} \Omega(\theta_i, \phi_i) \right). \tag{3.13}$$

Notice that P_{SFN} and I_{SFN} have the factor $P_{\text{tx}} k e^{\chi_{\text{c}}}$ in common, therefore we can rewrite (3.11) as follows

$$S_{\text{SFN}} = \frac{\hat{P}_{\text{SFN}}}{\frac{P_{\text{N}}}{P_{\text{tx}} k e^{\chi_{\text{c}}}} + \hat{I}_{\text{SFN}}}, \tag{3.14}$$

where $\hat{P}_{\text{SFN}}$ and $\hat{I}_{\text{SFN}}$ are P_{SFN} and I_{SFN} divided by $P_{\text{tx}} k e^{\chi_{\text{c}}}$, respectively.

3.2.4 SINR Probability Distribution

When a UE perceives a low SINR, a high bandwidth is needed to satisfy a certain capacity requirement. However, the network cannot allocate all resources to a single user. Thus, generally, users with a bad link quality are left out of service. The probability of a receiver being out of service is called the Outage Probability (p_{o}) and is defined as

$$p_{\text{o}} = \mathbb{P}[S \leq s], \tag{3.15}$$

where S is a random variable (RV) representing the SINR and s is a fixed SINR value. The outage probability is the Cumulative Distribution Function (CDF) of the SINR. Conversely, the probability of a receiver being covered is called the Coverage Probability (p_{c}) and it is defined as

$$p_{\text{c}} = \mathbb{P}[S > s], \tag{3.16}$$

which is the Complementary Cumulative Distribution Function (CCDF) of the SINR. Therefore, $p_{\text{o}} = 1 - p_{\text{c}}$.

3.2.5 SINR comparison - Unicast versus MBSFN

We calculate the CDF of the SINR perceived by a user when receiving in UC mode and MBSFN mode using the Monte Carlo method. We consider a very large surface to locate the BSs and analyze each transmission mode separately. In MBSFN mode, we consider PPP-distributed BSs as in Figure 3.1 but with all BSs belonging to the MBSFN area. In theory, when considering a very large (infinite) cellular network with PPP distributed BSs, the placement of the UEs is not important because the distribution of the distances between the UE and the BS does not change. Therefore, we consider a UE located in the center of the simulated surface, the origin of the plane. We also consider tri-sector base stations for UC and MBSFN, and beamforming only for UC mode. In each iteration a new PPP for the BS location is generated and the SINR for a UE in UC and MBSFN modes are calculated based on (3.4) and (3.14). To be compliant with 3GPP standards, most of the simulation parameters were taken from [3, Table C.6] and are given in Table 3.1.

PARAMETER	VALUE
Area of the surface	$1600\,\mathrm{km}^2$
System Bandwidth (W)	5 MHz
Carrier Frequency (f_c)	2000 MHz
UE Noise Figure (γ)	9 dB
BS Transmission Power (P_{tx})	43 dBm
Useful OFDM Symbol Time (T_{u})	66.7 µs
Cyclic Prefix Length (T_{CP})	16.67 µs
Trisectored antenna gain (G_A)	15 dBi
Antenna frontback ratio (G_{FB})	20 dBi
3 dB beam width (θ_{3dB})	65°
Shadowing Standard Deviation (σ_{dB})	10 dB
Shadowing Correlation Coefficient (ρ)	0.5
Noise Power (P_{N})	−98 dBm
Path Loss Exponent (α)	3.76
Path Loss Factor (k)[1]	0.0295
Target coverage probability ($p_{\mathrm{c_T}}$)	95 %

[1] For distance in meters.

Table 3.1 – Simulation parameters

Figure 3.5 presents the average useful signal power the UE perceives in each transmission mode. We evaluate 2 different BS densities, $\lambda_{\mathrm{BS}_1} = 0.25$ BS/km^2 and $\lambda_{\mathrm{BS}_2} = 2$ BS/km^2. In UC mode we consider four cases: tri-sector base stations without beamforming, and beamforming with 2, 4 and 8 antennas per sector. We see that the difference between UC without beamforming and MBSFN is small. This means that most of the useful signal power in MBSFN mode comes from the serving cell. However, when beamforming is used, the useful signal power level in UC increases with the number of antennas per sector. Using $M = 2$ the average signal power in UC is already higher than in MBSFN. Furthermore, we see that both transmission modes provides a higher signal power with the higher BS density. However, the gap between beamforming with 8 antennas and MBSFN is reduced.

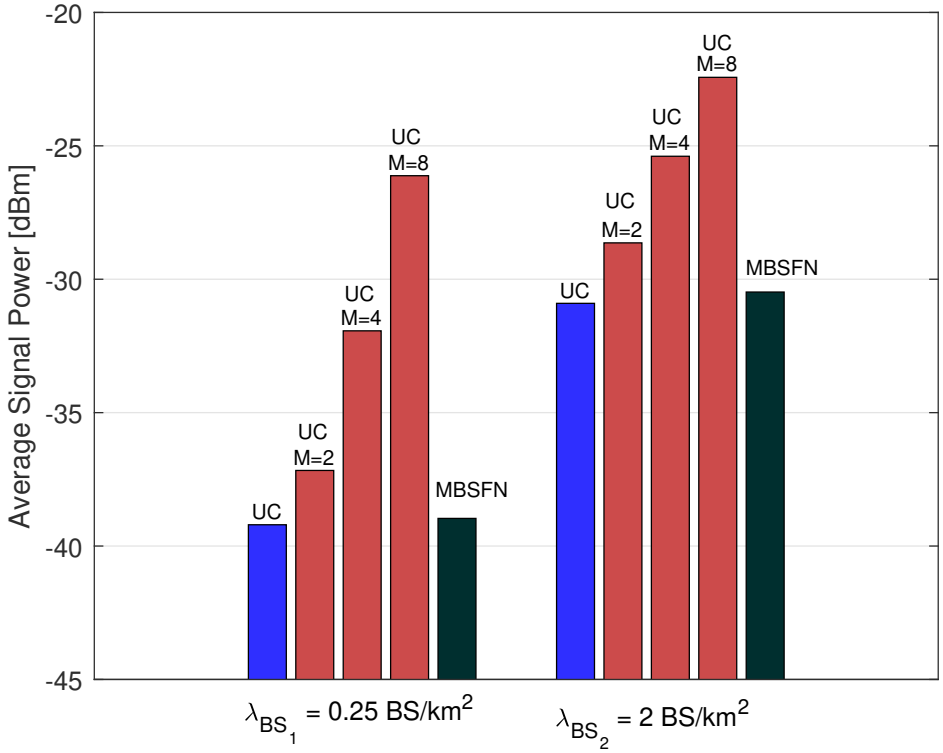

Figure 3.5 – Average Signal power for UC mode, including beamforming with different number of antennas M, and BC mode, considering all BSs as part of the SFN area, for different values of BS density λ_{BS}.

In terms of interference, it is clear that in MBSFN the interference is drastically reduced when compared to UC, see Figure 3.6. This was expected since all cells in the MBSFN area transmit the same signal. On the other hand, under the assumptions and context of

our work, the reduction of interference due to beamforming in UC mode is small. Take into account that we consider the same transmission power for all BSs.

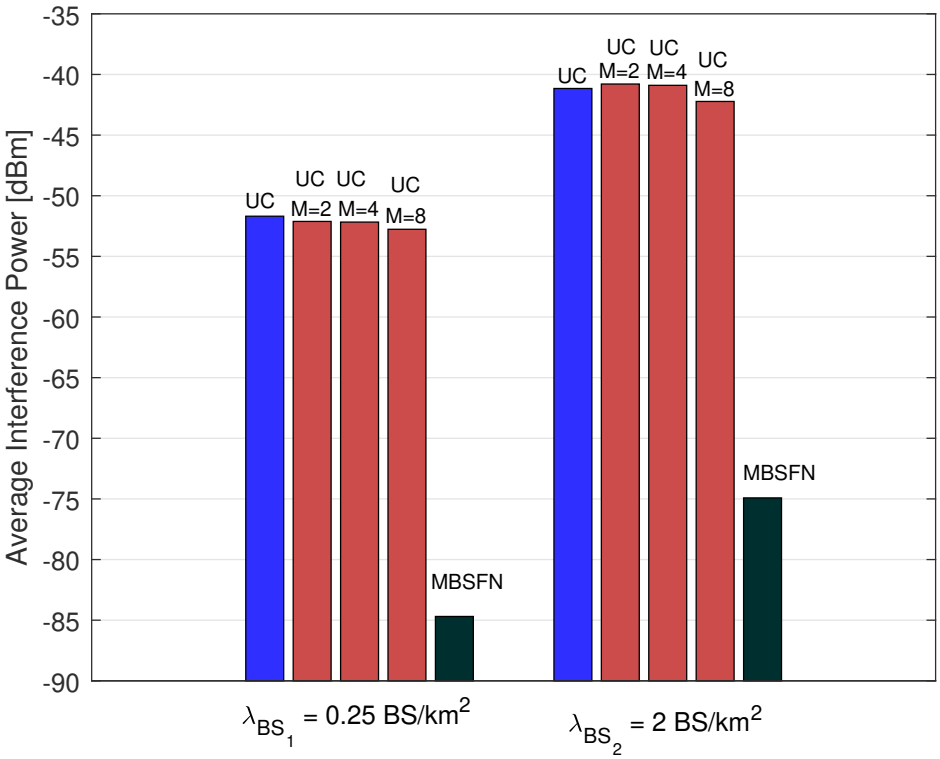

Figure 3.6 – Average Interference power for UC mode, including beamforming with different number of antennas M, and BC mode, considering all BS as part of the MBSFN area, for different values of BS density λ_{BS}.

Figure 3.7 shows the SINR CDF for a receiver in UC mode, including beamforming with a different number of antennas per sector (M), and MBSFN mode when considering a large MBSFN area, 1600 km^2. As expected, the beamforming technique increases the SINR in UC mode, the higher the number of antennas per sector (M), the higher the SINR, thanks to the increased signal power, as seen in Figure 3.5. However, the MBSFN mode provides a higher SINR that all UC cases due to the reduced interference power as seen in Figure 3.6. Notice in Figure 3.7 that the BS density does not have a significant effect when transmitting in UC mode. As seen in Figure 3.6 the interference power increases when increasing the BS density attenuating the effect of the increase in signal power. In contrast, when transmitting in MBSFN mode, the higher the BS density the higher the SINR. A higher number of BS in the MBSFN area increases the signal power while maintaining a

low interference.

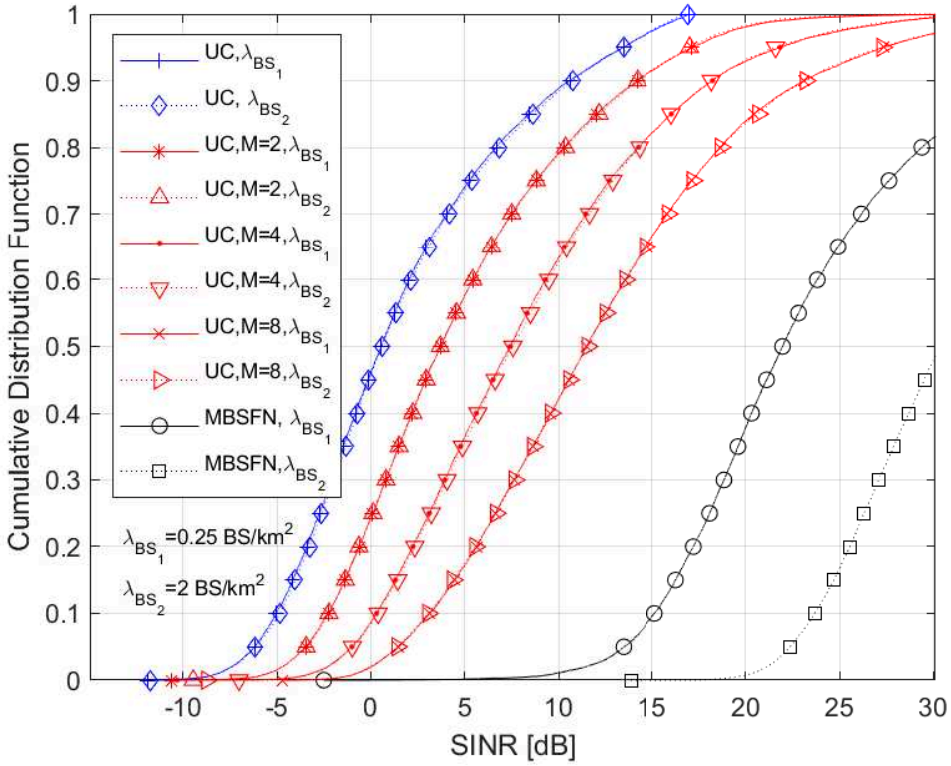

Figure 3.7 – Cumulative Distribution Function of the SINR perceived by a UE in UC mode, including beamforming with different number of antennas M, and MBSFN mode, considering all BS as part of the MBSFN area, for different values of BS density λ_{BS}.

3.2.6 SINR with fixed size MBSFN areas

The assumption that all the BS in the simulated surface belong to the MBSFN area is valid if we consider an MBSFN area in the scale of a Nation wide deployment. However, MBSFN areas can have different sizes depending on the coverage objective or application. Figure 3.8 shows the CDF of the SINR in MBSFN mode when the MBSFN area is formed by the N_{BS} BSs closer to the origin of the plane, as in Figure 3.1. BSs outside the MBSFN area generate interference. Two different BS densities are considered $\lambda_{\text{BS}_1} = 0.25\,\text{BS/km}^2$ and $\lambda_{\text{BS}_2} = 2\,\text{BS/km}^2$. In this case, we limit the maximum value of N_{BS} based on the maximum geographical size of the MBSFN area. It is set to half the size of the total simulated surface, i.e. 800 km^2. This is $N_{\text{BS}} = 200$ BS and $N_{\text{BS}} = 1600$ BS for λ_{BS_1} and

λ_{BS_2} respectively. Keep in mind that each BS represents three cells. As expected, the SINR increases with the number of BSs in the MBSFN area. Notice that for the same value of N_{BS}, the BS density doesn't have an important effect on the SINR. However, if N_{BS} is fixed, with a reduced BS density the MBSFN area covers a larger geographical area. On the other hand, if the objective is to increase the SINR in a surface with a fixed size, i.e. $800\,\mathrm{km}^2$, the operator should deploy more BS as part of the MBSFN area, thus, increase the BS density. As seen in Figure 3.8, an MBSFN area with $N_{\mathrm{BS}} = 1600$ BS provides a higher SINR than an MBSFN area with $N_{\mathrm{BS}} = 200$ BS.

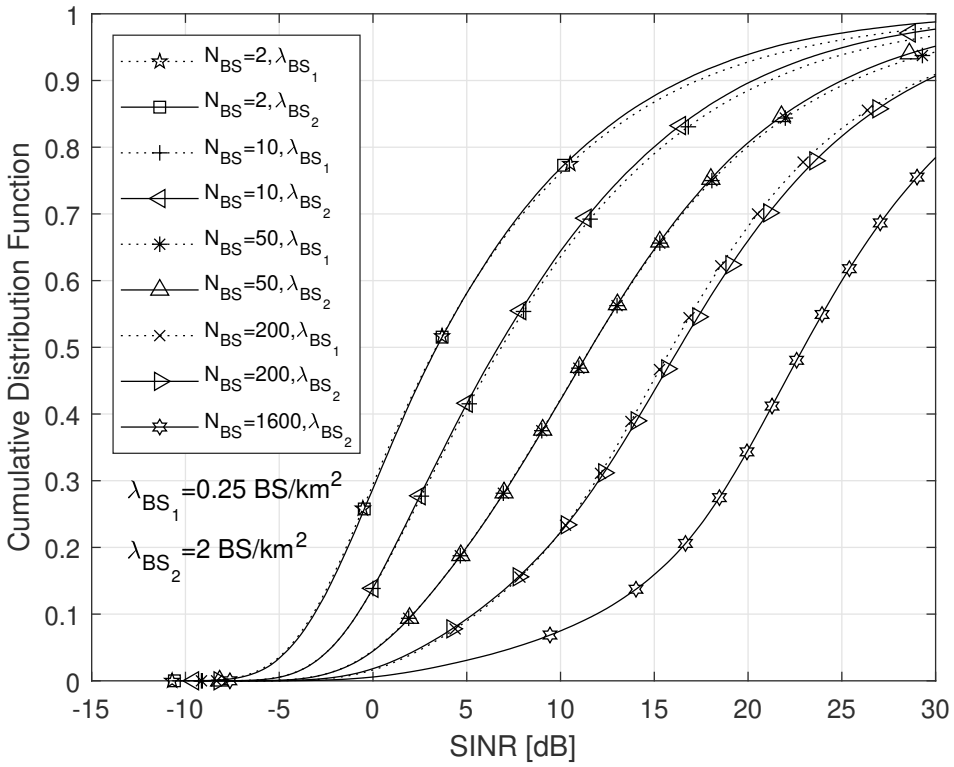

Figure 3.8 – Cumulative Distribution Function of the SINR for a UE in MBSFN mode considering MBSFN areas with a fixed number of BS (N_{BS}) for different values of BS density λ_{BS}.

3.3 Radio Resource Utilization

Hereafter we present the resource utilization model we use to compare the efficiency of UC and MBSFN transmission modes. Consider a certain service with a capacity requirement

(C) in bits per second (bps). According to Shannon's theorem, the capacity of a system (C) can be calculated as $C = W \log_2(1 + S)$, where W represents the system bandwidth and S the SINR. Then, the bandwidth required to transmit a service with a capacity requirement C, can be calculated as

$$W = C \frac{1}{\log_2(1 + S)}. \tag{3.17}$$

3.3.1 Resource utilization in Unicast mode

The UC transmission mode uses link adaptation. Thus, to calculate the average bandwidth used per UC user (W_{UC}), we take the expected value of (3.17). It is usual in mobile networks to fix a target coverage probability ($p_{\mathrm{c_T}}$) to determine an acceptable percentage of users that can be let out of service such that $p_{\mathrm{c_T}} = \mathbb{P}[S > s_m]$, where s_m is the minimum SINR to cover. Therefore, W_{UC} is calculated as

$$W_{\mathrm{UC}} = C\,\mathbb{E}\left[\frac{1}{\log_2(1 + S_{\mathrm{UC}})}\middle| S_{\mathrm{UC}} > S_{\mathrm{m_{UC}}}\right] = C\Gamma_{\mathrm{UC}}, \tag{3.18}$$

where S_{UC} is a RV representing the SINR for a UE receiving in UC mode, $S_{\mathrm{m_{UC}}}$ is the minimum SINR to cover in UC mode to get the target coverage probability and Γ_{UC} is the ratio between bandwidth and capacity in UC mode.

3.3.2 Resource utilization in MBSFN mode

MBSFN transmissions do not benefit from link adaptation. Thus, transmissions are done aiming to cover the users with the lowest SINR in the UC group. The average bandwidth used per cell in MBSFN mode (W_{SFN}) is given by

$$W_{\mathrm{SFN}} = C \frac{1}{\log_2(1 + s_{\mathrm{m_{SFN}}})} = C\Gamma_{\mathrm{SFN}}, \tag{3.19}$$

where $s_{\mathrm{m_{SFN}}}$ is the target SINR of the MBSFN transmission which is fixed based on the coverage requirement, and Γ_{SFN} is the ratio between bandwidth and capacity in MBSFN mode.

3.3.3 User Threshold

Consider an MBSFN area formed by N_{SFN} cells and N_{U} users demanding the same content. Notice that $N_{\mathrm{SFN}} = 3N_{\mathrm{BS}}$ in tri-sector BS deployments. In such scenario, the UC transmission mode consumes more resources than the MBSFN transmission mode if

$$N_{\mathrm{U}} W_{\mathrm{UC}} > N_{\mathrm{SFN}} W_{\mathrm{SFN}}. \tag{3.20}$$

We define the User Threshold (U_{T}) as the number of users per cell in the MBSFN area from which the UC mode consumes more resources than the MBSFN mode. It can be calculated by solving (3.20) for N_{U} and dividing by N_{SFN} as follows

$$\begin{aligned} N_{\mathrm{U}} &> \frac{W_{\mathrm{SFN}} N_{\mathrm{SFN}}}{W_{\mathrm{UC}} N_{\mathrm{SFN}}} \\ &> \frac{C\Gamma_{\mathrm{SFN}}}{C\Gamma_{\mathrm{UC}}} \\ &> \frac{\Gamma_{\mathrm{SFN}}}{\Gamma_{\mathrm{UC}}}, \end{aligned} \tag{3.21}$$

therefore,

$$U_{\mathrm{T}} = \frac{\Gamma_{\mathrm{SFN}}}{\Gamma_{\mathrm{UC}}}. \tag{3.22}$$

Figure 3.9 presents the User threshold (U_{T}) versus the number of cells in the MBSFN area (N_{SFN}) for different UC configurations. Notice that even when an MBSFN area is formed by only 2 base stations (6 cells) and UC transmissions are performed using beamforming with 8 antennas per sector, MBSFN outperforms UC when there are at least 8 users per cell demanding the same content.

3.4 Summary

In this chapter we analyze and compare the performance of UC transmission and MBSFN transmission from a resource utilization perspective. We started with a review of the definition of MBMS and MBSFN transmission in cellular networks. Then, we epitomize the evolution of MBMS in 3GPP standards from its beginnings in Release 6 to the enhancements expected in Release 17. Afterwards, a state of the art on the comparison

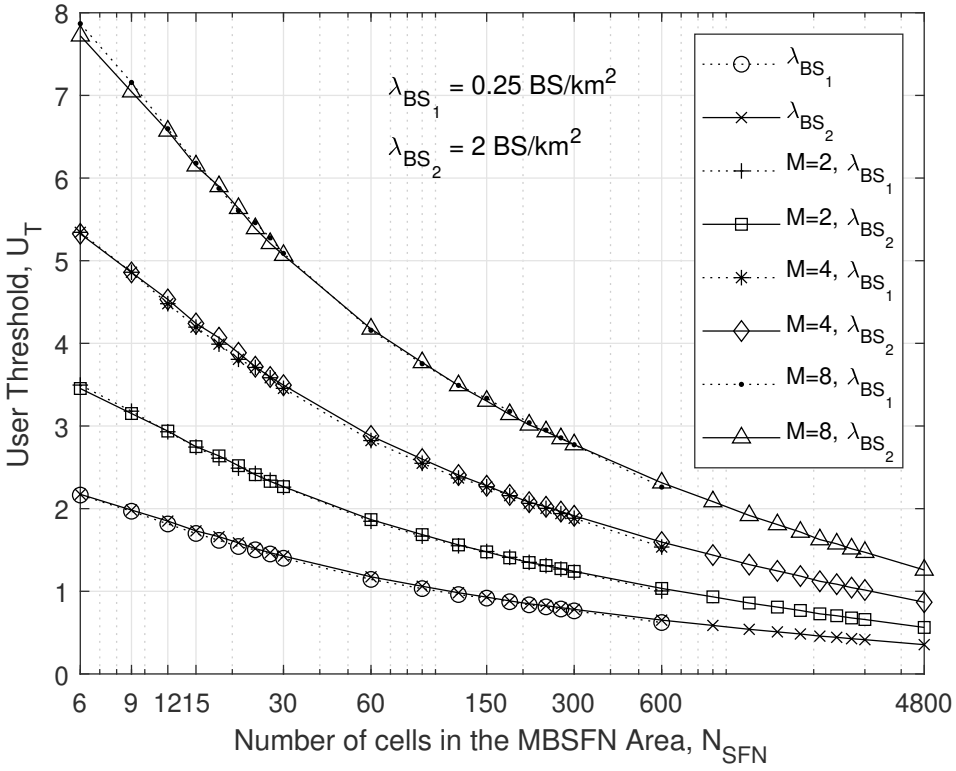

Figure 3.9 – User Threshold (U_{T}) versus Number of cells in the MBSFN Area (N_{SFN}) for different UC configurations and different values of BS density λ_{BS}.

between UC and MBSFN is presented. One of the major contributions of this chapter is the development of models to calculate the SINR in UC mode and MBSFN mode considering Poisson distributed base stations, tri-sector antennas, MBSFN areas with different number of base stations and beamforming in UC mode.

We observe that the main advantage of MBSFN over UC is the reduction of interference power. When considering large MBSFN areas, the useful signal power in UC with beamforming can surpass that of MBSFN, but the interference power is always much higher in UC than in MBSFN. This leads to MBSFN to provide a higher SINR than UC, specially in dense base station deployments. However, if the MBSFN area is formed by a small number of cells, the SINR in UC with beamforming can surpass the SINR in MBSFN mode.

An important part of the chapter presents the model we use to compare the radio resource utilization in UC mode and MBSFN mode based on Shannon's theorem. We propose a method to calculate the number of users per cell in the MBSFN area from which

the MBSFN mode is more efficient than the UC mode. Results show that even when an MBSFN area is formed by only 2 base stations and UC transmissions are performed using beamforming with 8 antennas per sector, MBSFN outperforms UC when there are at least 8 users per cell demanding the same content.

In this chapter we use an approach that is common when studying PPP distributed BS deployments in cellular networks, we study the case of a user located in the origin of the plane. This assumption is well established for UC studies and very large MBSFN areas. However, in the case of a small MBSFN area it is interesting to consider the case of users located close to the borders of the MBSFN area since they are expected to have the lowest SINR. In Chapter 4 we study this scenario and propose an analytical method to calculate the SINR distribution of users located at any place inside the MBSFN area.

Chapter 4

A Tractable Approach to resource utilization and energy consumption in MBMS

This chapter presents analytical expressions to calculate the SINR distribution for users receiving in UC, MBSFN and SC-PTM transmission modes. The analytical expressions are developed using tools from stochastic geometry. We integrate these expressions with the user threshold model from Chapter 3 and propose a method to calculate it analytically. We also present an energy consumption model for MBMS. We develop analytical expressions to calculate the energy consumption of the BSs and UE when receiving in unicast, MBSFN and SC-PTM. Using these expressions we calculate the user threshold to switch from unicast to BC in order to reduce energy consumption.

In Section 4.1 we present a short overview of the analysis of UC and BC transmission modes using stochastic geometry. We emphasize the related work that set the basis or our study. Then, in Section 4.2 we develop an expression to calculate the SINR Complementary Cumulative Distribution Function (CCDF) (probability of coverage) for a user receiving in MBSFN mode located at any place inside the MBSFN area. We confirm the correctness of this expression by comparing its results with the ones obtained through Monte Carlo simulations. Afterwards, in Section 4.3 we propose analytical methods to calculate the user threshold to reduce radio resource utilization by switching from unicast to MBSFN or SC-PTM.

The second part of this chapter is centered on energy consumption. In Section 4.4 we present analytical models to calculate the energy consumption in unicast, MBSFN , and SC-PTM transmission modes from the BS and UE sides. We use power consumption models from the literature and the analytical expressions for the SINR distribution for each transmission mode. We compare the energy consumption in unicast and MBMS and show that MBMS allows to reduce BS and UE energy consumption in various scenarios. Then,

in Section 4.5 we compute the user threshold to reduce BS and UE energy consumption analytically. We prove that the user threshold to reduce BS energy consumption is the same than the user threshold to reduce radio resource utilization. However, the user threshold to reduce UE energy consumption is lower.

4.1 Stochastic Geometry and Cellular Networks

Stochastic geometry refers to the study of random spatial patterns, the most important one being the Poisson Point Process (PPP). A point process is a countable random collection of points that reside in some measure space, usually the Euclidean space $\mathbb{R}^d$. In this thesis, the location of the base stations over the two-dimensional plane is modeled as a point process, thus, the PPP takes place in the Euclidean space $\mathbb{R}^2$.

In cellular network analysis, modeling the location of Base Stations (BS) as a PPP enables stochastic geometry concepts and theorems to be used. This approach allows the development of mathematical expressions to estimate performance indicators as the probability of coverage or the data rate [11][45]. Furthermore, the results obtained when considering a PPP distribution for the BS are pessimistic compared to actual cellular network deployments [11]. This allows to guarantee a minimum performance level.

Researchers have developed expressions to calculate the probability of coverage of a user when receiving in unicast and MBSFN transmission modes using stochastic geometry.

4.1.1 Probability of coverage in unicast

Andrews, Baccelli, and Ganti developed in [11] an expression to calculate the probability of coverage (SINR CCDF) of a user in unicast mode. They consider omnidirectional BSs located according to a PPP of density λ_{BS}, as in Figure 3.1 but with all BSs transmitting in unicast mode. The path loss model is based on Okumura-Hata-Cost231 with fading. The path loss exponent is denoted as α and the path loss factor as k. Rayleigh fading is modeled as an exponential Random Variable (RV) h with unit rate and shadowing is not considered. Under these assumptions, the probability of coverage in unicast ($p_{\mathrm{c_{UC}}}$), which is the probability that the SINR is above the threshold s as presented in (3.16), is calculated as

$$p_{\mathrm{c_{UC}}}(s) = \pi\lambda_{\mathrm{BS}} \int_0^\infty e^{-\pi\lambda_{\mathrm{BS}} v(1+\rho(s,\alpha)) - s\frac{p_{\mathrm{N}}}{P_{\mathrm{tx}}k} v^{\alpha/2}}\, dv, \tag{4.1}$$

where

$$\rho(s,\alpha) = s^{2/\alpha} \int_{s^{-2/\alpha}}^{\infty} \frac{1}{1+u^{\alpha/2}}\, du, \tag{4.2}$$

where P_{tx} denotes the BS transmission power and s is the SINR threshold.

Figure 4.1 presents the CDF in unicast mode considering different BS densities and path loss exponents, α. We compare the CDF obtained using (4.1) with the one obtained through Monte Carlo simulations and the curves match perfectly. Notice that for the same value of α we get the same CDF for different λ_{BS} values. This is because with a higher BS density the received signal power increases but also does the interference. With the transmission power considered, the noise is much lower than the interference. Therefore, for these α values and the considered noise power, the SINR CDF in unicast mode is practically the same as the Signal to Interference Ratio (SIR) CDF and thus it does not depend on the BS density.

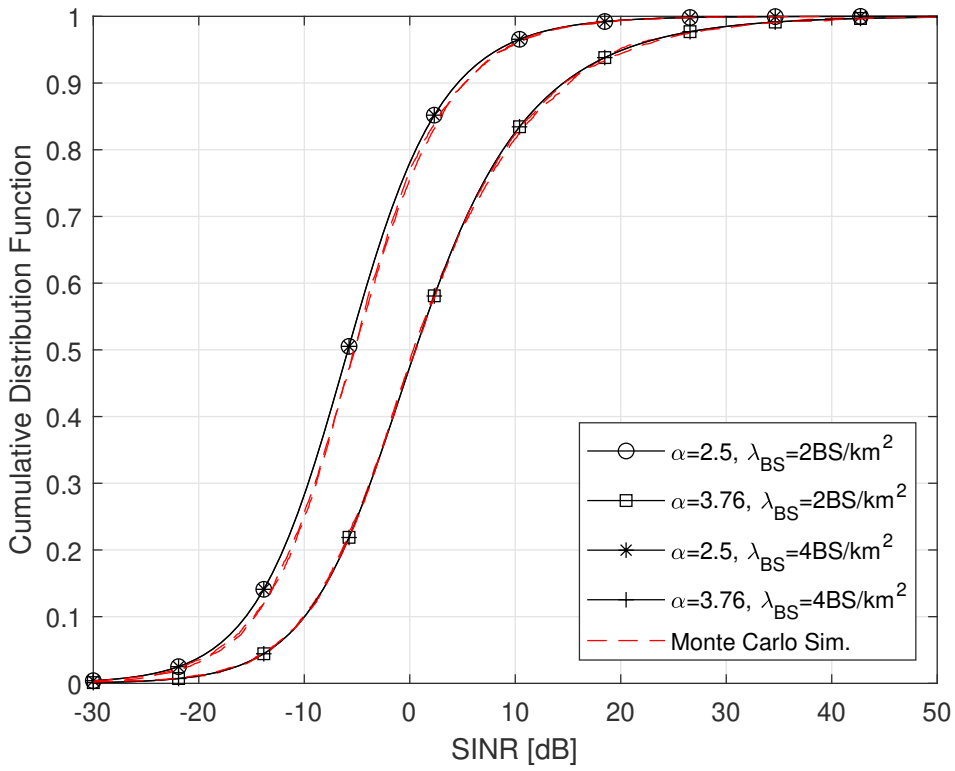

Figure 4.1 – CDF of the SINR for a UE in unicast mode considering different values of α and λ_{BS}. Curves obtained via the analytical expression (4.1) and Monte Carlo simulations.

4.1.2 Probability of coverage in MBSFN

Most recently, Sahu, Chaurasia, and Gupta found an expression to calculate the probability of coverage for a user receiving in MBSFN mode [45]. The propagation model is the same than in [11]. They consider PPP-distributed BS located in a circular surface of radius R and a UE located at the origin of the plane. The model assumes that all the BS belong to the MBSFN area but only those located at a distance shorter or equal to R_{s} provide useful signal power. BSs at a distance larger than R_{s} generate interference because their signals are delayed. R_{s} is called the connectivity radius. See Figure 4.2. Under these assumptions, the probability of coverage ($p_{\mathrm{c_{SFN}}}$), which the probability than the SINR is higher than a threshold s, is calculated as

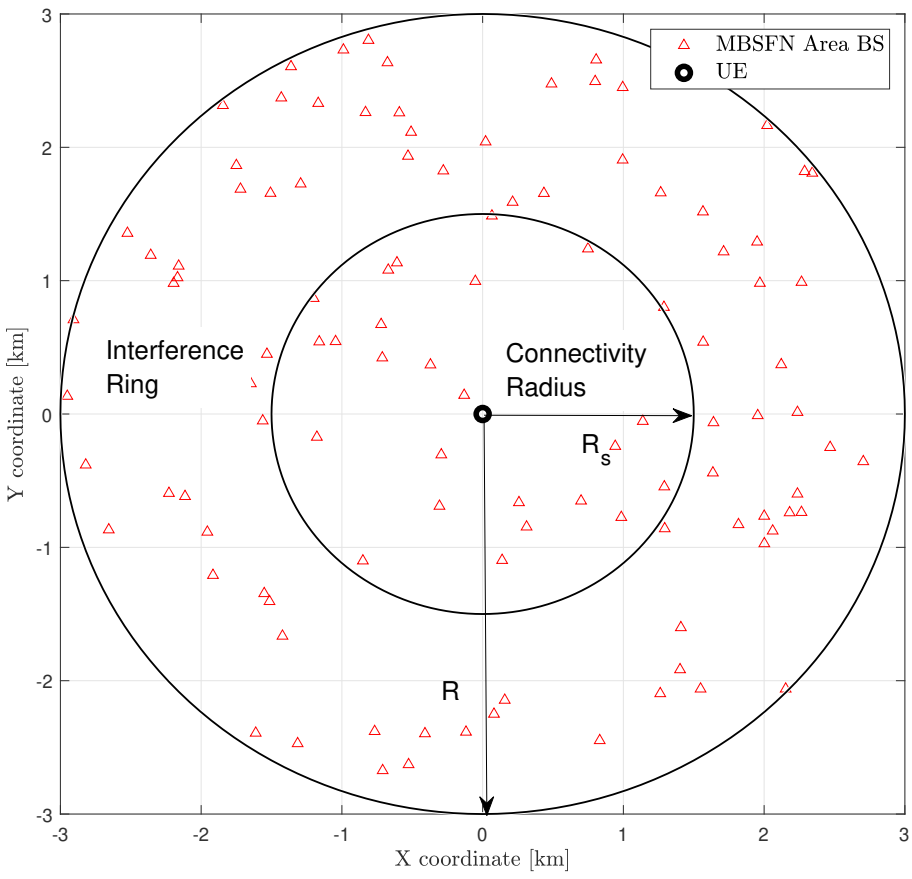

Figure 4.2 – Model considered by Sahu, Chaurasia, and Gupta.

$$p_{c_{\mathrm{SFN}}}(s) = \frac{1}{2} + \frac{1}{\pi}\int_0^\infty \frac{1}{t}\,\mathrm{Im}\left[e^{-jts\frac{p_{\mathrm{N}}}{P_{\mathrm{tx}}k}} e^{-2\pi\lambda_{\mathrm{BS}}t^{2/\alpha}(M(t,s)+jN(t,s))/(2\alpha)}\right] dt, \tag{4.3}$$

where

$$\begin{aligned} M(t,s) = s^{2/\alpha}\Bigg[& \mathrm{B}\left(\frac{1}{\alpha}, -\frac{1}{\alpha}+1; \frac{1}{1+t^2s^2R^{-2\alpha}}\right) \\ & - \mathrm{B}\left(\frac{1}{\alpha}, -\frac{1}{\alpha}+1; \frac{1}{1+t^2s^2R_{\mathrm{s}}^{-2\alpha}}\right)\Bigg] \\ & - \mathrm{B}\left(\frac{1}{\alpha}, -\frac{1}{\alpha}+1; \frac{1}{1+t^2R_{\mathrm{s}}^{-2\alpha}}\right), \end{aligned} \tag{4.4}$$

$$\begin{aligned} N(t,s) = s^{2/\alpha}\Bigg[& \mathrm{B}\left(\frac{1}{\alpha}+\frac{1}{2}, -\frac{1}{\alpha}+\frac{1}{2}; \frac{1}{1+t^2s^2R^{-2\alpha}}\right) \\ & - \mathrm{B}\left(\frac{1}{\alpha}+\frac{1}{2}, -\frac{1}{\alpha}+\frac{1}{2}; \frac{1}{1+t^2s^2R_{\mathrm{s}}^{-2\alpha}}\right)\Bigg] + \\ & \mathrm{B}\left(\frac{1}{\alpha}+\frac{1}{2}, -\frac{1}{\alpha}+\frac{1}{2}; \frac{1}{1+t^2R_{\mathrm{s}}^{-2\alpha}}\right) \end{aligned} \tag{4.5}$$

and $\mathrm{B}(x, y; z)$ is the incomplete Beta function which is defined as

$$\mathrm{B}(x,y;z) = \int_0^z u^{x-1}(1-u)^{y-1}\,du. \tag{4.6}$$

This expression considers a user at the center of the MBSFN area, as in Figure 4.2. This is an ideal case in MBSFN since the BSs surrounding the user provide useful signal power but, in reality, we can find UEs located at the border of the MBSFN area. In that case, the interference, generated by the BSs located at a distance $r > R_{\mathrm{s}}$ from the origin, increases and the SINR for the user is lower.

4.2 Location dependent SINR distribution in MBSFN

In MBSFN transmission mode, the MCS, and therefore the data rate, are fixed. The values are based on the users in the broadcast group with the lowest SINR and the coverage target. Therefore, it is important to find an expression to calculate the probability of

coverage in MBSFN mode for a UE located anywhere in the MBSFN area. This allows to extend the performance analysis, notably to consider the case of a user at the border of the MBSFN area.

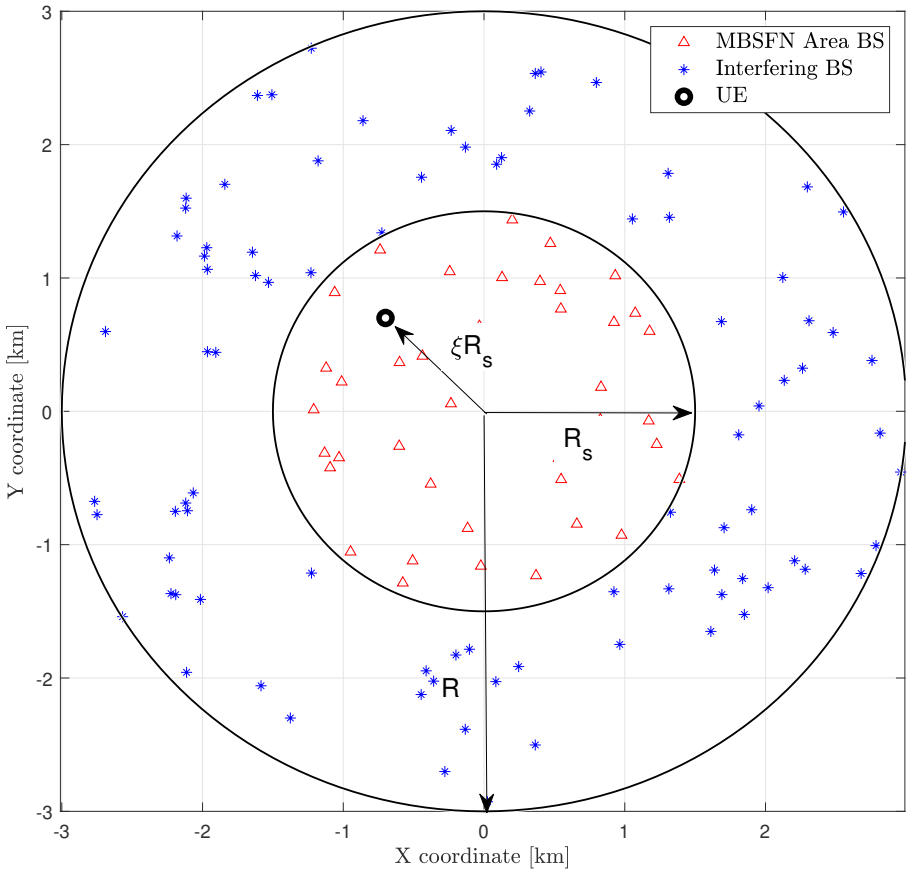

Figure 4.3 – Extended Model for the SINR distribution in MBSFN mode.

We consider that the MBSFN area is formed by the BSs located at a distance $r \leq R_s$ from the origin. The UE can be located at any distance ξR_s from the origin, such that $0 \leq \xi \leq 1$ as shown in Figure 4.3. The model in [45] considers only the case $\xi = 0$. However, the assumption that the signals from all the BSs inside the MBSFN area are useful for a user at the border ($\xi = 1$) is valid for values of $R_s < 2.5$ km when using the Orthogonal Frequency-Division Multiplexing (OFDM) extended CP. This is because $c \times T_{CP} = 5$ km, where c denotes the speed of electromagnetic waves and $T_{CP} = 16.67$ µs the CP length. This length of R_s is useful for scenarios with a coverage area smaller than 20 km^2.

We can also think of ξR_s as the radius of a target service area, see Figure 4.4. It is the size of the area where the users are located. In that case, UEs located at a distance ξR_s from the origin have the lowest SINR.

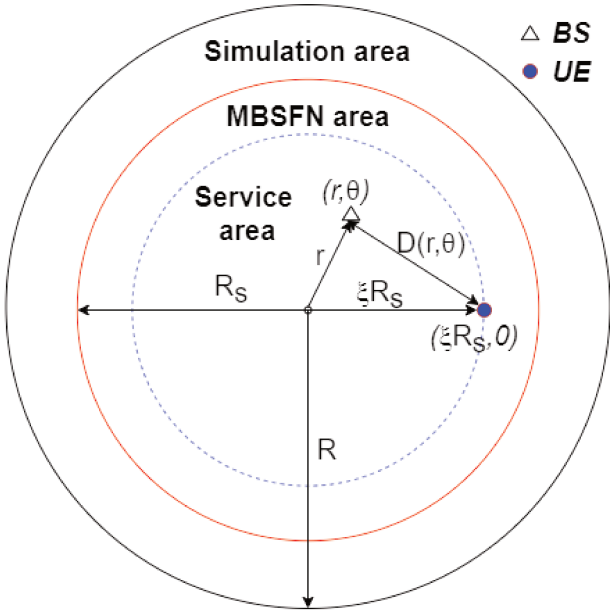

Figure 4.4 – Extended model for the SINR distribution in MBSFN mode. Service area with radius ξR_s.

As presented in [45], the probability of coverage of a user in a MBSFN network, $p_{c_{SFN}}$, is obtained by calculating the Laplace transform of the interference (I) and the Laplace transform of the useful signal power (P) such that

$$p_{c_{SFN}}(s) = \frac{1}{2} + \frac{1}{\pi}\int_0^\infty \frac{1}{t}\,\mathrm{Im}\left[\mathscr{L}_I(jts)e^{-jts\frac{P_N}{P_{\mathrm{tx}^k}}}\mathscr{L}_P(-jt)\right]dt. \tag{4.7}$$

In [45] P and I are random variables because they are dependant on fading which is modeled as an exponential random variable.

The objective is to calculate the probability of coverage in MBSFN mode for a user located at a distance ξR_s from the origin as shown in 4.4. The Laplace transform of P is calculated as a function of the distance between a BS and the UE. The location of a BS can be represented as a vector x in polar coordinates, such that $||x|| = r \leq R_s$, see Figure 4.5. When considering the user located at the origin of the plane, $||x|| = r$ is the BS-UE distance. In our case, we denote the UE location (vector) as y and the distance between the BS and the UE is $||x - y||$. Therefore, the Laplace transform of P can be

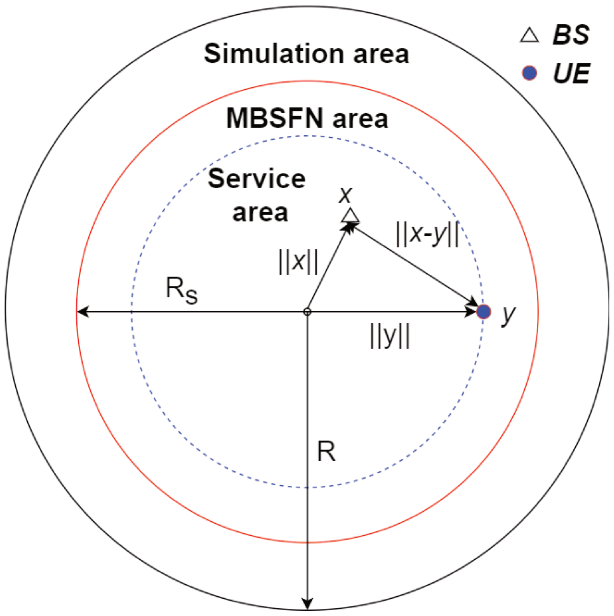

Figure 4.5 – Representation of vectors x and y for the location of BS and UE, respectively.

calculated as

$$\mathscr{L}_P(s_{\mathrm{L}}) = \exp\left(-\lambda \int_{A_{UE}} \left(1 - \mathbb{E}_h\left[e^{-s_{\mathrm{L}} h ||x-y||^{-\alpha}}\right]\right) dy\right), \tag{4.8}$$

where A_{UE} is the area where the UE can be located. We add the sub-index L to the traditional s of the Laplace transform (s_{L}) to avoid confusion with the variable s that denotes an SINR value. To solve the expected value in (4.8) we use the moment generating function of the exponential RV h which is calculated as

$$\mathrm{M}_h(a) = \mathbb{E}[e^{ah}] = \frac{1}{1-a}. \tag{4.9}$$

Afterwards, we express the integral over $\mathbb{R}^2$ in polar coordinates. The distance between the UE and the BS, $D(r,\theta)$ in Figure 4.4, is given by

$$D(r,\theta) = ||x-y|| = ((\xi R_{\mathrm{s}})^2 + r^2 - 2\xi R_{\mathrm{s}} r\cos(\theta))^{\frac{1}{2}}. \tag{4.10}$$

Then, the Laplace transform of P in polar coordinated is calculated as

$$\mathscr{L}_{P,\xi}(s_{\mathrm{L}}) = \exp\left(-\lambda \int_0^{R_{\mathrm{s}}} \int_0^{2\pi} \frac{s_{\mathrm{L}} r}{s_{\mathrm{L}} + D(r,\theta)^{\alpha}} d\theta dr\right). \tag{4.11}$$

Replacing (4.10) in (4.11) we get

$$\mathscr{L}_{P,\xi}(s_{\mathrm{L}}) = \exp\left(-\lambda \int_0^{R_{\mathrm{s}}} \int_0^{2\pi} \frac{s_{\mathrm{L}} r}{s_{\mathrm{L}} + ((\xi R_{\mathrm{s}})^2 + r^2 - 2\xi R_{\mathrm{s}} r\cos(\theta))^{\frac{\alpha}{2}}} d\theta dr\right). \tag{4.12}$$

Similarly, the Laplace transform for I can be calculated as

$$\mathscr{L}_{I,\xi}(s_{\mathrm{L}}) = \exp\left(-\lambda \int_{R_{\mathrm{s}}}^{R} \int_0^{2\pi} \frac{s_{\mathrm{L}} r}{s_{\mathrm{L}} + ((\xi R_{\mathrm{s}})^2 + r^2 - 2\xi R_{\mathrm{s}} r\cos(\theta))^{\frac{\alpha}{2}}} d\theta dr\right), \tag{4.13}$$

the only difference being the integration limits for r since interfering BS are at a distance r such that $R_{\mathrm{s}} < r < R$. By replacing (4.12) and (4.13) in (4.7) with the respective value of s_{L}, we obtain the probability of coverage for a UE located at a distance ξR_{s} from the origin in MBSFN mode. There is not a close form expression for the integrals in (4.12) and (4.13). Therefore, they are calculated numerically.

4.2.1 Confirmation of the analytical expression

PARAMETER	VALUE
Radius of the simulation area	10 km
System Bandwidth (W)	10 MHz
Carrier Frequency (f_{c})	700 MHz
BS Transmission Power (P_{tx})	46 dBm
Noise Power (P_{N})	−95 dBm
Path Loss Exponent (α)	3.76
Path Loss Factor (k)[1]	0.267
Target coverage probability ($p_{\mathrm{c_T}}$)	95 %

[1] For distance in meters.

Table 4.1 – Simulation parameters for Analytical Model.

A comparison between the outage probability (SINR CDF) obtained using the analytical expression in (4.7) and Monte Carlo simulations is presented in Figure 4.6. Simulation parameters are presented in Table 4.1. The first observation from these results is that the analytical and simulation curves match almost exactly. The 95% confidence intervals were calculated but they are not presented since they are small. This confirms the analytical

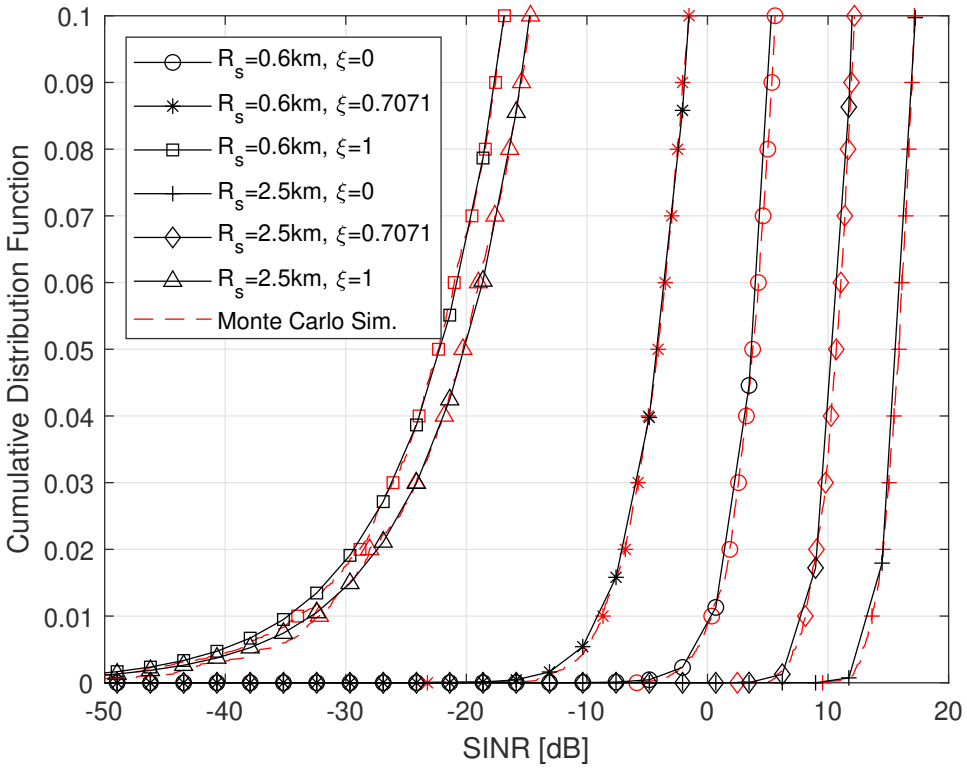

Figure 4.6 – CDF for a user receiving in MBSFN mode considering different values of ξ, R_s and $\lambda_{BS} = 12$ BS/km^2. Curves obtained via the Analytical expression in (4.7) and Monte Carlo simulations.

expression in (4.7). Now, the most pessimistic scenario for MBSFN is $\xi = 1$ because the interference generated by the cells outside the MBSFN area is high for a user at the border. Actually, it is possible that the BS providing the highest signal power is not in the MBSFN area. On the other hand, $\xi = 0$ is the most optimistic scenario since the user is in the middle of the MBSFN area. It is the model considered in [45]. We can observe that for an outage probability of 0.05 and $R_s = 2.5$ km, the SINR difference between the optimistic ($\xi = 0$) and pessimistic ($\xi = 1$) scenarios is 36 dB. A good compromise is to take the median value. Assuming that in a real deployment the UEs are uniformly distributed in the entire broadcast surface or radius R_s, half of the users are in the inner circle of radius $R_s/\sqrt{2}$. The SINR difference between the optimistic approach and the median approach for $R_s = 2.5$ km is 6 dB. Furthermore, we consider two radius of MBSFN area, $R_s = 0.6$ km and $R_s = 2.5$ km. Notice that for the same ξ value, the outage probability decreases when increasing R_s. This is because more cells participate in the MBSFN transmission

and therefore the SINR increases. However, this difference is smaller when $\xi = 1$ since the interference from cells outside the broadcast area increases drastically in both cases.

4.3 Tractable Calculation of the User Threshold

We defined the user threshold as the number of users per cell from which broadcast transmission becomes more efficient than unicast.

4.3.1 Unicast to SC-PTM

SC-PTM transmission is more efficient than unicast in terms of resource utilization if

$$N_{\mathrm{U}} W_{\mathrm{UC}} > N_{\mathrm{SC}} W_{\mathrm{SC}}, \tag{4.14}$$

where N_{U} is the number of users demanding the broadcast service, W_{UC} is the average bandwidth used by each user calculated using (3.18), N_{SC} is the number of cells that transmit in SC-PTM mode and W_{SC}, the bandwidth used by each cell in SC-PTM mode, is calculated as

$$W_{\mathrm{SC}} = C \left[\frac{1}{\log_2(1 + S_{\mathrm{m_{SC}}})} \right] = C\Gamma_{\mathrm{SC}}, \tag{4.15}$$

where $S_{\mathrm{m_{SC}}}$ is the minimum SINR to cover in the cell and can be calculated using (4.1) and the target coverage probability. Therefore, we can calculate the User Threshold for SC-PTM as

$$U_{\mathrm{T_{SC}}} = \frac{\Gamma_{\mathrm{SC}}}{\Gamma_{\mathrm{UC}}}. \tag{4.16}$$

As seen in (4.15), Γ_{SC} can be obtained using (4.1) and the coverage target.

In Subsection 3.3.3, Γ_{UC} is calculated through Monte Carlo simulations using (3.18). In this chapter, instead of Monte Carlo simulations we calculate Γ_{UC} using the law of the unconscious statistician: the expected value of a measurable function g of a RV X, given that X has a PDF $f(x)$, is given by:

$$\mathbb{E}\left[g(X)\right] = \int_{-\infty}^{\infty} g(x) f(x)\, dx. \tag{4.17}$$

The PDF of X, $f(x)$, can be obtained from its CDF, $F(x)$, as $f(x) = \frac{d}{dx} F(x)$. In our

case $X = S$ and $F(S)$ can be calculated using (4.1) since $F(S) = 1 - p_{\mathrm{c_{UC}}}(S)$. Furthermore, the function $g(S) = \frac{1}{log_2(1+S)}$, therefore

$$\Gamma_{\mathrm{UC}} = \int_{S_{\mathrm{m_{UC}}}}^{S_{\mathrm{M_{UC}}}} g(S) \left(\frac{d}{dS} F(S) \right) dS, \tag{4.18}$$

where $S_{\mathrm{M_{UC}}}$ is the maximum SINR value expected in unicast mode. (4.18) has the form of a Riemann integral. Then, since $F(S)$ is continuously differentiable, (4.18) can be transformed into a Riemann-Stieltjes integral such that

$$\Gamma_{\mathrm{UC}} = \int_{S_{\mathrm{m_{UC}}}}^{S_{\mathrm{M_{UC}}}} g(S)\, dF(S). \tag{4.19}$$

Solving the Riemann–Stieltjes integral in (4.19) by parts, we can calculate Γ_{UC} as

$$\Gamma_{\mathrm{UC}} = g(S_{\mathrm{M_{UC}}})F(S_{\mathrm{M_{UC}}}) - g(S_{\mathrm{m_{UC}}})F(S_{\mathrm{m_{UC}}}) - \int_{S_{\mathrm{m_{UC}}}}^{S_{\mathrm{M_{UC}}}} F(S)\, dg(S), \tag{4.20}$$

where

$$dg(S) = \frac{-\ln(2)}{(1+S)(\ln(S+1))^2}\, dS, \tag{4.21}$$

and the value of $S_{\mathrm{m_{UC}}}$ can be calculated numerically using (4.1) and the coverage target.

Figure 4.7 presents the ratio between bandwidth and bitrate in unicast mode (Γ_{UC}) vs the path-loss exponent (α). In the case of Monte Carlo results, we present the 95% confidence interval for Γ_{UC}, obtained for each α value. Notice that the curve for the analytical calculation of Γ_{UC} is slightly below Monte Carlo results. This is because the expression in (4.1) considers an infinite surface and we consider $R = 10$ km. However, this confirms the analytical expression in (4.20).

The user threshold to switch from unicast to SC-PTM vs the path-loss exponent (α) for two different values of λ_{BS} is presented in Figure 4.8. In SC-PTM mode, the user threshold does not depend on λ_{BS}, R_{s} or ξ. The number of UE per cell to switch from unicast to SC-PTM is between 8.61 and 8.85 in all cases. Therefore, if 9 UE/cell demand the same multimedia content, SC-PTM is more efficient than unicast.

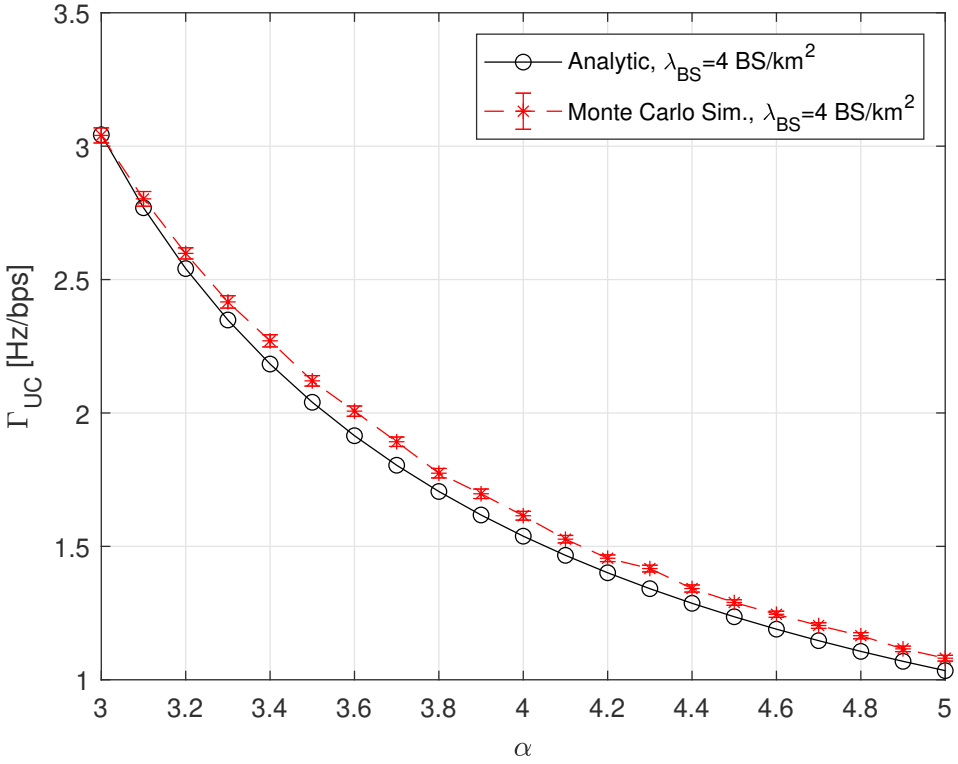

Figure 4.7 – Γ_{UC} vs path-loss exponent α. Analytical calculation vs Monte Carlo simulation.

4.3.2 Unicast to MBSFN

In Subsection 3.3.3 we present a model to calculate the number of users per cell in the MBSFN area to switch from unicast to MBSFN in order to reduce radio resource utilization as follows

$$U_{\mathrm{T_{SFN}}} = \frac{\Gamma_{\mathrm{SFN}}}{\Gamma_{\mathrm{UC}}}. \tag{4.22}$$

In Subsection 3.3.3, Γ_{UC} and Γ_{SFN} are calculated through Monte Carlo simulations using (3.18) and (3.19) respectively. In this chapter, instead of Monte Carlo simulations we get Γ_{SFN} using (4.7), (4.11) and (4.13). We calculate numerically the value of SINR threshold (s) at which the coverage probability ($p_{\mathrm{c_{SFN}}}$) is equal to the target, typically 95% [2] [44]. The obtained SINR value is $S_{\mathrm{m_{SFN}}}$. On the other hand Γ_{UC} is calculated using (4.20). Therefore, the user threshold to switch from unicast to MBSFN is obtained by replacing (4.20) and the value of Γ_{SFN} in (4.22).

The user threshold to switch from unicast to MBSFN vs ξ is presented in Figure 4.9.

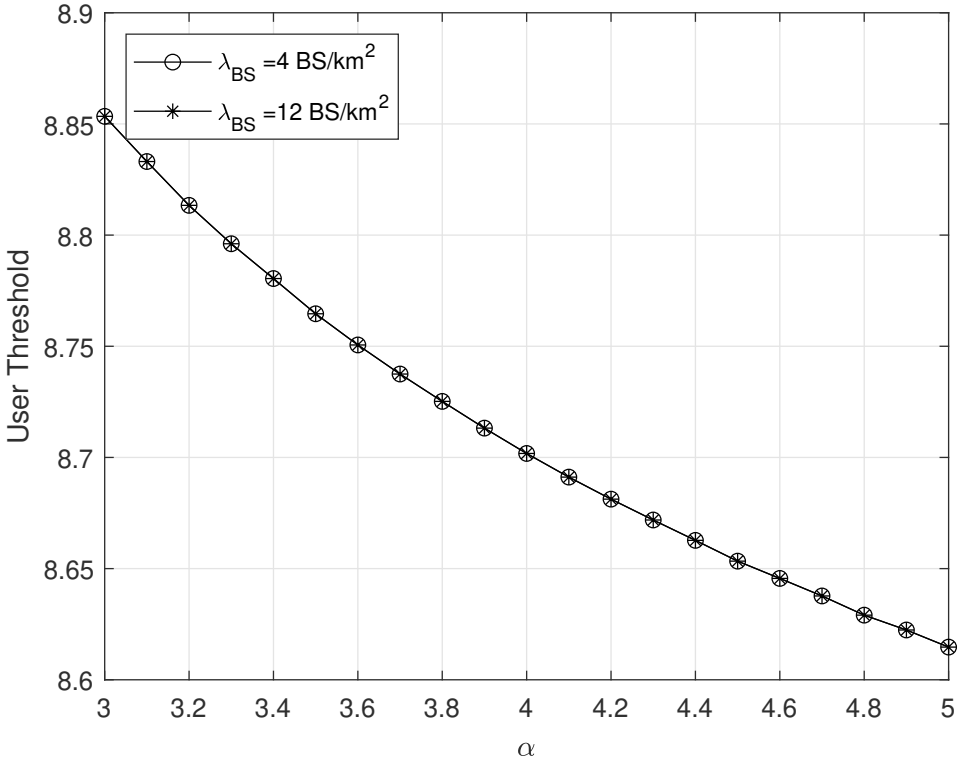

Figure 4.8 – User threshold to switch from unicast to SC-PTM mode vs α considering different λ_{BS} values. Curves are obtained via the analytical expression in (4.16).

These results were obtained using the analytical expressions in (4.1), (4.7) and (4.20). The coverage target is 95% and we set $S_{\mathrm{M_{UC}}} = 30$ dB. We consider two values for the BS density, $\lambda_{\mathrm{BS}} = 4$ BS/km^2 and $\lambda_{\mathrm{BS}} = 12$ BS/km^2. The first observation is that for the same R_{s} value the user threshold is lower for the higher BS density. This is because the SINR provided by a MBSFN transmission increases with higher BS densities [45][56]. On the other hand, the probability of coverage in unicast does not depend on the BS density [11]. Therefore, for the set of parameters considered in this study, the value of the user threshold depends on the MBSFN network configuration. Furthermore, a high user threshold means that many users are needed for MBSFN to be more efficient than unicast. Thus, when deploying a MBSFN network it is better to keep a low user threshold. In Figure 4.9 we observe that the value of user threshold remains almost constant for $R_{\mathrm{s}} = 2.5$ km in the interval $0 < \xi < 0.5$, particularly for the higher BS density. As consequence, the expression (4.3) provided in [45] could be used if the radius of the MBSFN area is large and twice the radius of the target service area. A bigger MBSFN area would not drastically improve

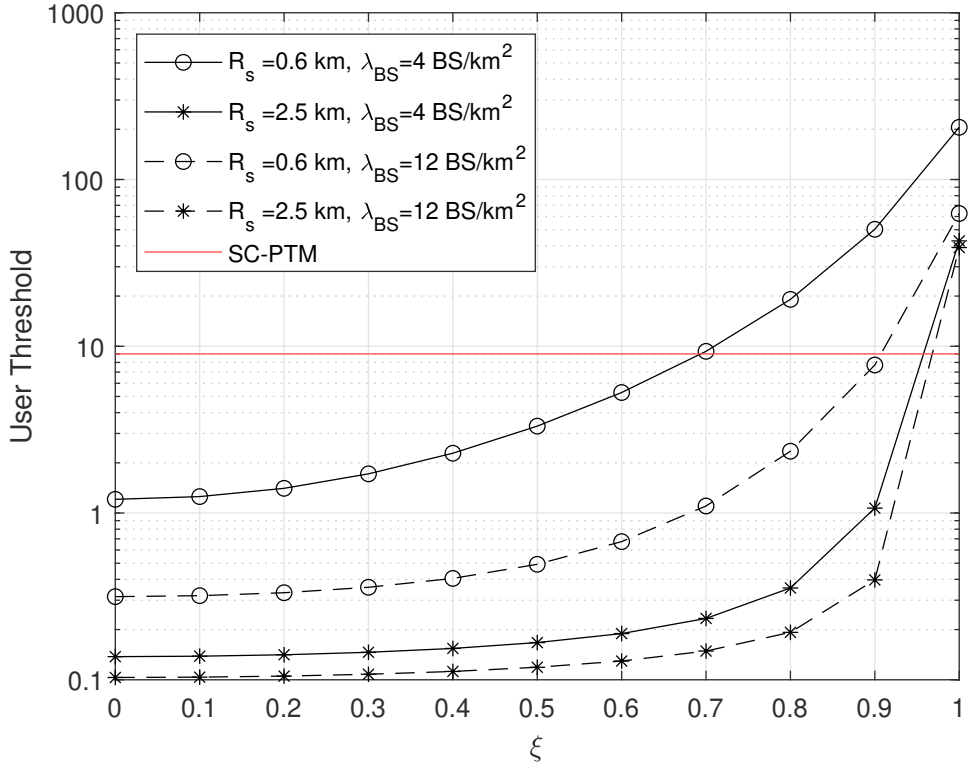

Figure 4.9 – User threshold to switch from unicast to MBSFN mode vs ξ considering different R_{s} and λ_{BS} values. Curves are obtained via the Analytical expression in (4.7).

MBSFN performance. On the other hand, if a small MBSFN area is considered or $\xi > 0.5$ or a higher precision in the user threshold calculation is required, (4.7) should be used. Furthermore, deployments in which users are located at a distance larger than $0.9R_{\mathrm{s}}$ from the origin should be avoided since the user threshold increases drastically in this region and the MBSFN mode may never be activated. Finally, observe that SC-PTM is a better solution when the MBSFN area is small, the BS density is low and users are located close to the border of the MBSFN area.

In Figure 4.10 we present the user threshold vs the radius of the MBSFN area (R_{s}) for different values of ξ and λ. We appreciate that the value of ξ has a more important impact on the user threshold than the BS density. Observe that the user threshold is higher when $\lambda_{\mathrm{BS}} = 12$ BS/km^2 and $\xi = 0.9$ than when $\lambda_{\mathrm{BS}} = 4$ BS/km^2 and $\xi = 0.7071$. This means that it is better to have an MBSFN area significantly larger than the service area with a low BS density than an MBSFN area with a similar size than the service area with a high BS density. However, for the same value of ξ, MBSFN does benefit from a higher BS

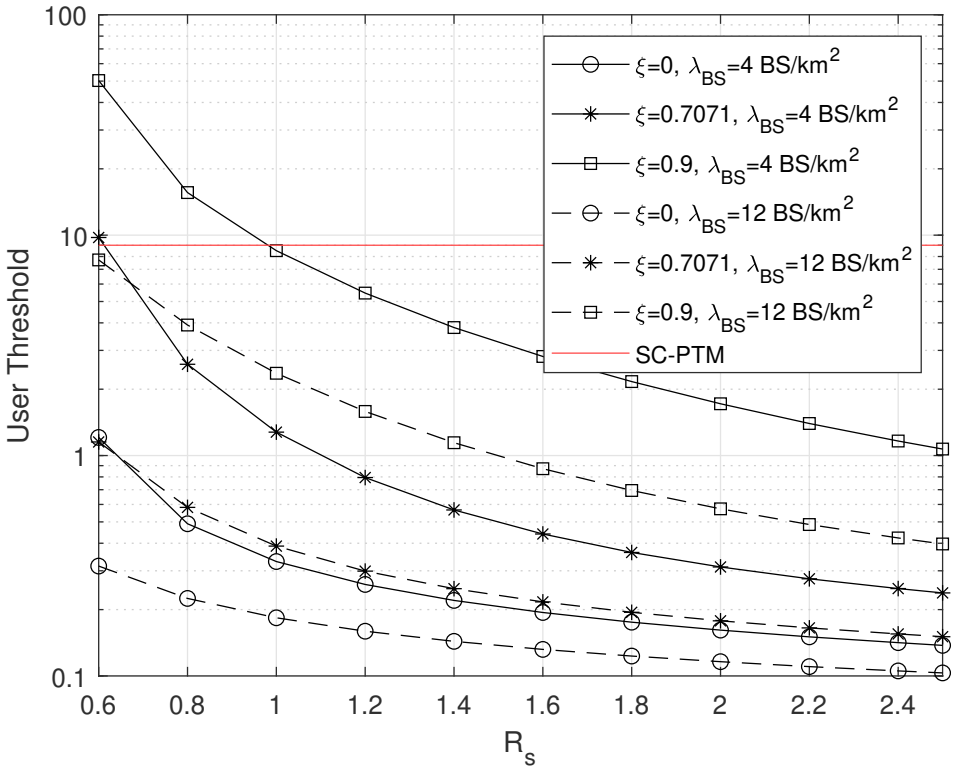

Figure 4.10 – User threshold to switch from unicast to MBSFN mode vs R_s considering different ξ and λ_{BS} values. Curves are obtained via the Analytical expression in (4.7).

density.

4.4 Energy Consumption in Unicast and MBMS

Energy consumption is a great concern in many fields of study due to the economic and environmental cost of energy production. Specifically, mobile networks account for 1-2% of the world energy consumption [39]. Thus, one of the main requirements for the fifth generation (5G) of cellular networks is a 90% reduction in network energy usage [30]. Broadcast transmission is a promising solution to reduce energy consumption in scenarios where many users demand the same content as sportive events or group communications in mission critical scenarios. However, few works study the energy consumption of broadcast transmission compared to unicast transmission.

Energy consumption depends on many system parameters: bitrate, transmission time, transmission power, bandwidth, transmission mode, network deployment, among others.

Providing a model that considers all these parameters is not an easy task. Authors in [52], proposed a scheduling algorithm to reduce UE energy consumption when receiving in MBSFN mode. They showed that MBSFN helps to reduce energy consumption on the UE compared to unicast. However, a model for SC-PTM and a BS energy consumption model are not provided.

This section studies BS and UE energy consumption in scenarios where many users demand the same content and broadcast transmission might be used. We present analytical models to calculate the energy consumption in unicast, MBSFN, and SC-PTM transmission modes.

4.4.1 Power Consumption Model

This section presents the UE and BS power consumption models used to calculate energy consumption.

User Equipment Model

In this study we consider the LTE UE power consumption model presented in [31]. According to this model the power consumed by a UE in Downlink (DL) is calculated as

$$P_{\mathrm{UE}} = P_{\mathrm{con}} + P_{\mathrm{Rx}} + P_{\mathrm{RxRF}}(U_{\mathrm{Rx}}) + P_{\mathrm{RxBB}}(C_{\mathrm{Rx}}), \tag{4.23}$$

where P_{con} is the average power consumption in Radio Resource Configuration (RRC) connected mode and P_{Rx} is the base power the UE signal-processing-chain consumes when active. The power consumed by the Radio Frequency (RF) parts, P_{RxRF}, is a function of the DL power level in dBm, U_{Rx}, and it is given by

$$P_{\mathrm{RxRF}}(U_{\mathrm{Rx}}) = p_{0_{\mathrm{RF}}} + p_{1_{\mathrm{RF}}} U_{\mathrm{Rx}}, \tag{4.24}$$

where $p_{0_{\mathrm{RF}}}$ and $p_{1_{\mathrm{RF}}}$ are constant values provided in [31] and presented in Table 4.2. Take into account that a high DL power level in the receiver (U_{Rx}) means that the gain of the amplifiers in the RF receive chain can be reduced and they may be powered off, to reduce power consumption. Therefore, the constant $p_{1_{\mathrm{RF}}}$ is negative. The constant $p_{0_{\mathrm{RF}}}$ is also negative but that is due to an adjustment of the model to avoid considering P_{con} and P_{Rx} twice when replacing (4.24) in (4.23) [31].

The power consumed by the Baseband (BB) parts, P_{RxBB}, is a function of the DL

bitrate in Mbit/s, C_{Rx}, and it is calculated as

$$P_{\mathrm{RxBB}}(C_{\mathrm{Rx}}) = p_{0_{\mathrm{BB}}} + p_{1_{\mathrm{BB}}} C_{\mathrm{Rx}}, \tag{4.25}$$

where $p_{0_{\mathrm{BB}}}$ and $p_{1_{\mathrm{BB}}}$ are constant values provided in [31] and presented in Table 4.2. Here, the power consumption increases with the bitrate. This is because the decoding complexity for the BB components, and thus the power consumption, scale linearly with the bitrate. Therefore, the constant $p_{1_{\mathrm{BB}}}$ is positive. The constant $p_{0_{\mathrm{BB}}}$ is negative for similar reasons than for $p_{0_{\mathrm{RF}}}$.

The values for P_{con}, P_{Rx} are constant and provided in [31] and presented in Table 4.2. Therefore, the UE power consumption depends on the DL power level (U_{Rx}) and the DL bitrate (C_{Rx}). In this study we use a fixed value for U_{Rx}, thus the UE consumed power can be expressed as

$$P_{\mathrm{UE}} = K + p_{1_{\mathrm{BB}}} C_{\mathrm{Rx}}, \tag{4.26}$$

where $K = P_{\mathrm{con}} + P_{\mathrm{Rx}} + P_{\mathrm{RxRF}}(U_{\mathrm{Rx}}) + p_{0_{\mathrm{BB}}}$.

Base Station Model

The BS power consumption is studied using the model presented in [15]. The model considers an LTE system with 10 MHz bandwidth and a BS maximum transmit power of 43 dBm. A BS antenna is served by a transceiver (TRX) that comprises: a power amplifier, an RF small-signal TRX module, a BB engine, a DC-DC power supply, an active cooling system and an AC-DC unit for connection to the electrical grid. Considering all these components, authors of [15] estimate the power consumption per TRX chain for LTE Macro BS (P_{BS}).

4.4.2 Energy Consumption Model

Consider a service area in which the users are located following a PPP of density λ_{UE}. This service area is a disk smaller than the MBSFN area and centered on it, see Figure 4.4. In MBSFN mode, the minimum SINR to cover (S_{mSFN}) sets the transmission bitrate. This minimum SINR is usually perceived by users close to the border of the MBSFN area since they receive a high interference power. Therefore, we fix the radius of the service area as ξR_{s} and calculate the probability of coverage for a user at the border in order to determine

the bitrate of the MBSFN transmission.

The UE power consumption depends on the transmission bitrate and the total energy consumption depends on the transmission time. Hereafter we present how to calculate these values and use them to obtain the energy consumption in unicast, MBSFN and SC-PTM.

Energy Consumption in Unicast

The average downlink bitrate in unicast mode is calculated as

$$C_{\mathrm{UC}} = W\,\mathbb{E}\left[\log_2(1+S)|S \geq S_{\mathrm{m_{UC}}}\right]. \tag{4.27}$$

The expected value in (4.27) can be calculated as in (4.20) by using $g(S) = \log_2(1+S)$ and, thus,

$$dg(S) = \frac{1}{S\ln(2) + \ln(2)}\,dS. \tag{4.28}$$

In unicast, the average transmission time [s/bit] is calculated as

$$t_{\mathrm{UC}} = \mathbb{E}\left[\frac{1}{W\log_2(1+S)}\middle| S \geq S_{\mathrm{m_{UC}}}\right] = \frac{\Gamma_{\mathrm{UC}}}{W}, \tag{4.29}$$

Notice that $\mathbb{E}\left[\frac{1}{X}\right] \neq \frac{1}{\mathbb{E}[X]}$ and thus $t_{\mathrm{UC}} \neq \frac{1}{C_{\mathrm{UC}}}$. Now, the energy consumption for all the BS is calculated as

$$E_{\mathrm{BS_{UC}}} = N_{\mathrm{BS_{UC}}} P_{\mathrm{BS}} D_{\mathrm{Tx}} t_{\mathrm{UC}} \frac{N_{\mathrm{U}}}{N_{\mathrm{BS_{UC}}}} = P_{\mathrm{BS}} D_{\mathrm{Tx}} t_{\mathrm{UC}} N_{\mathrm{U}}, \tag{4.30}$$

where $N_{\mathrm{BS_{UC}}}$ is the total number of BS that transmit in unicast mode, P_{BS} is the BS power consumption, D_{Tx} is the amount of data to be transmitted and $N_{\mathrm{U}} = \lambda_{\mathrm{UE}}\pi(\xi R_{\mathrm{s}})^2$ is the average number of users in the service area. Since BS in unicast do not transmit if there aren't any users camped on them, $N_{\mathrm{BS_{UC}}} = \min\left\{N_{\mathrm{U}}, \lambda_{\mathrm{BS}}\pi(\xi R_{\mathrm{s}})^2\right\}$. The factor $\frac{N_{\mathrm{U}}}{N_{\mathrm{BS_{UC}}}}$ accounts for the fact that radio resources are shared in unicast. The more users per cell, the longer the time to transmit a certain data to all of them. Notice that $E_{\mathrm{BS_{UC}}}$ does not depend on the BS density.

The energy consumption of all the UE is calculated as

$$\begin{aligned} E_{\mathrm{UE_{UC}}} &= N_{\mathrm{U}} D_{\mathrm{Tx}} t_{\mathrm{UC}} \frac{N_{\mathrm{U}}}{N_{\mathrm{BS_{UC}}}} \left(K + p_{1_{\mathrm{BB}}} C_{\mathrm{UC}} \frac{N_{\mathrm{BS_{UC}}}}{N_{\mathrm{U}}} \right) \\ &= {N_{\mathrm{U}}}^2 \frac{D_{\mathrm{Tx}} t_{\mathrm{UC}} K}{N_{\mathrm{BS_{UC}}}} + N_{\mathrm{U}} D_{\mathrm{Tx}} t_{\mathrm{UC}} p_{1_{\mathrm{BB}}} C_{\mathrm{UC}}. \end{aligned} \tag{4.31}$$

Take into account that the UE power model considers the bitrate in Mbit/s. Furthermore, the average bitrate in unicast is multiplied by $\frac{N_{\mathrm{BS_{UC}}}}{N_{\mathrm{U}}}$ because the capacity of each cell is divided equally among the users of the cell.

Energy Consumption in MBSFN

The DL bitrate in MBSFN is calculated as

$$C_{\mathrm{SFN}} = W \left[\log_2(1 + S_{\mathrm{m_{SFN}}}) \right], \tag{4.32}$$

and the average transmission time is $t_{\mathrm{SFN}} = \frac{1}{C_{\mathrm{SFN}}} = \frac{\Gamma_{\mathrm{SFN}}}{W}$. Then, the energy consumption for all the BS is calculated as

$$E_{\mathrm{BS_{SFN}}} = N_{\mathrm{BS_{SFN}}} P_{\mathrm{BS}} D_{\mathrm{Tx}} t_{\mathrm{SFN}}, \tag{4.33}$$

where $N_{\mathrm{BS_{SFN}}} = \lambda_{\mathrm{BS}} \pi {R_{\mathrm{s}}}^2$, is the number of BS in the MBSFN area. Notice that $E_{\mathrm{BS_{SFN}}}$ does not depend on the UE density. On the other hand, the energy consumption for all the UEs is calculated as

$$E_{\mathrm{UE_{SFN}}} = N_{\mathrm{U}} D_{\mathrm{Tx}} t_{\mathrm{SFN}} (K + p_{1_{\mathrm{BB}}} C_{\mathrm{SFN}}). \tag{4.34}$$

Figure 4.11 presents the ratio between the BS energy consumption in unicast mode ($E_{\mathrm{BS_{UC}}}$) and MBSFN mode ($E_{\mathrm{BS_{SFN}}}$). Simulation parameter are presented in Table 4.1 and Table 4.2. We consider an MBSFN area of 19.6 km^2 ($R_{\mathrm{s}} = 2.5$ km) and a service area of 9.8 km^2 ($\xi = 0.7071$). With MBSFN transmission the BSs consume less energy than in unicast mode when the user density is higher than 3.8 UE/km^2 for $\lambda_{\mathrm{BS}} = 12$ BS/km^2. For lower BS densities, until 1.2 BS/km^2, the value of λ_{UE} that makes $\frac{E_{\mathrm{BS_{UC}}}}{E_{\mathrm{BS_{SFN}}}} = 1$ decreases. However, if $\lambda_{\mathrm{BS}} < 1.2$ BS/km^2 more users are necessary for MBSFN to be more efficient. In this scenario, $\lambda_{\mathrm{BS}} = 1.2$ BS/km^2 minimizes the BS energy consumption in MBSFN mode for all UE densities. Additionally, observe that the BS energy ratio increases with the user density, e.g., with $\lambda_{\mathrm{BS}} = 4$ BS/km^2 and $\lambda_{\mathrm{UE}} = 10$ UE/km^2 the BSs consume 5

PARAMETER	VALUE
BS power consumption (P_{BS})	225 W
UE RX power consumption (U_{Rx})	−40 dBm
P_{con}	1.53 W
P_{Rx}	0.42 W
$p_{0_{\mathrm{RF}}}$	-60.7×10^{-3} W
$p_{1_{\mathrm{RF}}}$	-1.11×10^{-3} W/dBm
$p_{0_{\mathrm{BB}}}$	-26.6×10^{-3} W
$p_{1_{\mathrm{BB}}}$	2.89×10^{-3} Ws/Mbit

Table 4.2 – Simulation parameters for Energy Consumption Simulation

times more energy in unicast mode than in MBSFN mode.

The ratio between UE energy consumption in unicast mode ($E_{\mathrm{UE_{UC}}}$) and MBSFN mode ($E_{\mathrm{UE_{SFN}}}$) is presented in Figure 4.12. Only when $\lambda_{\mathrm{BS}} < 0.8$ BS/km^2 and $\lambda_{\mathrm{UE}} < 3.4$ UE/km^2 the UE energy consumption is lower in unicast than in MBSFN. Apart from that, we see that in most cases the UEs energy consumption is lower when receiving in MBSFN than in unicast. This is because the UEs perceive a higher SINR in MBSFN mode due to a reduced interference and therefore, they receive at a higher bitrate and transmission is faster. In Fig. Figure 4.12 we appreciate one surface when $\lambda_{\mathrm{UE}} \geq \lambda_{\mathrm{BS}}$ and other when $\lambda_{\mathrm{UE}} < \lambda_{\mathrm{BS}}$, this is due to the definition of $N_{\mathrm{BS_{UC}}}$. If in average there is one or less users per BS, the UE energy consumption in unicast is constant for a given λ_{BS}, however if there is more than one user per BS, the UE energy consumption increases due to the resource sharing in unicast. Similarly with the BS energy consumption, $\lambda_{BS} = 1.2$ BS/km^2 minimizes UE energy consumption in MBSFN mode for all UE densities and the UE energy consumption ratio increases with λ_{UE} when $\lambda_{\mathrm{UE}} \geq \lambda_{\mathrm{BS}}$. As an example, if $\lambda_{\mathrm{BS}} = 4$ BS/km^2 and $\lambda_{\mathrm{UE}} = 10$ UE/km^2 the UEs consume 10 times more energy in unicast mode than in MBSFN mode.

Energy Consumption in SC-PTM

The downlink bitrate in SC-PTM is calculated as

$$C_{\mathrm{SC}} = W\left[\log_2(1 + S_{\mathrm{m_{SC}}})\right], \tag{4.35}$$

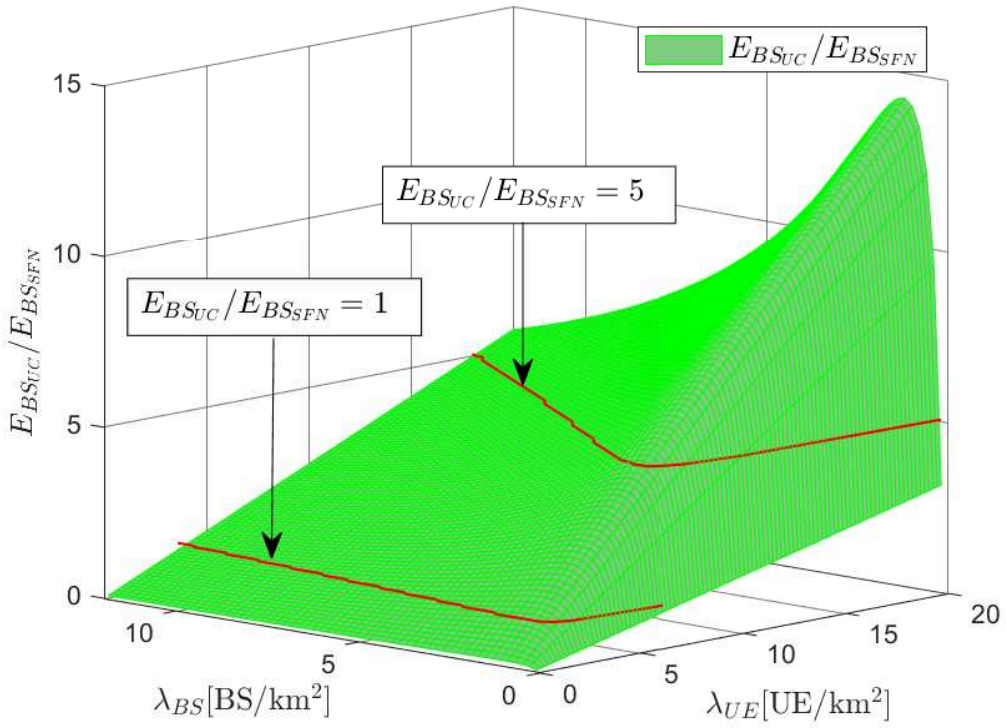

Figure 4.11 – Ratio between the BS Energy Consumption in unicast and MBSFN modes for different λ_{BS} and λ_{UE} values, considering $R_s = 2.5$ km and $\xi = 0.7071$.

and the average transmission time is $t_{\mathrm{SC}} = \frac{1}{C_{\mathrm{SC}}} = \frac{\Gamma_{\mathrm{SC}}}{W}$. Notice that $S_{\mathrm{m_{SC}}} = S_{\mathrm{m_{UC}}}$. Then, the energy consumption for all the BS is calculated as

$$E_{\mathrm{BS_{SC}}} = N_{\mathrm{BS_{SC}}} P_{\mathrm{BS}} D_{\mathrm{Tx}} t_{\mathrm{SC}}, \tag{4.36}$$

where $N_{\mathrm{BS_{SC}}} = N_{\mathrm{BS_{UC}}}$, is the number of BS that transmit in SC-PTM mode. On the other hand, the energy consumption for all the UE is calculated as

$$E_{\mathrm{UE_{SC}}} = N_{\mathrm{U}} D_{\mathrm{Tx}} t_{\mathrm{SC}} (K + p_{1_{\mathrm{BB}}} C_{\mathrm{SC}}). \tag{4.37}$$

Figure 4.13 presents the ratio between the BS energy consumption in unicast mode ($E_{\mathrm{BS_{UC}}}$) and SC-PTM mode ($E_{\mathrm{BS_{SC}}}$). First notice that the axis for λ_{BS} and λ_{UE} are inverted with respect to Figure 4.11 and Figure 4.12. We see that in most cases BSs consume more energy in SC-PTM mode than in unicast mode. However, the BSs consume less energy when transmitting in SC-PTM mode when λ_{BS} is low. This is because in unicast the BS

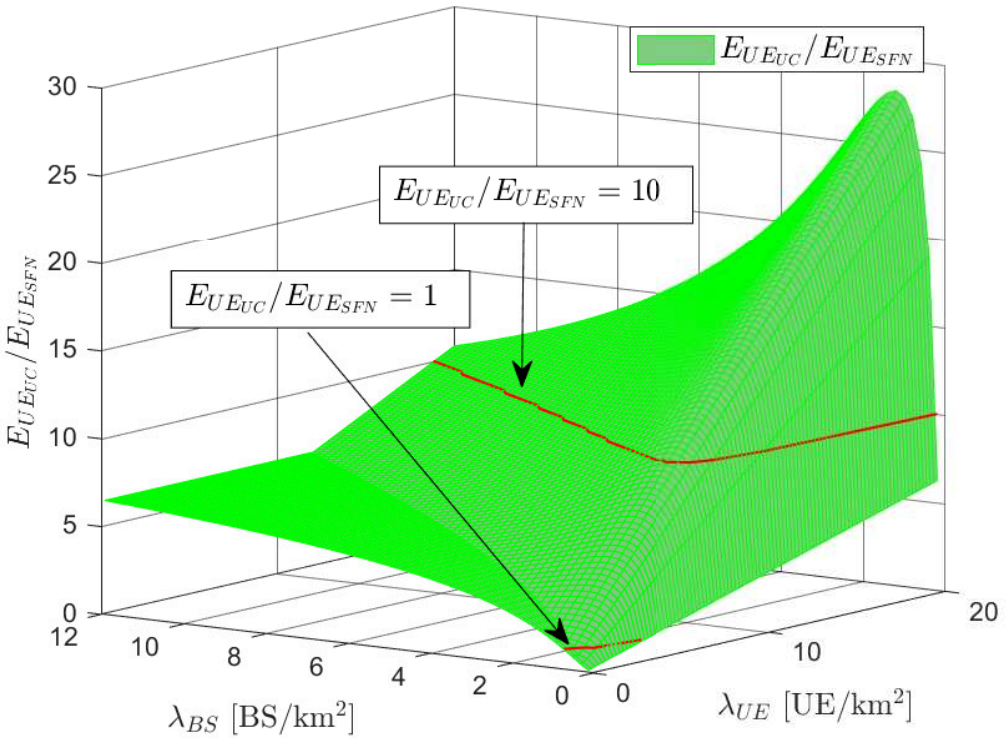

Figure 4.12 – Ratio between the User Equipment Energy Consumption in unicast and MBSFN modes for different λ_{BS} and λ_{UE} values, considering $R_s = 2.5$ km and $\xi = 0.7071$.

energy consumption does not depend on the BS density, the more BS the lower the number of user in each BS and therefore, the transmission is faster. However, in SC-PTM mode, BSs energy consumption increases linearly with the BS density. On the other hand, the BS energy consumption in unicast increases with λ_{UE} while $E_{\mathrm{BS_{SC}}}$ does not depend on the UE density. This is why the energy ratio increases with λ_{UE}. If we consider $\lambda_{\mathrm{BS}} = 2$ BS/km^2, SC-PTM helps to reduce BS energy consumption only if $\lambda_{\mathrm{UE}} > 17.6$ UE/km^2.

4.5 User Threshold to Reduce Energy Consumption

This section provides an analytical model to calculate the number of users per cell to switch from UC to BC (MBSFN or SC-PTM) to reduce BS and UE energy consumption.

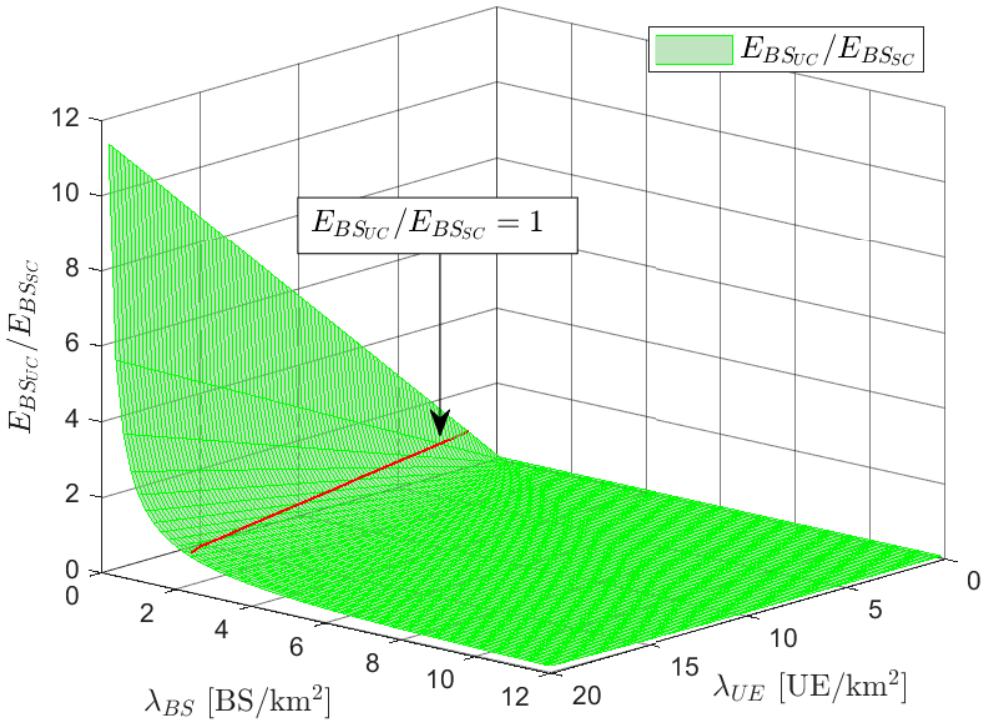

Figure 4.13 – Ratio between the Base Station Consumption in unicast and SC-PTM modes for different λ_{BS} and λ_{UE} values.

4.5.1 Unicast to MBSFN

Base Stations Side

The comparison of BS energy consumption between unicast and MBSFN is as follows

$$P_{\mathrm{BS}} D_{\mathrm{Tx}} t_{\mathrm{UC}} N_{\mathrm{U}} > N_{\mathrm{BS_{SFN}}} P_{\mathrm{BS}} D_{\mathrm{Tx}} t_{\mathrm{SFN}}. \tag{4.38}$$

The user threshold, in number of user per cell in the MBSFN area, is the value of N_{u} that makes (4.38) an equality divided by $N_{\mathrm{BS_{SFN}}}$, thus

$$U_{\mathrm{SFN_{BS}}} = \frac{t_{\mathrm{SFN}}}{t_{\mathrm{UC}}} = \frac{\Gamma_{\mathrm{SFN}}}{\Gamma_{\mathrm{UC}}}, \tag{4.39}$$

which is the same value of user threshold when aiming to optimize radio resource utilization.

User Equipment Side

On the other hand, considering UE power consumption the comparison is as follows

$$E_{\mathrm{UE_{UC}}} > E_{\mathrm{UE_{SFN}}} \tag{4.40}$$

By combining (4.31) and (4.34), we get

$$a{N_u}^2 - bN_u \geq 0, \tag{4.41}$$

where

$$a = \frac{D_{\mathrm{Tx}} t_{\mathrm{UC}} K}{N_{\mathrm{BS_{UC}}}}, \tag{4.42}$$

and

$$b = D_{\mathrm{Tx}}(-t_{\mathrm{UC}} p_{1_{\mathrm{BB}}} C_{\mathrm{UC}} + t_{\mathrm{SFN}}(K + p_{1_{\mathrm{BB}}} C_{\mathrm{SFN}})). \tag{4.43}$$

Since $N_u \geq 0$, inequation (4.41) is verified if $N_u \geq b/a$. Thus, the user threshold in UE per MBSFN area cell for which the energy consumption on the UE side is reduced when transmitting in MBSFN mode is given by

$$U_{\mathrm{SFN_{UE}}} = \frac{N_{\mathrm{BS_{UC}}}}{N_{\mathrm{BS_{SFN}}}} \left[\frac{t_{\mathrm{SFN}}}{t_{\mathrm{UC}}} - \frac{p_{1_{\mathrm{BB}}}}{K} \left(C_{\mathrm{UC}} - \frac{1}{t_{\mathrm{UC}}} \right) \right]. \tag{4.44}$$

As stated before, $N_{\mathrm{BS_{UC}}} = \min\{N_{\mathrm{u}}, \lambda_{\mathrm{BS}} \pi (\xi R_{\mathrm{s}})^2\}$ therefore, $U_{\mathrm{SFN_{UE}}}$ has two definitions depending on the values of λ_{UE} and λ_{BS} because

$$\frac{N_{\mathrm{BS_{UC}}}}{N_{\mathrm{BS_{SFN}}}} = \begin{cases} \xi^2 & \lambda_{UE} \geq \lambda_{BS} \\ \frac{\lambda_{UE}}{\lambda_{BS}} \xi^2 & \lambda_{UE} < \lambda_{BS} \end{cases} \tag{4.45}$$

Since $\frac{N_{\mathrm{BS_{UC}}}}{N_{\mathrm{BS_{SFN}}}} \leq 1$, K is always positive and $C_{\mathrm{UC}} > \frac{1}{t_{\mathrm{UC}}}$, because $\mathbb{E}[X] > \frac{1}{\mathbb{E}[\frac{1}{X}]}$, thus, we prove that $U_{\mathrm{SFN_{UE}}} < U_{\mathrm{SFN_{BS}}}$. This means that switching from unicast to MBSFN considering the user threshold in (4.22) and (4.39), helps to reduce radio resource utilization and energy consumption on the BS side and the UE side.

4.5.2 Unicast to SC-PTM

Base Stations Side

Following a similar procedure than for MBSFN, we obtain the number of users per cell from which the BS energy consumption in SC-PTM is lower than in unicast, as follows

$$U_{\mathrm{SC}_{\mathrm{BS}}} = \frac{t_{\mathrm{SC}}}{t_{\mathrm{UC}}} = \frac{\Gamma_{\mathrm{SC}}}{\Gamma_{\mathrm{UC}}}, \tag{4.46}$$

which is the same user threshold to reduce radio resource utilization.

User Equipment Side

Furthermore, the number of users per cell from which the UE energy consumption is lower in SC-PTM than in unicast is calculated as

$$U_{\mathrm{SC}_{\mathrm{UE}}} = \frac{t_{\mathrm{SC}}}{t_{\mathrm{UC}}} - \frac{p_{1_{\mathrm{BB}}}}{K}\left(C_{\mathrm{UC}} - \frac{1}{t_{\mathrm{UC}}}\right). \tag{4.47}$$

This proves that $U_{\mathrm{SC}_{\mathrm{UE}}} < U_{\mathrm{SC}_{\mathrm{BS}}}$. However, the difference between $U_{\mathrm{SC}_{\mathrm{BS}}}$ and $U_{\mathrm{SC}_{\mathrm{UE}}}$ is negligible because $p_{1_{\mathrm{BB}}}$ is of the order of 10^{-3}.

The user thresholds to switch from unicast to MBSFN or SC-PTM in order to reduce energy consumption in the BSs or UE are presented in Figure 4.14. We consider $\lambda_{\mathrm{BS}} = 4$ BS/km^2 and MBSFN areas ranging from 3.1 km^2 ($R_{\mathrm{s}} = 1$ km) up to 19.6 km^2 ($R_{\mathrm{s}} = 2.5$ km). The service areas have half the size ($\xi = 0.7071$) and 80% the size ($\xi = 0.9$) of the MBSFN area. First, notice that $U_{\mathrm{SC}_{\mathrm{BS}}}$ and $U_{\mathrm{SC}_{\mathrm{UE}}}$ are equal to 8.7 UE/cell. These values do not depend on λ_{UE} or λ_{BS}. On the other hand, the user thresholds for MBSFN decrease with the MBSFN area size. The bigger the MBSFN area, the higher the SINR and therefore the lower the energy consumption in MBSFN. We see as well that the size of the Service area has an important impact on the user threshold, e.g., if $R_{\mathrm{s}} = 1$ km, $U_{\mathrm{SFN}_{\mathrm{BS}}}$ increases from 1.27 UE/cell to 8.5 UE/cell when increasing ξ from 0.7071 to 0.9. This is due to the higher interference perceived by the users at the border of the service area. Now, when $\lambda_{\mathrm{UE}} \geq \lambda_{\mathrm{BS}}$, the difference between $U_{\mathrm{SFN}_{\mathrm{BS}}}$ and $U_{\mathrm{SFN}_{\mathrm{UE}}}$ is lower than 2 UE/cell in all cases. However, if $\lambda_{\mathrm{UE}} \geq \lambda_{\mathrm{BS}}$, $U_{\mathrm{SFN}_{\mathrm{UE}}}$ can be significantly lower than $U_{\mathrm{SFN}_{\mathrm{BS}}}$. For example, if $R_{\mathrm{s}} = 1$ km, $U_{\mathrm{SFN}_{\mathrm{UE}}} = 3.44$ UE/cell while $U_{\mathrm{SFN}_{\mathrm{BS}}} = 8.5$ UE/cell.

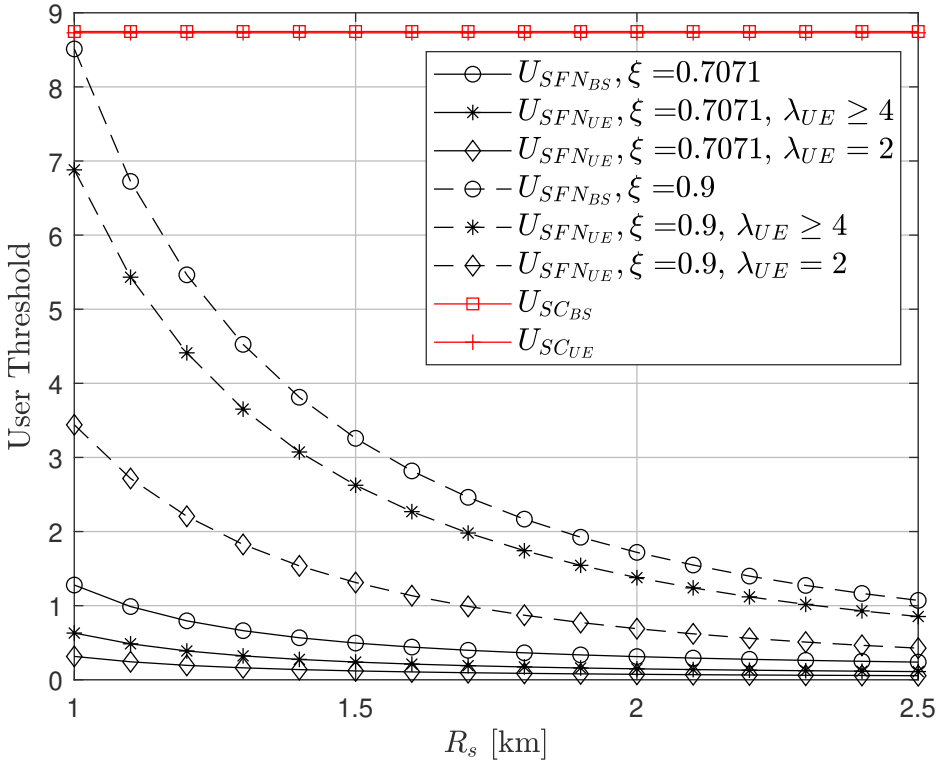

Figure 4.14 – User Threshold to switch from unicast to MBSFN or SC-PTM in order to reduce Energy Consumption on the Base Stations or User Equipment for different service area and MBSFN area configurations and user densities.

4.6 Summary

This chapter presents an analytical expression to calculate the probability of coverage for a user located at any point between the origin of the plane and the border of the MBSFN area when receiving in MBSFN mode. Furthermore, we use this expression and the formula for the probability of coverage in unicast mode, to develop an expression to calculate the user threshold to switch from unicast to MBSFN mode or SC-PTM mode in order to reduce radio resource utilization.

Our approach can be used to make an accurate estimation of the user threshold. Either in real time by obtaining the location of the user further away from the origin (closer to the border of the MBSFN area) or beforehand by knowing the radius of the service area, where the users are expected to be. In both cases, the distance should be smaller than the radius of the MBSFN area (R_s).

We also present an analytical model to calculate the energy consumption in the BS and UE when transmitting using UC, SC-PTM and MBSFN mode. Furthermore, we developed expressions to calculate the number of users per cell from which SC-PTM or MBSFN reduce BS or UE energy consumption with respect to unicast.

We proved that the user threshold to reduce BS energy consumption are the same as the user threshold to reduce radio resource utilization, in both SC-PTM and MBSFN mode. We also proved that the user threshold to reduce UE energy consumption is lower than the user threshold to reduce BS energy consumption, in particular for MBSFN. The results show that MBSFN is a better solution than SC-PTM to reduce energy consumption in most cases.

Analytical expressions allow fast computation of system metrics, like SINR or user threshold, compared to Monte Carlo simulations. However, some simplifications are done with respect to real deployments. For instance, in this chapter we consider BS with omnidirectional antennas, we do not consider reserved cells in the MBSFN area or the possibility of some users remaining in unicast mode even after MBSFN activation. These aspects are contemplated for MBMS but are difficult to consider using analytical methods. Therefore, the following chapter uses Monte Carlo simulations to analyze a more realistic MBMS deployment scenario, particularly focused on MCC.

Chapter 5

Comparison of MBSFN, SC-PTM and Unicast for Mission Critical Communication

MCC Services are currently provided through secure and reliable PMR dedicated networks. These services include voice, data and video delivery. During an emergency, timely access to video streaming can increase situational awareness and enhance life-saving operations. Therefore, to improve the capabilities of PMR networks and benefit from the advantages of mutualization, standard cellular technologies based on 4G and 5G were adopted for MCC. In particular, the MBMS is suitable for the transmission of group communication services. In this chapter, we compare MBSFN, SC-PTM and UC in MC scenarios from a resource use perspective.

In Section 5.1 we present the definition of MCC and review the standardization history with special attention to the use of MBMS for group communications. Then, Section 5.2 details the system model we propose for the study of MBMS in MC scenarios. Additionally, the equations used to calculate the SINR perceived by the MC users are presented. Afterwards, in Section 5.3 we developed the radio resource utilization model, principally focused on the calculation of the System Spectral Efficiency (SSE) in each transmission mode. Monte Carlo simulation results for the SSE are presented and discussed. Section 5.4 is centered on the calculation of the user threshold which in this chapter is defined as the number of users per square kilometer from which MBMS becomes more efficient than UC. Finally, the main conclusions and more important contributions are highlighted in Section 5.5.

5.1 Mission Critical Communications

MCC refer to the timely and reliable exchange of information between first responders in emergency situations where human life and other values for society are at risk [26]. Emergencies can take place in different scenarios. They can affect a small area (e.g. a building on fire or a bank robbery) or an entire city (e.g., an earthquake or a tsunami). Furthermore, the number of MC Agents changes according to the severity and scale of the emergency. According to [37], over 1000 officers including companies of specialist riot teams and 1400 stewards were deployed in the surroundings of the Stade de France during a football game between France and Turkey in 2020. In emergency conditions, people of rescue or security teams should share information in real time. **Group Communications**, intended to distribute the same content to multiple users in a controlled manner, are thus of prime importance to ensure efficient operations.

MCC depend on secure PMR networks. PMR networks are used by private actors (companies, local authorities, police forces, firemen) to deploy dedicated, reliable and secure networks in given areas (cities, port areas, airports, industrial complexes, stadiums, campuses) operating in multicast, broadcast or unicast mode. The first PMR technologies, Terrestrial Trunked Radio (TETRA), Terrestrial Trunked Radio Police (TETRAPOL) and Association of Public-Safety Communications Officials (APCO) Project 25 (P25), used specific waveforms and multiplexing methods. They offered mainly voice services but they had a limited possibility to support data services. Moreover, they work on narrow channels (25 kHz for TETRA, 6.25 or 12.5 kHz for APCO-P25 and 10 or 12.5 kHz for TETRAPOL) in the Ultra High Frequency (UHF) band (around 400MHz). In parallel, public networks and devices advanced rapidly with the deployment of Third-Generation cellular networks (3G), 4G LTE and nowadays 5G. 4G and 5G networks and terminals offer bit rates and functionalities superior to those of PMR. Because of this, the working group PMR Tetra and Critical Communication Association (TCCA) partnered with the 3GPP to achieve in Release 13 the definition of high-bitrate PMR services working on LTE bands. These services include Mission Critical Push-to-Talk (MCPTT), Device-to-Device (D2D) communication and group communication. Afterwards, in Release 14 two new MC services were specified: MC Video and MC Data (including messaging services and file distribution). These three MC services (MCPTT, MCVideo and MCData) currently work in LTE bands and respond to the requirements of private communications. These MC services are not as exigent in terms of latency as Ultra-Reliable Low-Latency Communication (URLLC)

services but they can be bandwidth consuming. Therefore, MBMS was adopted to support PMR Group Communication. Today, there exist two BC technologies used in mobile networks: MBSFN and SC-PTM.

5.1.1 MBMS for Mission Critical Communications

The 3GPP presents in [29] a comparison between SC-PTM and MBSFN for public safety. They conclude that SC-PTM is more efficient that MBSFN when UE are only located in some cells of the MBSFN area. This is because they consider a static MBSFN area in which all cells participate in the MBSFN transmission even if they do not have UE camped on them, while in SC-PTM only the cells with users are activated. They also observed that SC-PTM is more efficient than single cell MBSFN in terms of Spectral Efficiency. This is because MBSFN only supports single antenna port transmission and extended CP while SC-PTM supports Transmit Diversity and uses the normal CP. Additionally, their simulations use a regular hexagonal model with an inter-site distance of 1732m (a BS density of $\sim$0.4 BS/km^2), which is low compared to actual deployments in big cities. At last, they consider at most 20 UEs per cell, which is low for MC Scenarios in massive events. The work in [18] compares MBSFN, SC-PTM and UC in terms of radio quality, system spectral efficiency and cell coverage. Their study considers 4 UE/cell in most simulations and a BS density of $\sim$0.31 BS/km^2 with omnidirectional antennas. Under this assumptions they conclude that SC-PTM outperforms both UC and MBSFN in terms of SSE. In our study we prove that this affirmation do not always hold true, specially for MC scenarios with high user densities and BS densities.

5.2 System Model for MBMS transmission in Mission Critical scenarios

In this section we describe the system model we consider in our work. The propagation model is based on Okumura-Hata-Cost231 with shadowing and fading following the 3GPP reference model [3]. Tri-sector base stations are considered with adapted antennas, as in Chapter 3. To take into account the irregularity of operational networks, we consider BSs located following a PPP of density λ_{BS}. It is assumed that all cells use the same transmission power and carrier frequency.

There exist different types of MBSFN area cells. Guard cells do not transmit any signal

while a broadcast transmission is taking place in order to reduce interference. Normally they are located at the border of the MBSFN area. There are also Additional cells which are MBSFN area cells that do transmit useful signal power but there are not any interested UE are camped on them. In this study we do not consider guard cells or additional transmitting cells in MBSFN mode. The findings from [29], [18] and our own simulations proved that the SINR gain of using guard cells or additional cells does not compensate the additional use of radio resources. On the other hand, an MBSFN area Reserved cell is defined as a cell that belongs to the MBSFN area but that does not transmit the broadcast content, instead it transmit for other services and therefore, generate interference.

In UC and SC-PTM modes each UE receives the content from its serving cell, i.e., the cell from which the UE perceives the highest SINR. All the other cells generate interference. On the other hand, in MBSFN mode the UE receives the signals from all the cells belonging to the MBSFN area except for the MBSFN Area Reserved Cells. In our study, we consider that a cell in the MBSFN area becomes a reserved cell if there are not any UE interested in the BC content camped on it. Additionally, we consider that reserved cells transmit for other services and therefore, generate interference [7].

We denote the cells from the MBSFN area that contribute to the MBSFN transmission as N_{SFNon}. The number of interfering reserved cells is denoted by N_{SFNint}. Therefore the total number of cells in the MBSFN area is $N_{\mathrm{SFN}} = N_{\mathrm{SFNon}} + N_{\mathrm{SFNint}}$. Furthermore, we define the area where the MC users (e.g., firemen) are located as the MC Area (A_{MC}). In our study, this area is a disk and users are assumed to be uniformly distributed in the disk, see Figure 5.1. The MBSFN area (A_{SFN}) is also a disk which is assumed to be equal or bigger than the MC area. The ratio between the size of both areas is δ_{MC} which is calculated as $\delta_{\mathrm{MC}} = A_{\mathrm{MC}}/A_{\mathrm{SFN}}$. Therefore, $0 < \delta_{\mathrm{MC}} < 1$ since $A_{\mathrm{SFN}} \geq A_{\mathrm{MC}}$.

5.2.1 SINR Probability Distribution

The SINR in unicast mode is calculated as in Subsection 3.2.2. Since SC-PTM mode refers to broadcast transmission in one cell, the SINR in SC-PTM mode is calculated the same way that the SINR in unicast mode. In the case of MBSFN, the SINR is calculated similarly to Subsection 3.2.3, but instead of considering all the BS in the MBSFN area, we consider only the active BS, N_{SFNon}. Thus, the useful signal power in MBSFN is calculated as

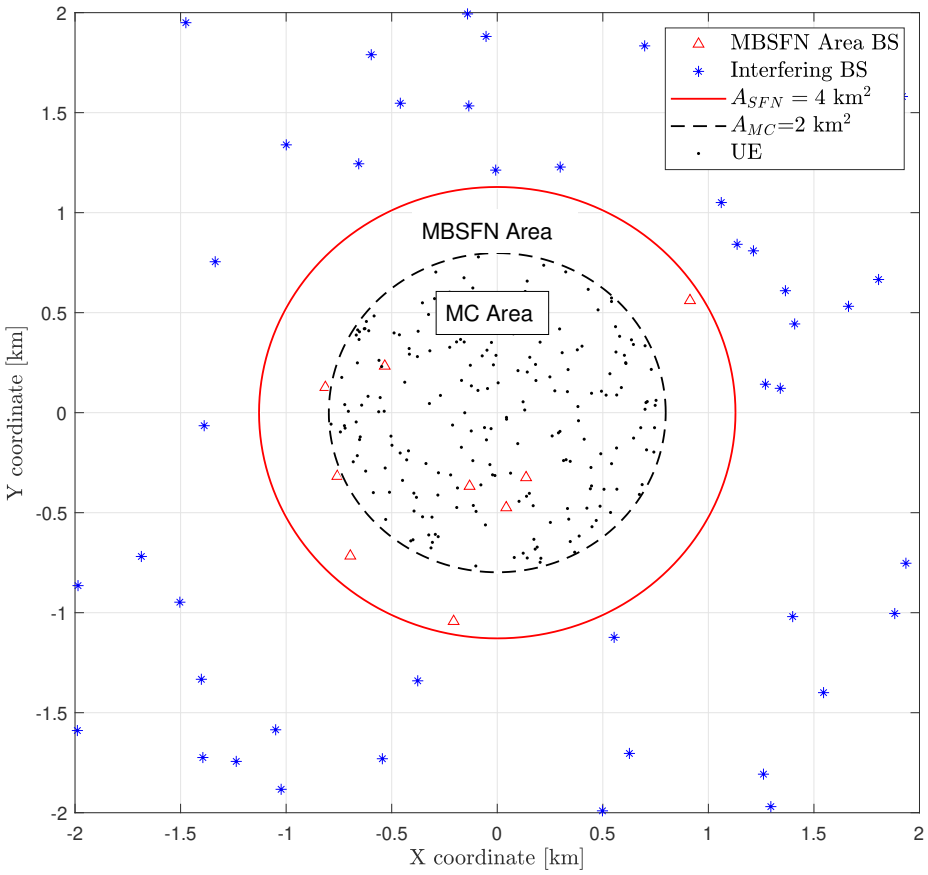

Figure 5.1 – MBSFN capable BS in the MBSFN Area and MC users in the Mission Critical Area considering $\lambda_{\text{BS}} = 4$ BS/km^2 and $\lambda_{\text{UE}} = 100$ UE/km^2.

$$P_{\text{SFN}} = P_{\text{tx}} k e^{\chi_c} \sum_{i \in N_{\text{SFNon}}} \delta_i r_i^{-\alpha} h_i e^{\chi_i} G(\theta_i), \tag{5.1}$$

and the interference power is obtained as

$$I_{\text{SFN}} = P_{\text{tx}} k e^{\chi_c} \left(\sum_{i \in N_{\text{SFNon}}} (1 - \delta_i) r_i^{-\alpha} h_i e^{\chi_i} G(\theta_i) + \sum_{i \notin N_{\text{SFNon}}} r_i^{-\alpha} h_i e^{\chi_i} G(\theta_i) \right). \tag{5.2}$$

5.2.2 Simulation Results for the SINR Distribution in MC Scenarios

Since this study is centered on MCC, we fix an exigent coverage requirement of 99% (4% higher than in [29]). Considering this model, we calculate the CDF of the SINR perceived by the UE in unicast mode and the CDF of the first percentile SINR (99% coverage) in SC-PTM and MBSFN modes. To do so, we use the Monte Carlo method. For a given set of system parameters (λ_{BS}, λ_{UE}, A_{SFN}, A_{MC}) we run several iterations and calculate the SINR perceived by the group of UE in each mode based on the equations presented in Section 3.2. To be compliant with 3GPP standards, most of the simulation parameters were taken from [3, Table C.1] and are given in Table 5.1. Simulation parameters not mentioned in Table 5.1 are presented in Table 3.1.

PARAMETER	VALUE
Total simulation area	$100\,\text{km}^2$
System Bandwidth (W)	20 MHz
Carrier Frequency (f_c)	700 MHz
BS Transmission Power (P_{tx})	46 dBm
Noise Power (P_{N})	-98 dBm
Path Loss Factor (k)[1]	0.2630

[1] For distance in meters.

Table 5.1 – Simulation parameters for MCC

Figure 5.2 and Figure 5.3 presents the CDF of the first percentile SINR in MBSFN (S_{mSFN}) for different λ_{BS} and λ_{UE} values and the CDF of the SINR in unicast mode, S_{UC}. In the former we set $A_{\text{SFN}} = 8$ km^2 and in the latter $A_{\text{SFN}} = 4$ km^2. Notice that the effect of the UE density changes depending on the BS density. When $\lambda_{\text{BS}} = 4$ BS/km^2, increasing the UE density results in a higher SINR. A gain of 3.35 dB is obtained when $A_{\text{SFN}} = 8$ km^2, see Figure 5.2. This is because the more users in the MC area the higher number of active cells in the MBSFN area (N_{SFNon}), see Figure 5.5. On the contrary, when $\lambda_{\text{BS}} = 1$ BS/km^2, increasing the UE density results in a lower SINR. In this case, N_{SFNon} does not increase significantly because the cells cover a larger surface and the new users are camped on the already active cells. Furthermore, the probability of having users at the border of the MBSFN area increases. In other words, to increase the SINR in MBSFN

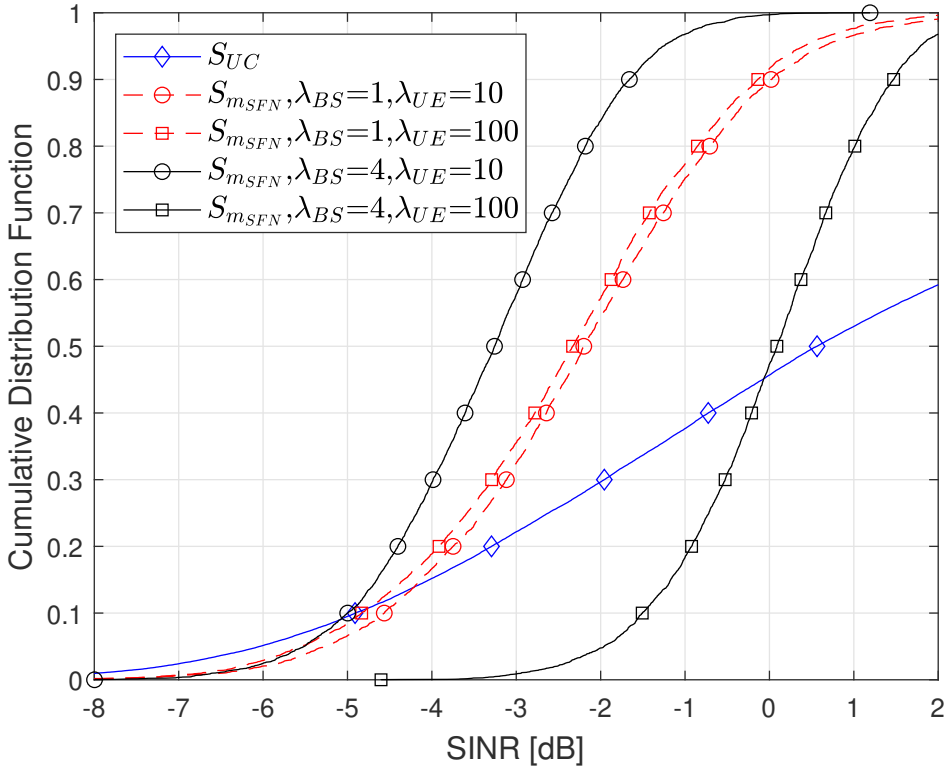

Figure 5.2 – CDF of the first percentile SINR in MBSFN mode (S_{mSFN}) and CDF of the SINR in UC (S_{UC}) considering $A_{\text{MC}} = 4$ km^2 and $A_{\text{SFN}} = 8$ km^2. λ_{BS} in BS/km^2, λ_{UE} in UE/km^2.

mode, for a high UE density it is convenient to have a high BS density and for a low UE density it is better to have a low BS density. Additionally, we appreciate that in most cases the first percentile SINR in MBSFN is lower than the SINR in Unicast. However, for high λ_{BS}, λ_{UE} and A_{SFN} values, the median S_{mSFN} value is close the median S_{UC} value. When comparing Figure 5.2 and Figure 5.3, we see that for the same λ_{BS} and λ_{UE} values, S_{mSFN} is higher when increasing the MBSFN area size (A_{SFN}). A SINR gain of ∼2.5 dB is obtained when $\lambda_{\text{BS}} = 4$ BS/km^2 and $\lambda_{\text{UE}} = 100$ UE/km^2.

The CDF of the first percentile SINR in SC-PTM (S_{mSC}) are presented in Figure 5.4. The simulations proved that when transmitting in SC-PTM mode we get a better performance when having a high BS density and low UE density. A gain > 1 dB can be obtained when increasing λ_{BS} from 1 BS/km^2 to 4 BS/km^2. At the same time, a maximum gain of 4.8 dB is obtained when reducing the UE density from 100 UE/km^2 to 10 UE/km^2. This is because the UE receive a higher useful signal power from its serving cell when having

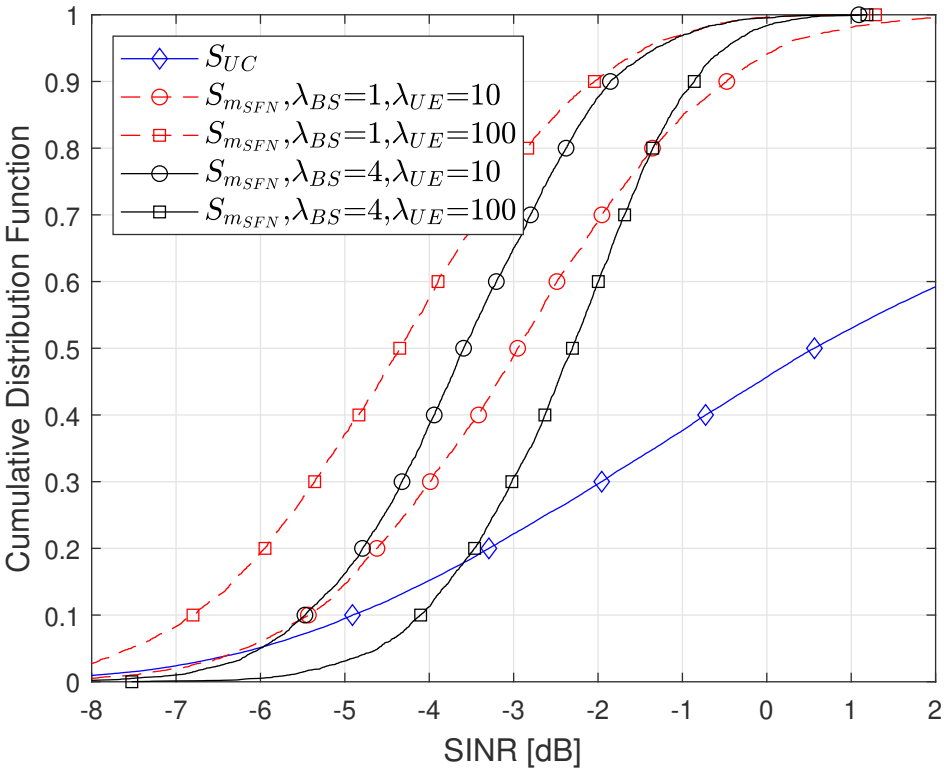

Figure 5.3 – CDF of the first percentile SINR in MBSFN mode (S_{mSFN}) and CDF of the SINR in UC (S_{UC}) considering $A_{\text{MC}} = 4$ km^2 and $A_{\text{SFN}} = 4$ km^2. λ_{BS} in BS/km^2, λ_{UE} in UE/km^2.

a high BS density. Additionally, having less UE per cell reduces the probability of them being at the cell border. As expected the target SINR in SC-PTM mode (S_{mSC}) is lower than S_{UC}.

Figure 5.5 presents the ratio between the MBSFN area cells that participate in the MBSFN transmission, N_{SFNon}, and all the cells in the MBSFN area, N_{SFN} versus the ratio between the MC area and the MBSFN area,

$$\varphi_{\text{MC}} = A_{\text{MC}}/A_{\text{SFN}}. \tag{5.3}$$

We observe that with a high UE density, more cells participate in the MBSFN transmission. This is because there are fewer empty cells. Similarly, as the MC area approaches the size of the MBSFN area ($\varphi_{\text{MC}} = 1$), more cells have users camped on them and participate in the MBSFN transmission. Notice that, if the ratio between A_{MC} and A_{SFN} is maintained, the size of the MC area does not have a significant effect on the fraction of cells that

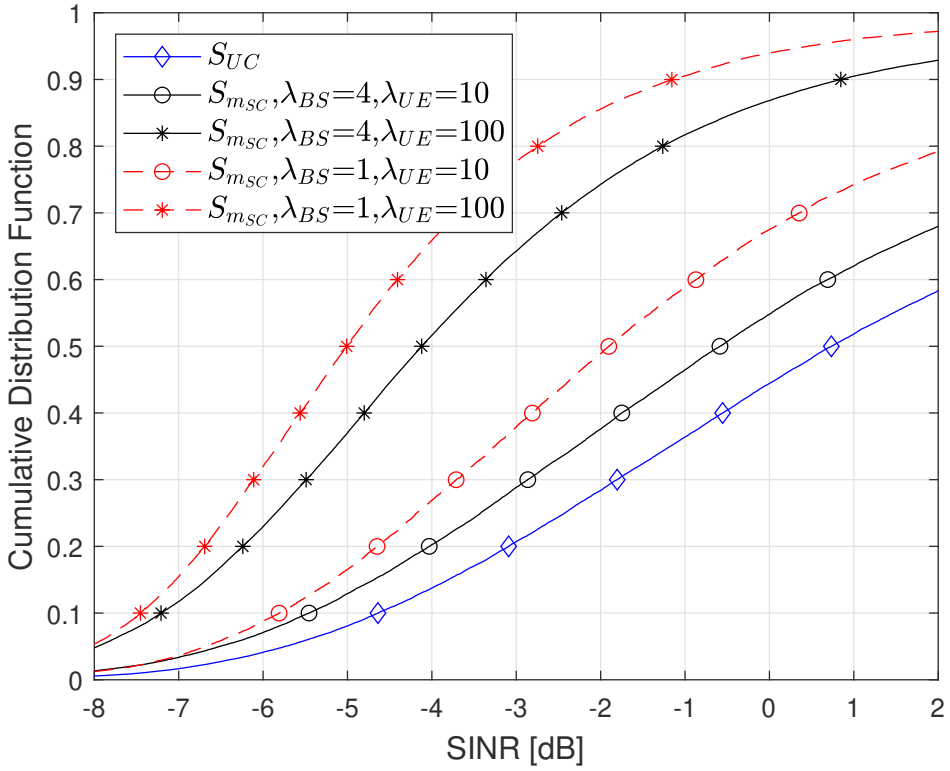

Figure 5.4 – CDF of the first percentile SINR in SC-PTM mode (S_{mSC}) and CDF of the SINR in UC (S_{UC}) for different scenarios considering $A_{\text{MC}} = 4$ km^2. λ_{BS} in BS/km^2 and λ_{UE} in UE/km^2.

participate in the MBSFN transmission.

5.3 Radio Resource utilization Model for MCC

This section describes the resource utilization model used to compare the radio efficiency of MBSFN, MBSFN and UC transmission modes. We fix a coverage requirement of 99%. In all the scenarios, we consider the transmission of a single content common to all the MC users. Users are located following a PPP of density λ_{UE}. We denote the number of MC users in the MC area as N_{u}. The value of N_{u} depends on λ_{UE} and the size of the Mission Critical Area (A_{MC}). For each transmission mode we derive the expressions for the SSE and we present the equation for the ratio between radio resources and capacity.

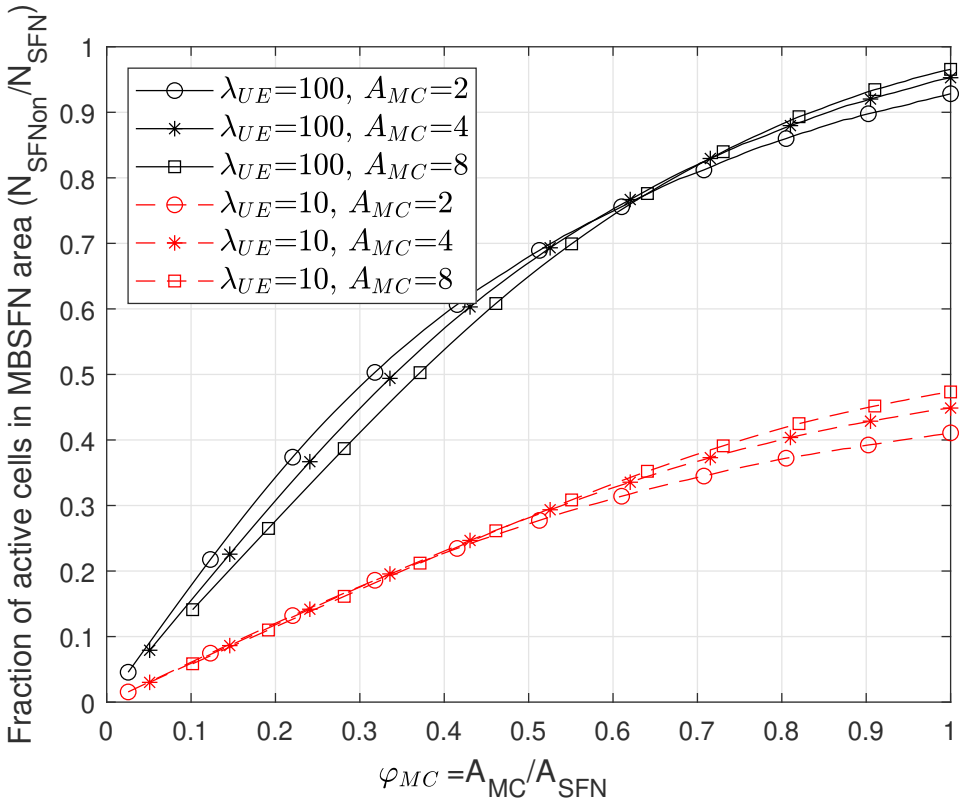

Figure 5.5 – Fraction of active cells in the MBSFN area ($N_{\text{SFNon}}/N_{\text{SFN}}$) versus the ratio between the MC area and the MBSFN area ($\varphi_{\text{MC}} = A_{\text{MC}}/A_{\text{SFN}}$) considering $\lambda_{\text{BS}} = 4$ BS/km^2. λ_{UE} in UE/km^2 and A_{MC} in km^2.

5.3.1 Resource utilization in MBSFN mode

When MBSFN available content is to be transmitted, the cells in the MBSFN Area that have MC users camped on them start the MBSFN transmission. The target SINR to cover (S_{mSFN}) is fixed as the lowest SINR among the 99% of these UE with the best channel conditions.

We calculate the SSE based on the Shannon Theorem. The capacity of a system (C) in bits per second (bits/s) is calculated as $C = W \log_2(1 + S)$, where W denotes the system bandwidth and S the SINR. We denote the radio resources used for MBSFN transmission as W_{SFN}. One realization of the PPP for the BS location and the PPP for the UE location is denoted as ζ. Thus, the SSE in MBSFN mode for a certain network deployment and MC users location,$E_{\text{SFN}}(\zeta)$, is calculated as

$$E_{\mathrm{SFN}}(\zeta) = \frac{C}{W_{\mathrm{SFN}}} = \frac{6}{7}\log_2(1 + S_{\mathrm{mSFN}}), \tag{5.4}$$

where the factor $\frac{6}{7}$ accounts for the longer cyclic prefix with MBSFN. Then, we take the expected value over several network deployments (PPP realizations) with the same λ_{BS} and λ_{UE} to obtain the average SSE in MBSFN mode

$$\overline{E_{\mathrm{SFN}}} = \mathbb{E}\left[E_{\mathrm{SFN}}\right]. \tag{5.5}$$

Since $\mathbb{E}\left[1/E_{\mathrm{SFN}}\right] \neq 1/\mathbb{E}\left[E_{\mathrm{SFN}}\right]$, we define the average ratio between radio resources and capacity in MBSFN mode as

$$\Gamma_{\mathrm{SFN}} = \frac{W_{\mathrm{SFN}}}{C} = \mathbb{E}\left[\frac{1}{E_{\mathrm{SFN}}}\right], \tag{5.6}$$

which is useful to calculate the User threshold in Section 5.4.

5.3.2 Resource utilization in SC-PTM mode

A cell transmitting in SC-PTM mode fixes the target SINR to cover (S_{mSC}) based on the 99% coverage requirement. The SSE for a certain network deployment and MC users location is calculated as

$$E_{\mathrm{SC}}(\zeta) = \frac{C}{W_{\mathrm{SC}}} = \log_2(1 + S_{\mathrm{mSC}}). \tag{5.7}$$

We assume that all cells are SC-PTM capable. Then, we take the expected value over several PPP realizations with the same λ_{BS} and λ_{UE} to obtain the average SSE in SC-PTM mode

$$\overline{E_{\mathrm{SC}}} = \mathbb{E}\left[E_{\mathrm{SC}}\right] \tag{5.8}$$

Finally, the average ratio between radio resources and capacity is given by

$$\Gamma_{\mathrm{SC}} = \frac{W_{\mathrm{SC}}}{C} = \mathbb{E}\left[\frac{1}{E_{\mathrm{SC}}}\right]. \tag{5.9}$$

5.3.3 Resource utilization in unicast mode

The UC mode uses link adaptation techniques and the radio resources per cell are shared among the users. Therefore the Spectral Efficiency (SE) is calculated for each MC

user as

$$E_{\mathrm{UE}} = \frac{C}{W_{\mathrm{UE}}} = \log_2(1 + S_{\mathrm{UC}}), \tag{5.10}$$

where W_{UE} is the bandwidth allocated to the user and S_{UC} the SINR. Each cell fixes the minimum SINR to cover (S_{mUC}) according to the coverage requirement. To calculate the SSE in UC mode for a certain network deployment and MC users location we average over all the values of SINR from S_{mUC} to the highest measured SINR

$$E_{\mathrm{UC}}(\zeta) = \mathbb{E}\left[\frac{E_{\mathrm{UE}}}{N_{\mathrm{u_{cell}}}}\middle| S_{\mathrm{UC}} \geq S_{\mathrm{mUC}}\right], \tag{5.11}$$

where $N_{\mathrm{u_{cell}}}$ is the number of users per cell. Therefore, the average SSE in unicast mode is calculated as

$$\overline{E_{\mathrm{UC}}} = \mathbb{E}\left[E_{\mathrm{UC}}\right]. \tag{5.12}$$

Additionally, the average ratio between radio resources and capacity in UC is calculated as

$$\Gamma_{\mathrm{UC}} = \frac{W_{\mathrm{UE}}}{C} = \mathbb{E}\left[\frac{1}{E_{\mathrm{UE}}}\middle| S_{\mathrm{UC}} \geq S_{\mathrm{mUC}}\right]. \tag{5.13}$$

The same reasoning is used to estimate the ratio between radio resources and capacity for users that remain in UC mode after MBSFN activation (Γ_{UCo}). We denote the average radio resources per UE for these users as W_{UEo}. The sub-index o stands for Outside the MBSFN area.

5.3.4 Simulation Results for the SSE in MC Scenarios

The System Spectral Efficiency for each transmission mode is presented in Figure 5.6. We consider $\lambda_{\mathrm{BS}} = 4$ BS/km^2 and $\lambda_{\mathrm{UE}} = 100$ BS/km^2. The ratio between the MC area and the MBSFN area is denoted as φ_{MC}. First, notice that the SSE in SC-PTM is ~ 0.2 bit/s/Hz higher than in UC for all the MC area sizes. The SSE in UC is reduced as the number of users per cell ($N_{\mathrm{u_{cell}}}$) increases, as stated in (5.11). Furthermore, we see that the smaller the MC area the higher the SSE for SC-PTM and UC. Doubling the size of the MC area reduces the SSE by $\sim$0.05 bit/s/Hz. As seen before, SC-PTM and UC benefit from a low number of users. On the other hand, the SSE in MBSFN mode increases by

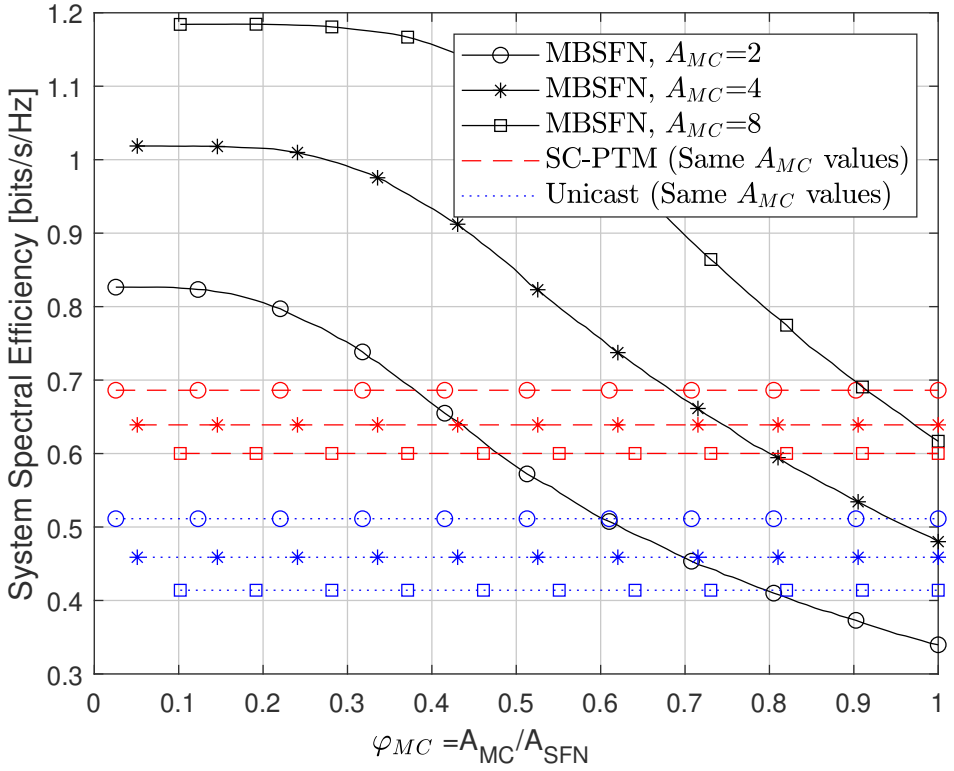

Figure 5.6 – System Spectral Efficiency in MBSFN, SC-PTM and Unicast transmission modes versus the ratio between the MC area and the MBSFN area ($\varphi_{\text{MC}} = A_{\text{MC}}/A_{\text{SFN}}$) for different scenarios considering $\lambda_{\text{BS}} = 4$ BS/km^2, $\lambda_{\text{UE}} = 100$ UE/km^2 and A_{MC} in km^2.

$\sim$0.2 bit/s/Hz when doubling the size of the MC area and MBSFN area. Additionally, we see that for each MC area there is a threshold for the MBSFN area size from which the SSE stops increasing. This is because cells located far from the MC area are not selected as serving cells by the UEs and therefore do not participate in the MBSFN transmission.

Simulation results considering $\lambda_{\text{UE}} = 10$ BS/km^2 are presented in Figure 5.7. The SSE in MBSFN mode is below 0.5 bit/s/Hz for all the A_{MC} and φ_{MC} values while the SSE for UC is above 1.2 bit/s/Hz and above 1.3 bit/s/Hz for SC-PTM. As presented in Figure 5.5, if the UE density is low, few cells from the MBSFN area participate in the MBSFN transmission. Furthermore, SC-PTM and unicast benefit from a low number of users per cell.

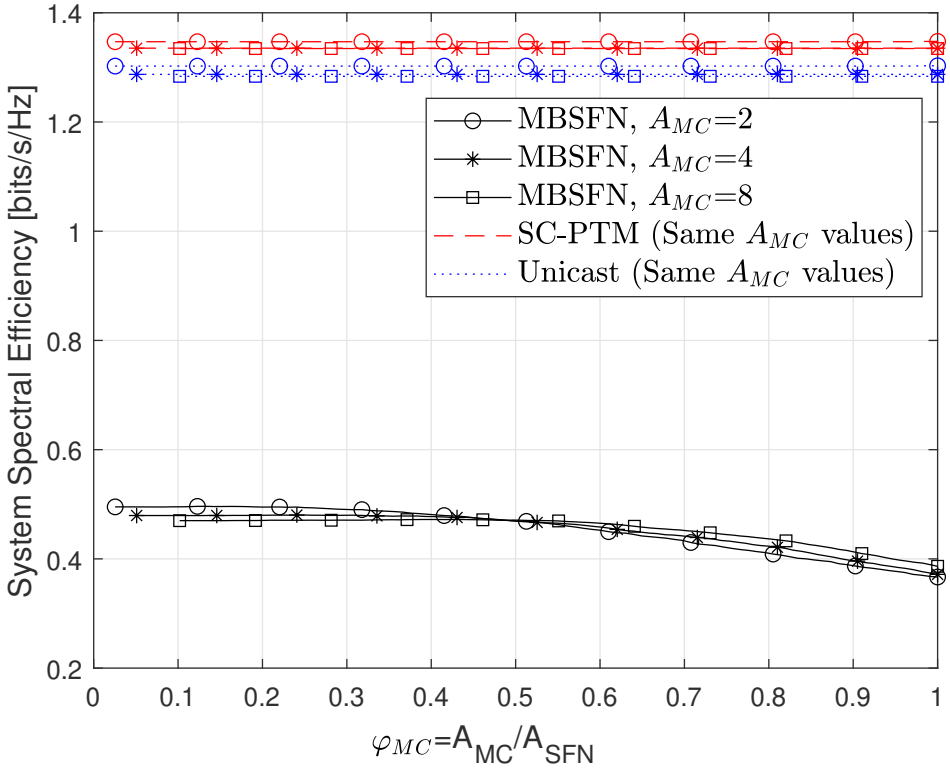

Figure 5.7 – System Spectral Efficiency in MBSFN, SC-PTM and Unicast transmission modes versus the ratio between the MC area and the MBSFN area ($\varphi_{\mathrm{MC}} = A_{\mathrm{MC}}/A_{\mathrm{SFN}}$) for different scenarios considering $\lambda_{\mathrm{BS}} = 4$ BS/km^2, $\lambda_{\mathrm{UE}} = 10$ UE/km^2 and A_{MC} in km^2.

5.4 User Threshold for Mission Critical Communications

In this chapter, we define the User Threshold as **the number of users per square kilometer** demanding the same MC service from which MBSFN or SC-PTM become more efficient than UC from a resource utilization perspective. We modify the definition of user threshold with respect to previous chapters to follow the thread of the chapter which assumes that the size of emergency areas (A_{MC}) and MBSFN areas A_{SFN} is measured in km^2 and not in number of cells. This facilitates the analysis.

A scenario that, to the best of our knowledge, has not been considered in previous works on the use of MBSFN transmission in MC Communications is: ***What happens with the MC users that request a content available in MBSFN mode but are served by cells outside the MBSFN Area?*** This scenario is highly probable if the

size of the MC area is equal to the size of the MBSFN area. In this study we examine two possibilities:

1. The SINR perceived by the UE from the active cells in the MBSFN area is higher than the minimum SINR targeted by the MBSFN transmission. In that case the UE starts a handover procedure and choose a serving cell among those in the MBSFN area to receive the content in BC mode.
2. The SINR perceived by the UE from the cells in the MBSFN area is lower than the minimum SINR targeted by the MBSFN transmission. Then, the UE remains receiving in UC mode from its serving cell.

The fraction of MC users in the MC area that receive the content in BC mode after MBSFN activation is denoted by γ_{SFN} such that $0 \leq \gamma_{\text{SFN}} \leq 1$.

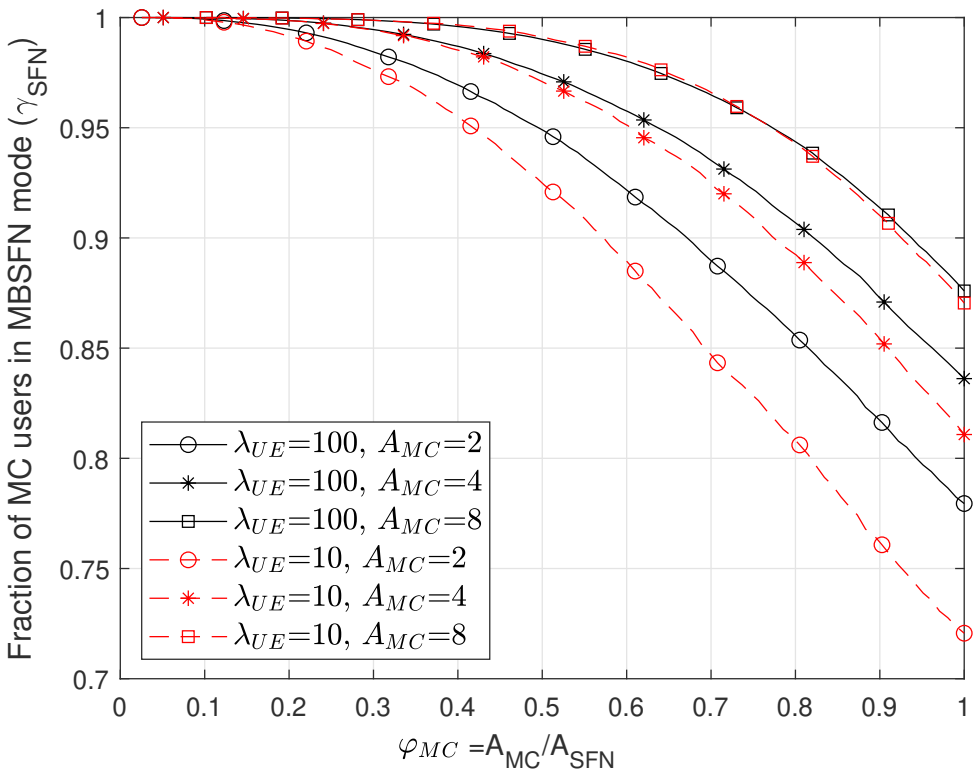

Figure 5.8 – Fraction of users that receive the content in MBSFN mode (γ_{SFN}) versus the ratio between the MC area and the MBSFN area ($\varphi_{\text{MC}} = A_{\text{MC}}/A_{\text{SFN}}$) considering $\lambda_{\text{BS}} = 4$ BS/km^2.

Figure 5.8 presents the fraction of users that receive the content in MBSFN mode (γ_{SFN}) versus φ_{MC}. As expected, if the size of the MC area approaches the size of the

MBSFN area ($\varphi_{\mathrm{MC}} = 1$), the number of users receiving in MBSFN mode decreases. If users are close to the border of the BC area, they may find a cell outside the MBSFN area that provides a higher signal power. Also notice that γ_{SFN} is higher for larger MC areas. Finally, we see that the worst case for MBSFN is a small MC area and a low UE density, almost 30% of the users remain in unicast mode after MBSFN activation. Since A_{MC} and A_{SFN} are correlated, the MBSFN area is also small and BS outside the MBSFN area are close to the MC users.

Unicast to MBSFN

Considering the proposed model, in terms of radio resource utilization MBSFN is more efficient than UC if

$$N_{\mathrm{u}} W_{\mathrm{UE}} > N_{\mathrm{SFNon}} W_{\mathrm{SFN}} + (1 - \gamma_{\mathrm{SFN}}) N_{\mathrm{u}} W_{\mathrm{UEo}}. \tag{5.14}$$

The user threshold for MBSFN ($U_{\mathrm{T_{SFN}}}$) is the value of N_{u} for which (5.14) is an equality. Thus, we obtain $U_{\mathrm{T_{SFN}}}$ by solving (5.14) for N_{u}, dividing by A_{MC} and replacing W_{UE} and W_{SFN} using (5.6) and (5.13) assuming the same target capacity (C) for unicast and MBSFN such that

$$U_{\mathrm{T_{SFN}}} = \frac{N_{\mathrm{SFNon}} \Gamma_{\mathrm{SFN}}}{A_{\mathrm{MC}} (\Gamma_{\mathrm{UC}} - (1 - \gamma_{\mathrm{SFN}}) \Gamma_{\mathrm{UCo}})}. \tag{5.15}$$

Keep in mind that $U_{\mathrm{T_{SFN}}}$ is the exact number of MC users demanding the MC service from which MBSFN becomes more efficient that UC while λ_{UE} is the average number of MC users on field.

Unicast to SC-PTM

Using SC-PTM, all the MC users are served in BC mode since there are not limitations in terms of broadcast area. Thus, the comparison in terms of radio resource utilization between UC and SC-PTM is as follows

$$N_{\mathrm{u}} W_{\mathrm{UE}} > N_{\mathrm{SC}} W_{\mathrm{SC}}, \tag{5.16}$$

where N_{SC} is the number of cells that transmit in SC-PTM mode. We obtain the User Threshold for SC-PTM ($U_{\mathrm{T_{SC}}}$) using a similar procedure to the one used to obtain (5.15):

$$U_{\mathrm{T_{SC}}} = \frac{N_{\mathrm{SC}}\Gamma_{\mathrm{SC}}}{A_{\mathrm{MC}}\Gamma_{\mathrm{UC}}}. \tag{5.17}$$

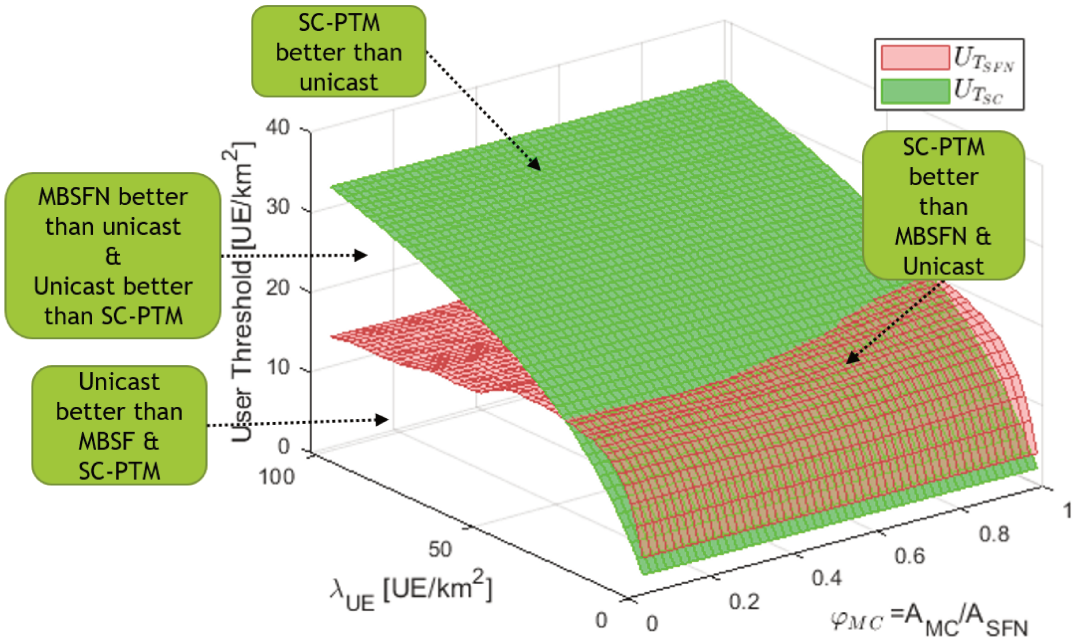

Figure 5.9 – User threshold for MBSFN ($U_{\mathrm{T_{SFN}}}$) and SC-PTM ($U_{\mathrm{T_{SC}}}$) for different scenarios considering $\lambda_{\mathrm{BS}} = 4$ BS/km^2 and $A_{\mathrm{MC}} = 4$ km^2.

The User Thresholds for MBSFN ($U_{\mathrm{T_{SFN}}}$) and SC-PTM ($U_{\mathrm{T_{SC}}}$) are presented in Figure 5.9. We consider $\lambda_{\mathrm{BS}} = 4$ BS/km^2 and $A_{\mathrm{MC}} = 4$ km^2. If $\varphi_{\mathrm{MC}} = 1$, the user threshold for MBSFN is higher than for SC-PTM when $\lambda_{\mathrm{UE}} < 38$ UE/km^2. For $\lambda_{\mathrm{UE}} = 38$ UE/km^2 and $\varphi_{\mathrm{MC}} = 1$ we get $U_{\mathrm{T_{SFN}}} = U_{\mathrm{T_{SC}}} = 21$ UE/km^2 (∼2UE/cell). If $\lambda_{\mathrm{UE}} > 38$ UE/km^2 then $U_{\mathrm{T_{SFN}}} < U_{\mathrm{T_{SC}}}$ and thus MBSFN should be preferred to SC-PTM. Furthermore, $U_{\mathrm{T_{SFN}}}$ decreases when increasing the size of the MBSFN area, which reinforces the interest of MBSFN compared to SC-PTM.

Additionally, simulations considering $A_{\mathrm{MC}} = 2$ km^2 are presented in Figure 5.10. In that case, we got higher values of λ_{UE}, $U_{\mathrm{T_{SFN}}}$ and $U_{\mathrm{T_{SC}}}$ at the crossing points. This means that the number of cases in which SC-PTM is more efficient increases for small MC areas. Conversely, MBSFN performs better in large MC areas.

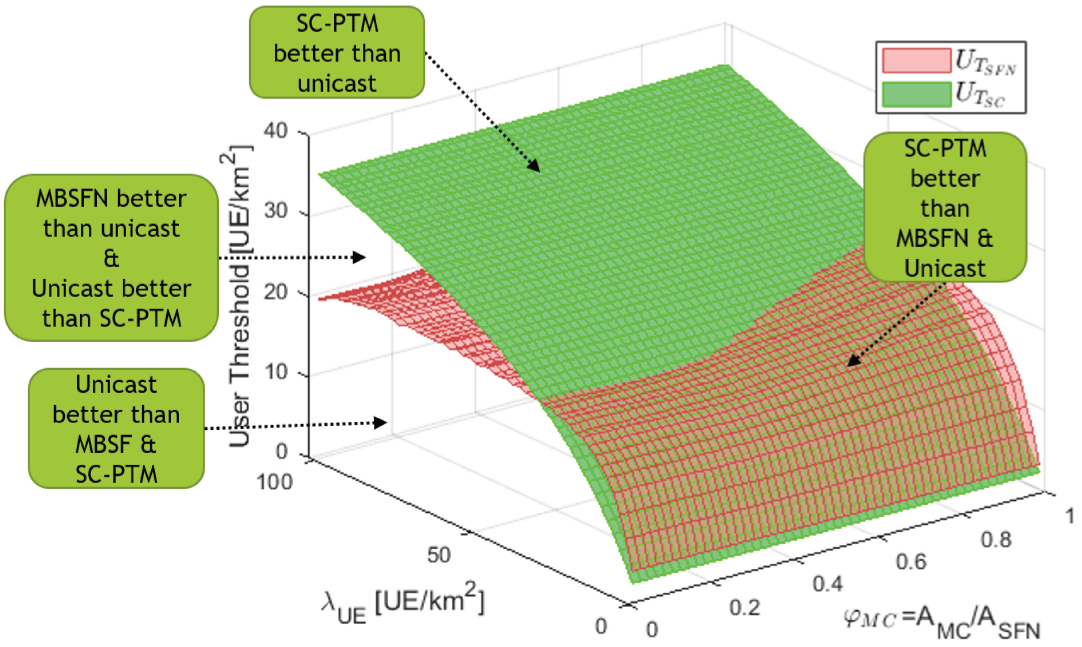

Figure 5.10 – User threshold for MBSFN ($U_{\mathrm{T_{SFN}}}$) and SC-PTM ($U_{\mathrm{T_{SC}}}$) for different scenarios considering $\lambda_{\mathrm{BS}} = 4$ BS/km^2 and $A_{\mathrm{MC}} = 2$ km^2.

5.5 Summary

In this chapter, we have provided a model to calculate the SINR for a MC user in a mobile network transmitting in MBSFN, SC-PTM and Unicast modes. We assumed that the cells in the MBSFN area can decide to not participate in the MBSFN transmission if there are not any interested UE camped on them. Furthermore, we consider the case in which MC users are camped on cells outside the MBSFN area and perform the handover procedure. Additionally, we develop a model to compare MBSFN and SC-PTM based on the SSE and the User Threshold.

Results showed that to increase the SINR in MBSFN when having a high UE density we need to increase the BS density. Conversely, if the UE density is low, a higher SINR is provided by reducing the BS density. On the other hand, the SINR in SC-PTM decreases with a high UE density and increases with higher BS densities. Additionally, the results in terms of SSE and user threshold showed that the dominant parameter is the UE density. If the UE density is high MBSFN is more efficient than SC-PTM. On the contrary, SC-PTM is more efficient than MBSFN for low UE densities. Furthermore, MBSFN performs better with large MBSFN areas and MC areas which makes it more suitable for emergencies during massive events. However, SC-PTM is the best solution for locally restricted and

small-scale emergencies.

Chapter 6

Conclusion

This thesis presents a comparison between unicast and broadcast transmission modes in cellular networks. It also provides solutions for the calculation of the user threshold for the switching between unicast and MBMS. Unicast transmission benefit from link adaptation and adaptive antennas. However, the same data is transmitted as many times as the number of users demanding the same content. On the other hand, MBMS transmission consist on a single transmission aiming to cover the group of users demanding the same content. The bitrate is the same for all users and is set based on the users with the worst channel quality. One broadcast technique, MBSFN, reduces interference at cells borders and increases the SINR thanks to the synchronized transmission from multiple neighboring cells. The second MBMS technique, SC-PTM, prioritizes compatibility with unicast to facilitate resource allocation and deployment. Thus, the calculation of the user threshold needs to consider the different nature of the three transmission techniques (Unicast, MBSFN and SC-PTM) and varying system parameters.

First we provide a comparison between unicast and MBSFN. We consider base stations equipped with tri-sector antennas located according to a Poisson distribution. We showed that when a MBSFN area covers a very large surface it outperforms unicast transmission in terms of SINR even if unicast uses beamforming with up to eight antennas per sector. Conversely, if the MBSFN area has a limited number of cells, the SINR is lower. The most challenging scenario for MBSFN is an MBSFN area of only two base stations versus unicast using beamforming with eight antennas per sector. In that case, the user threshold from which MBSFN becomes more efficient than unicast is eighth UE per cell.

Then, considering the dynamicity of users location, we aim to provide a faster way to calculate the user threshold. We developed an equation to calculate the SINR distribution for a UE located in any place inside the MBSFN area. Using this equation and the formula for the probability of coverage in unicast, we propose an analytical method to calculate the user threshold to switch from unicast to MBSFN or SC-PTM. The key parameter of this method is the location of the user closer to the border of the MBSFN area. If

this parameter is updated in real time, the value of the user threshold could be adjusted dynamically.

Afterwards, we developed an analytical model to calculate the energy consumption of UE and BS when using MBSFN and SC-PTM based on unicast models from the literature. Furthermore, we developed equations to calculate the user threshold from which MBSFN and SC-PTM reduce UE or BS energy consumption with respect to unicast. We proved that the user threshold to reduce BS energy consumption is the same as the user threshold to reduce radio resource utilization, in both SC-PTM and MBSFN mode. We also proved that the user threshold to reduce UE energy consumption is lower than the user threshold to reduce BS energy consumption, in particular for MBSFN.

One of the most important use cases for MBMS is group communication in mission critical scenarios. We consider a model in which the cells in the MBSFN area can decide to not participate in the MBSFN transmission if there are not any interested UE camped on them. Furthermore, we consider the case in which MC users are camped on cells outside the MBSFN area and have to decide if remaining in unicast or doing handover to a broadcast cell. The UE are located following a Poisson distribution, as well as the BS. Our results showed that to increase the SINR in MBSFN when having a high UE density we need to increase the BS density. Conversely, if the UE density is low, a higher SINR is provided by reducing the BS density. On the other hand, the SINR in SC-PTM decreases with the UE density and increases with the BS density. Additionally, the results in terms of SSE and user threshold showed that the dominant parameter is the UE density. If the UE density is high MBSFN is more efficient than SC-PTM. On the contrary, SC-PTM is more efficient than MBSFN for low UE densities.

6.1 Perspectives

The contributions of this thesis should be complemented by additional studies. There are open issues that are not addressed in our work and could be studied in the future:

— When comparing unicast and MBSFN we considered the use of beamforming in unicast with up to eight antennas per sector. Nowadays, with the advent of 5G, new technologies are available for unicast. These technologies include Multiple-Input Multiple-Output (MIMO) transmission, massive antenna arrays with up to 256 antennas per sector, Extremely High Frequency (EHF) transmission (up to 100

GHz), advanced scheduling algorithms, etc. Therefore, a comparison between 5G unicast, considering the implementation of these technologies, and LTE-based 5G broadcast is pertinent for future cellular networks.

— In our work we propose an analytical method to calculate the user threshold for the switching between unicast and MBMS. To develop this method we do some simplifications to the system model, notably the use of omnidirectional antennas instead of tri-sector antennas. Our method can be extended with a model for beamforming analysis using stochastic geometry. An equation to calculate the SINR distribution of users receiving in unicast mode when beamforming is used would enable an extension of our user threshold model.

— Machine learning algorithms could be used to predict when it is more efficient to use broadcast instead of unicast. Using data from real cellular deployments, a algorithm could be trained to predict with some minutes of advance when the use of MBSFN or SC-PTM can reduce radio resource utilization. The algorithm should be light because calculations would be done in real time. Furthermore, a large quantity of data is needed, particularly data from broadcast deployments.

— The use of broadcast is bound to many users demanding the same content at the same time. This is common in specific scenarios as Mission Critical or sportive events but rather uncommon for general public. However, many users can access the same content at different times of the day. Therefore, caching systems can make broadcast useful in many different scenarios. The caching system should predict what the user will watch and download it before user explicit demand. Machine learning prediction algorithms could be used.

— Enensys technologies has products (hardware and software) that enable an end-to end MBMS transmission. Analysing the performance of unicast and broadcast using real lab equipment would be an interesting compliment of our work. Furthermore, the implementation and evaluation of the user threshold calculation method on Enensys products is a possibility.

BIBLIOGRAPHY

[1] 3GPP. « Overview of 3GPP Release 11 ». In: (2014), p. 179.

[2] 3GPP. *Evolved Universal Terrestrial Radio Access (E-UTRA); Study on single-cell point-to-multipoint transmission for E-UTRA*. TR 36.890. Version 13.0.0. June 2015.

[3] 3GPP. *Evolved Universal Terrestrial Radio Access (E-UTRA); Radio Frequency (RF) system scenarios*. TR 36.942. Version 15.0.0. June 2018.

[4] 3GPP. *Multimedia Broadcast/Multicast Service (MBMS); Application Programming Interface and URL*. TS 26.347. Version 16.3.1. July 2020.

[5] 3GPP. *Multimedia Broadcast/Multicast Service (MBMS); Protocols and codecs*. TS 26.346. Version 16.6.1. Oct. 2020.

[6] 3GPP. *Non-Access-Stratum (NAS) protocol for 5G System (5GS); Stage 3*. TS 24.501. Version 16.13.0. Aug. 2020.

[7] 3GPP. *Technical Specification Group Radio Access Network; Evolved Universal Terrestrial Radio Access (E-UTRA) and Evolved Universal Terrestrial Radio Access Network (E-UTRAN); Overall description; Stage 2*. TS 36.300. Version 16.3.0. Sept. 2020.

[8] 3GPP. *5G Media Streaming (5GMS); General description and architecture*. TS 26.501. Version 17.2.0. June 2022.

[9] 3GPP. *5G multicast–broadcast services; User Service architecture*. TS 26.502. Version 17.2.0. Sept. 2022.

[10] 5G-Xcast. *5G-Xcast website*. 2022. URL: `https://5g-xcast.eu/` (visited on 08/03/2022).

[11] Jeffrey G. Andrews, Francois Baccelli, and Radha Krishna Ganti. « A Tractable Approach to Coverage and Rate in Cellular Networks ». In: *IEEE Transactions on Communications* 59.11 (Nov. 2011), pp. 3122–3134.

[12] P. Angot, V. Lepec, A. Nochimowski, P. Gonon, C. Thienot, and **Vargas-Rubio, J.C.** « Taking Steps Towards Greener Streaming ». In: *IBC 2022 International Broadcasting Convention 2022*. Amsterdam, Netherlands, Sept. 12, 2022.

[13] Muhammad Moiz Anis, Xavier Lagrange, and Ramesh Pyndiah. *Overview of evolved Multimedia Broadcast Multicast Services (eMBMS)*. Mar. 2016.

[14] IMT Atlantique. *IMT Atlantique website*. 2022. URL: https://www.imt-atlantique.fr/fr (visited on 09/29/2022).

[15] Gunther Auer et al. « How much energy is needed to run a wireless network? » In: *IEEE Wireless Communications*. Oct. 2011, pp. 40–49.

[16] Seon Yeob Baek, Young-Jun Hong, and Dan Keun Sung. « Adaptive Transmission Scheme for Mixed Multicast and Unicast Traffic in Cellular Systems ». In: *IEEE Transactions on Vehicular Technology* 58.6 (July 2009), pp. 2899–2908.

[17] Estevan Barjau et al. « Broadcast and Multicast Communication Enablers for the Fifth-Generation of Wireless Systems; Deliverable D4.1 Mobile Core Network ». In: (2019). Ed. by Tuan Tran.

[18] A. Daher, M. Coupechoux, P. Godlewski, P. Ngouat, and P. Minot. « SC-PTM or MBSFN for Mission Critical Communications? » In: 2017 IEEE 85th Vehicular Technology Conference (VTC Spring). June 2017, pp. 1–6. DOI: 10.1109/VTCSpring.2017.8108444.

[19] Erik Dahlman, Stefan Parkvall, and Johan Sköld. « Chapter 19 - Multimedia Broadcast/Multicast Services ». In: *4G LTE-Advanced Pro and The Road to 5G (Third Edition)*. Academic Press, Jan. 1, 2016, pp. 421–431.

[20] Harpreet S. Dhillon and Jeffrey G. Andrews. « Downlink Rate Distribution in Heterogeneous Cellular Networks under Generalized Cell Selection ». In: *IEEE Wireless Communications Letters* 3.1 (Feb. 2014), pp. 42–45.

[21] Marcin Dryjanski. *5G Core Network Functions*. Mar. 2, 2018. URL: https://www.grandmetric.com/2018/03/02/5g-core-network-functions/ (visited on 08/11/2022).

[22] Neila El Heni and Xavier Lagrange. « Multicast vs Multiple Unicast Scheduling in High-Speed Cellular Networks ». In: VTC Spring 2008 - IEEE Vehicular Technology Conference. May 2008, pp. 2456–2460.

[23] Ericsson. *Ericsson Mobility Report*. White Paper. June 2022.

[24] Hao Feng, Zhiyong Chen, and Hui Liu. « Performance Analysis of Push-Based Converged Networks With Limited Storage ». In: *IEEE Transactions on Wireless Communications* 15.12 (Dec. 2016), pp. 8154–8168.

[25] Tim Frost and Calnex Solutions. *Synchronization for Fronthaul and O-RAN Timing Architectures*. White Paper. March 2021.

[26] GSMA. « Network 2020: Mission Critical Communications ». In: 2020.

[27] Jordi Joan Gimenez, Jose Luis Carcel, Manuel Fuentes, Eduardo Garro, Simon Elliott, David Vargas, Christian Menzel, and David Gomez-Barquero. « 5G New Radio for Terrestrial Broadcast: A Forward-Looking Approach for NR-MBMS ». In: *IEEE Transactions on Broadcasting* 65.2 (June 2019), pp. 356–368.

[28] David Gomez-Barquero, David Navratil, Steve Appleby, and Matt Stagg. « Point-to-Multipoint Communication Enablers for the Fifth Generation of Wireless Systems ». In: *IEEE Communications Standards Magazine* 2.1 (Mar. 2018), pp. 53–59.

[29] Huawei, HiSilicon, TDTech, SouthernLINC, Potevio, China Unicom, MediaTek Inc, and CATT. « Comparison of SC-PTM and MBSFN use for Public Safety ». In: 3GPP TSG-RAN WG2. Apr. 2015.

[30] GSMA Intelligence. *Understanding 5G: Perspectives on future technological advancements in mobile*. White Paper. 2014.

[31] Anders R. Jensen, Mads Lauridsen, Preben Mogensen, Troels B. Sørensen, and Per Jensen. « LTE UE Power Consumption Model: For System Level Energy and Performance Optimization ». In: *2012 IEEE Vehicular Technology Conference (VTC Fall)*. Sept. 2012, pp. 1–5.

[32] Rafael Kaliski, Ching-Chun Chou, Hsiang-Yun Meng, and Hung-Yu Wei. « Dynamic Resource Allocation Framework for MooD (MBMS Operation On-Demand) ». In: *IEEE Transactions on Broadcasting* 62.4 (Dec. 2016), pp. 903–917.

[33] X. Lagrange. *CIR cumulative distribution in a regular network*. Research report. ENST Paris, 2000.

[34] Xavier Lagrange. « Allocation de ressources radios dans les réseaux radiomobiles ». In: (2000).

[35] William C.Y. Lee. « Chapter 9 - Diversity Schemes ». In: *Mobile Communications Engineering: Theory and Applications (2 Ed.)* McGraw-Hil, 1997, pp. 327–345.

[36] A. Ligeti. « Coverage probability estimation in single frequency networks in presence of correlated useful and interfering components ». In: Gateway to 21st Century Communications Village. VTC 1999-Fall. IEEE VTS 50th Vehicular Technology Conference (Cat. No.99CH36324). Vol. 4. Sept. 1999, 2408–2412 vol.4.

[37] The Local. « Police in Paris on high alert for France vs Turkey Euro 2020 clash ». In: 2019.

[38] Masood Maqbool, Marceau Coupechoux, and Philippe Godlewski. « Comparison of Various Frequency Reuse Patterns for WiMAX Networks with Adaptive Beamforming ». In: VTC Spring 2008 - IEEE Vehicular Technology Conference. May 2008, pp. 2582–2586.

[39] Meysam Masoudi et al. « Green Mobile Networks for 5G and Beyond ». In: *IEEE Access* 7 (2019), pp. 107270–107299.

[40] Nokia. *Policy control function*. URL: `https://www.nokia.com/networks/core-networks/policy-control-function/` (visited on 08/11/2022).

[41] Cisco White Paper. *Cisco Visual Networking Index: Global Mobile Data Traffic Forecast Update, 2017–2022*. White Paper. February 2019.

[42] Cisco White Paper. *Cisco Annual Internet Report (2018–2023)*. White Paper. March 2020.

[43] Alberto Rico-Alvariño, Imed Bouazizi, Miguel Griot, Prasad Kadiri, Le Liu, and Thomas Stockhammer. « 3GPP Rel-17 Extensions for 5G Media Delivery ». In: *IEEE Transactions on Broadcasting* 68 (June 2022), pp. 422–438.

[44] Letian Rong, Olfa Ben Haddada, and Salah-Eddine Elayoubi. « Analytical Analysis of the Coverage of a MBSFN OFDMA Network ». In: *IEEE GLOBECOM 2008 - 2008 IEEE Global Telecommunications Conference*. IEEE GLOBECOM 2008 - 2008 IEEE Global Telecommunications Conference. Nov. 2008, pp. 1–5.

[45] Reena Sahu, Kanchan K. Chaurasia, and Abhishek K. Gupta. « SINR and Rate Coverage of Broadcast Networks using Stochastic Geometry ». In: *2020 International Conference on Signal Processing and Communications (SPCOM)*. July 2020, pp. 1–5.

[46] Mikko Saily, Carlos Barjau, David Navratil, David Gomez-Barquero, and Fasil B. Tesema. « 5G Radio Access Networks: Enabling Efficient Point-to-Multipoint Transmissions ». In: *IEEE Vehicular Technology Magazine* 14.4 (Dec. 2019), pp. 29–37.

[47] Ahmad Shokair, Jean-Francois Helard, Oussama Bazzi, Matthieu Crussiere, and Youssef Nasser. « Analysis of the Coverage Probability of Cellular Multicast Single Frequency Networks ». In: *2019 International Conference on Wireless and Mobile Computing, Networking and Communications (WiMob)*. Oct. 2019, pp. 1–6.

[48] Vinay Kumar Shrivastava, Sangkyu Baek, and Youngkyo Baek. « 5G Evolution for Multicast and Broadcast Services in 3GPP Release 17 ». In: *IEEE Communications Standards Magazine* (2022), p. 7.

[49] Enensys Technologies. *Enensys Technologies website*. 2022. URL: `https://www.enensys.com/` (visited on 09/29/2022).

[50] Enensys Technologies. *Enensys website*. 2022. URL: `https://www.enensys.com/news/expway-extends-lte-broadcast-to-multi-media-distribution-over-5g/` (visited on 08/03/2022).

[51] T. T. Vu, L. Decreusefond, and P. Martins. « An analytical model for evaluating outage and handover probability of cellular wireless networks ». In: The 15th International Symposium on Wireless Personal Multimedia Communications. Sept. 2012, pp. 643–647.

[52] Chaoan Wu, Xuekang Sun, and Tiankui Zhang. « A power-saving scheduling algorithm for mixed multicast and unicast traffic in MBSFN ». In: *2012 Computing, Communications and Applications Conference*. Jan. 2012, pp. 170–174.

[53] SeungJune Yi, SungDuck Chun, YoungDae Lee, SungJun Park, and SungHoon Jung. *Radio protocols for LTE and LTE-advanced*. Wiley, 2012. 339 pp.

[54] **Vargas, Juan**, Cedric Thienot, and Xavier Lagrange. « Analytical Calculation of the User Threshold for the Switching between Unicast and Broadcast in Cellular Networks ». In: *NOMS 2022 IEEE/IFIP Network Operations and Management Symposium*. Budapest, Hungary, Apr. 25, 2022, pp. 1–6.

[55] **Vargas, Juan**, Cedric Thienot, and Xavier Lagrange. « MBSFN and SC-PTM as Solutions to Reduce Energy Consumption in Cellular Networks ». In: *ISCC 2022 IEEE Symposium on Computers and Communications*. Rhodes Island, Greece, June 30, 2022.

[56] **Vargas, Juan**, Cédric Thienot, Christophe Burdinat, and Xavier Lagrange. « Broadcast-Multicast Single Frequency Network versus Unicast in Cellular Systems ». In: *WiMob 2020 16th International Conference on Wireless and Mobile Computing, Networking and Communications*. Oct. 2020.

[57] **Vargas, Juan**, Cédric Thienot, and Xavier Lagrange. « Comparison of MBSFN, SC-PTM and Unicast for Mission Critical Communication ». In: *WPMC 2021 24th International Symposium on Wireless Personal Multimedia Communications*. Dec. 2021.

COLLEGE SCIENCES
DOCTORAL POUR L'INGENIEUR
BRETAGNE ET LE NUMERIQUE

IMT Atlantique
Bretagne-Pays de la Loire
École Mines-Télécom

Titre : Monodiffusion versus Diffusion dans les Réseaux Cellulaires

Mots clés : Monodiffusion, Diffusion, MBSFN, SC-PTM, beamforming, géométrie stochastique

Résumé : Le trafic de données sur les réseaux mobiles, notamment les contenus vidéos, augmente chaque année. Cependant, le spectre est limité et cher et les opérateurs cherchent à en optimiser l'utilisation. Si le même contenu est transmis en même temps à de nombreux appareils dans une zone géographique, la solution privilégiée pour réduire l'utilisation de bande passante est la diffusion. L'unicast bénéficie des techniques d'adaptation de liaison. Cependant, le même contenu est transmis autant de fois que le nombre d'utilisateurs demandant le service. À l'inverse, une seule diffusion peut couvrir un grand nombre d'utilisateurs. Néanmoins, le débit de la diffusion est fixé en tenant compte des utilisateurs dont la qualité du canal est la plus mauvaise. Dans le mode appelé MBSFN, un groupe de cellules synchronisées transmet le même signal. En revanche, avec SC-PTM chaque cellule effectue une diffusion de manière indépendante. Le problème est de déterminer quand il est préférable d'utiliser l'unicast, le MBSFN ou le SC-PTM. Dans ce travail, nous comparons les performances de l'unicast, du MBSFN et du SC-PTM par le biais de simulations et de modèles analytiques. Nous considérons des stations de base situées selon des distributions de Poisson, la formation de faisceaux et différentes configurations de réseaux. Nous proposons une méthode analytique pour calculer le nombre d'utilisateurs demandant le même contenu à partir duquel le MBSFN ou le SC-PTM deviennent plus efficaces que l'unicast. Nous prouvons qu'un mécanisme de commutation basé sur ce seuil réduit l'utilisation de la bande passante et la consommation d'énergie.

Title : Unicast versus Broadcast in Cellular Networks

Keywords : Unicast, Broadcast, MBSFN, SC-PTM, MooD, beamforming, stochastic geometry

Abstract : Data traffic on mobile networks increases every year, especially video content. However, spectrum is scarce and expensive, and operators need to optimize its use. In scenarios where the same content is transmitted at the same time to many devices in the same geographical area, the preferred solution to reduce bandwidth consumption is broadcast transmission. Unicast transmission benefits from link adaptation techniques. However, the same content is transmitted as many times as the number of users demanding the same service. Conversely, a single broadcast transmission can cover many users. Nevertheless, the bitrate in broadcast is fixed considering the users with the worst channel quality. Multicast-Broadcast Single-Frequency-Network (MBSFN) is a broadcast technique in which a group of synchronized cells transmit the same waveform. On the other hand, with Single-Cell Point-To-Multipoint (SC-PTM) each cell performs broadcast transmission independently. The problem is to determine when it is better to use unicast, MBSFN or SC-PTM. In our work, we compare the performance of unicast, MBSFN and SC-PTM through system level simulations and analytical models. We consider base stations located according to Poisson distributions, the use of beamforming in unicast and different broadcast configurations. Furthermore, we propose an analytical method to calculate the number of users demanding the same content from which MBSFN or SCPTM become more efficient than unicast. We prove that a switching mechanism based on this user threshold reduces bandwidth utilization and energy consumption. This method is based on stochastic geometry results for wireless networks.